國立臺灣大學醫學院腫瘤醫學研究所

博士論文

Graduate Institute of Oncology
College of Medicine
National Taiwan University
Doctoral Dissertation

利用 CDK4/6 抑制劑的協同細胞毒殺與腫瘤微環境調控最佳化乳癌放射治療成效

Optimizing Radiotherapy Efficacy in Breast Cancer: Synergistic Tumor Cell Killing and Tumor Microenvironment Reprogramming with CDK4/6 Inhibitors

楊文綺

Wen-Chi Yang

指導教授：郭頌鑫 教授

Advisor: Professor Sung-Hsin Kuo, M.D. Ph.D.

中華民國 114 年 9 月

September 2025

doi:10.6342/NTU202504448

國立臺灣大學博士學位論文
口試委員會審定書

利用 CDK4/6 抑制劑的協同細胞毒殺與腫瘤微環境調控

最佳化乳癌放射治療成效

Optimizing Radiotherapy Efficacy in Breast Cancer: Synergistic Tumor Cell Killing and Tumor Microenvironment Reprogramming with CDK4/6 Inhibitors

本論文係 楊文綺 君（學號 D07453002）在國立臺灣大學腫瘤醫學研究所完成之博士學位論文，於民國 114 年 9 月 4 日承下列考試委員審查通過及口試及格，特此證明

口試委員：

郭頌鑫 （簽名）

（指導教授）

盧彥仲　　劉峻宇

李欣倫　　[illegible]

所長：葉坤輝 （簽名）

doi:10.6342/NTU202504448

Acknowlegement

七年前申請腫瘤所博士班的時候，就知道醫師念博士班並不是很容易。但這條路走來，不容易之處與最開始的預期有很大的不同。一邊學習成為獨當一面的主治醫師，掌握治療病人細節；學習當一個母親，成為孩子的主要照顧者跟教養者；學習當一個學生，拾起基礎知識和教科書通過考試；最後學習成為一個研究者，發想設計並執行自己的研究取得成果。

年輕時會羨慕可以放下一切去讀書的人，虛長幾歲之後反倒是感謝學校以及研究所這樣的課程設計，能讓我在念書的這段時間，沒有錯過自己身為放射腫瘤科醫師的培養，也沒有錯過孩子的成長。早知道人生沒有兼得，只有取捨；走的越遠，越感謝生活中的師長同事家人，讓我在取捨的夾縫中，能逐步雕琢出未來的形狀。

感謝魏名峰博士，扮演著亦師亦友的角色，在這段路上的扶持；感謝助理瑀玟和群凱，分擔了各種瑣碎的細節，讓我更有餘裕得以前進。感謝余松良教授、沈盈君醫師以及第三共研，在設備及技術上的的各種協助。感謝學長姐許峯銘醫師、呂紹綸醫師、賴詩璠醫師、江韻醫師提供各種經驗上的分享告訴我如何少走一些冤枉路。感謝論文指導委員會的劉峻宇教授及盧彥伸教授，給予許多價值連城的意見和指導。最後感謝指導老師郭頌鑫教授一直以來的教導和支持，感謝老師給了我很大的自由空間去探索，並且永遠在我背後當最強大的後盾。

感謝一路上支持我的先生陳科廷以及女兒俐瑀，從來不因我的成功或失敗而改變你們的支持；但同時也感謝那些曾碰過的障礙和困難，這一路的險阻教會我如何謹慎行事、腳踏實地。走到最後一刻才發現，那些日復一日乍看瑣碎的臨床工作及家庭生活，才是穩固一切的錨。曾經也有想放棄的時刻，但想起女兒說的：「畢業或者不畢業，你做的事情有什麼不一樣嗎？不是都還是要念書、工作、看病人、做研究？」，所有的困頓與不安，盡皆驅散。

doi:10.6342/NTU202504448

中文摘要

本研究旨在透過結合臨床觀察與前臨床實驗，評估 CDK4/6 抑制劑、放射治療及免疫療法之治療策略，以期達成乳癌治療的最佳化，提供個人化治療的依據。

在臨床分析中，我們針對接受系統性治療並合併不同放射治療方式的早期乳癌患者進行預後評估。研究結果顯示，單純鎖骨上淋巴區域放射治療的成效與更廣泛的區域性淋巴結放射治療（含內乳淋巴結）相當。此外，針對病理分期為 N3 的患者，額外增加腋下淋巴結放射治療並未顯著提升治療成效，暗示對於此類高風險患者，加強系統性治療可能較擴大放療範圍更具療效。

在前臨床實驗部分，我們探討 CDK4/6 抑制劑合併 RT 於荷爾蒙受體陽性、人類表皮生長因子受體 2 (HER2)陰性乳癌的治療效果。研究顯示 CDK4/6 抑制劑可透過抑制 ERK 及 NF-κB/c-Myc 訊息傳導路徑，以及干擾 DNA 雙股斷裂修復，明顯提升細胞對放射治療的敏感性。此外，本研究進一步以具免疫功能的三陰性乳癌小鼠模式（4T1 及 EMT6），評估 CDK4/6 抑制劑、放射治療與抗 PD-L1 免疫療法的三合一治療策略。結果證實此三合一療法能有效抑制腫瘤生長，增加血液中干擾素-γ（IFN-γ）濃度，並促進 CD4+ T 細胞、CD8+ T 細胞及 M1 型巨噬細胞浸潤腫瘤組織，成功將腫瘤微環境轉變為較具免疫刺激性的狀態。

整體而言，本研究成果凸顯 CDK4/6 抑制劑合併放射治療對於提升各種亞型乳癌的治療成效，以及促進免疫療法療效的潛力。上述前臨床研究結果值得未來進一步推展至臨床驗證，以期提升乳癌患者的整體預後及存活率。

關鍵詞：乳癌、放射治療、放射增敏作用、CDK4/6 抑制劑、免疫療法、腫瘤微環境

doi:10.6342/NTU202504448

ABSTRACT

This study aimed to optimize breast cancer treatment by integrating clinical insights and preclinical evaluations of CDK4/6 inhibitor, radiotherapy (RT), and immunotherapy, supporting personalized therapeutic strategies.

Clinically, we analyzed outcomes in early-stage breast cancer patients receiving systemic therapy combined with various radiotherapy approaches. Supraclavicular radiotherapy (SCF-RT) alone showed comparable results to extensive regional nodal irradiation, including the internal mammary chain. Additionally, extending radiotherapy to axillary nodes did not improve outcomes for pathologically N3 patients, suggesting intensified systemic therapy might be more effective.

Preclinically, we assessed CDK4/6 inhibitors combined with RT in HR-positive, HER2-negative breast cancer. CDK4/6 inhibitors increased radiosensitivity by suppressing ERK and NF-κB/c-Myc signaling and impairing DNA double-strand break repair. Furthermore, combining CDK4/6 inhibitors, RT, and anti-PD-L1 immunotherapy in immunocompetent triple-negative breast cancer (TNBC) mouse models effectively inhibited tumor growth, increased circulating IFN-γ levels, and enhanced immune cell infiltration, shifting the tumor microenvironment towards immunostimulation.

Overall, this integrated approach highlights the promise of combining CDK4/6 inhibitors with RT to enhance therapeutic effects in breast cancer across various subtypes and improve the efficacy of immunotherapy. These promising preclinical results warrant further clinical investigation to potentially enhance treatment outcomes and patient survival.

Keywords: Breast cancer, Radiotherapy, Radiosensitization, CDK4/6 inhibitor, Immunotherapy, Tumor microenvironment.

doi:10.6342/NTU202504448

CONTENT

doi:10.6342/NTU202504448

doi:10.6342/NTU202504448

doi:10.6342/NTU202504448

LIST OF FIGURES

doi:10.6342/NTU202504448

doi:10.6342/NTU202504448

doi:10.6342/NTU202504448

LIST OF TABLES

doi:10.6342/NTU202504448

CHAPTER 1. INTRODUCTION

1.1 INTRODUCTION OF BREAST CANCER

Breast cancer is the most common malignancy among women, not only in Western countries but also in Taiwan. In 2018, over 12,000 women were diagnosed with breast cancer, making it the most prevalent cancer type among women and the second most common malignancy overall. The increasing breast cancer incidence was shown in Taiwan Cancer registry[1]. The etiology of breast cancer has been explored from Taiwan National Health Insurance Research Database which showed that benign breast diseases, obesity, endometriosis, uterine leiomyoma, hypertensive diseases, and disorders of lipid metabolism were associated with increased subsequent breast cancer risk[2].

Breast cancer is classified into molecular subtypes based on distinct biological characteristics and their prognostic implications[3]. Using immunohistochemistry and fluorescence in situ hybridization (FISH) to assess estrogen receptor (ER), progesterone receptor (PR), and human epidermal growth factor receptor 2 (HER2) expression, breast cancer heterogeneity is categorized into four major subtypes: luminal A/B [hormone receptor (HR)+/HER2−, HR+, ER+, and/or PR+], luminal HER2 (HR+/HER2+), HER2-enriched (HR−/HER2+), and triple-negative breast cancer (TNBC; HR−/HER2−).

Beyond HR and HER2 status, the Ki-67 index was proposed by Cheang *et al.*[4] as a key marker to differentiate luminal A from luminal B breast cancer. According to the immunohistochemical classification, luminal A breast cancer is defined as HR+/HER2− with low Ki-67 expression (Ki-67 index <14%), while luminal B breast cancer is characterized by HR+/HER2− status with high Ki-67 expression (Ki-67 index ≥14%)[5]. The correlation between this immunohistochemical classification and genetic profiling has been validated, leading to its routine clinical application. HR status and HER2

doi:10.6342/NTU202504448

overexpression have been shown to strongly correlate with treatment response and clinical outcomes[6]. Consequently, HR and HER2 expression have been incorporated into the published 8th edition of the AJCC cancer staging system[7].

Breast cancer treatment strategies vary significantly depending on the molecular subtype, as each subtype exhibits distinct biological behaviors and therapeutic responses. In the past, most breast cancer cases were treated with a one-size-fits-all approach, primarily relying on surgery, radiotherapy, and chemotherapy. However, with advancements in molecular biology and precision medicine, treatment has become increasingly personalized, incorporating targeted therapies tailored to the specific molecular characteristics of each tumor subtype. Hormone receptor-positive breast cancers, including luminal A and luminal B subtypes, are primarily treated with endocrine therapy, often in combination with CDK4/6 inhibitors for advanced disease[8], which has significantly improved progression-free survival. Luminal B tumors, due to their higher proliferative activity and poorer prognosis, may also require chemotherapy in addition to hormonal therapy. HER2-positive breast cancers, including both luminal HER2 and HER2-enriched subtypes, are treated with HER2-targeted therapies such as trastuzumab and pertuzumab, often combined with chemotherapy, which has dramatically improved survival rates. Triple-negative breast cancer, which lacks ER, PR, and HER2 expression, was historically treated solely with chemotherapy, but recent breakthroughs in immunotherapy, particularly immune checkpoint inhibitors targeting the PD-1/PD-L1 pathway, have provided new hope for patients with advanced or metastatic disease[9]. Additionally, novel combinations of immunotherapy with chemotherapy and radiotherapy are being explored to enhance treatment efficacy. These advancements highlight the transition from generalized treatment approaches to tailored, molecularly driven therapies, aiming to maximize efficacy while minimizing unnecessary toxicity for each patient.

doi:10.6342/NTU202504448

1.2 CHALLENGES IN THE TREATMENT OF LUMINAL-TYPE BREAST CANCER

Luminal A breast cancer is the most prevalent subtype, accounting for approximately 40% of all breast cancer cases, whereas luminal B represents around 20%. Due to the dependence of luminal-type breast cancer on hormone receptor signaling, patients with this subtype generally experience favorable clinical outcomes, primarily owing to the efficacy of endocrine therapy. For those diagnosed at an early stage, the standard treatment approach includes breast-conserving surgery, followed by adjuvant whole-breast radiotherapy and long-term endocrine therapy[10]. However, despite the overall favorable prognosis, luminal B breast cancer presents notable therapeutic challenges. This subtype is associated with higher expression of genes related to cellular proliferation, variable HER2 expression levels, and an increased risk of local recurrence. As a result, patients with luminal B tumors tend to have a poorer prognosis compared to those with luminal A breast cancer.

Luminal-type breast cancer exhibits limited responsiveness to conventional chemotherapy[11]. This presents a significant challenge, particularly in cases where patients develop resistance to endocrine therapy. Once endocrine resistance emerges, tumors may continue to progress despite ongoing anti-hormonal treatment, leaving patients with fewer effective therapeutic options. Additionally, a key concern in luminal breast cancer is the potential for late recurrence, where disease relapse can occur many years after the initial treatment, necessitating long-term disease monitoring and management[12].

The introduction of CDK4/6 inhibitors has revolutionized the treatment landscape for recurrent or advanced luminal-type breast cancer. These inhibitors have demonstrated substantial clinical benefits, effectively delaying disease progression and improving progression-free survival in patients with hormone receptor-positive, HER2-negative breast cancer[8, 13-15]. However, while CDK4/6

doi:10.6342/NTU202504448

inhibitors represent a major breakthrough, the search for optimal combination strategies to further enhance their therapeutic efficacy remains an active area of investigation.

1.3 THERAPEUTIC LIMITATION IN TRIPLE NEGATIVE BREAST CANCER

Among all breast cancer subtypes, TNBC is associated with the poorest prognosis, primarily due to its inherently aggressive nature and the lack of well-defined molecular targets for treatment[16]. The different clinical outcomes for different subtypes of breast cancer were varied [17]. Unlike hormone receptor-positive or HER2-positive breast cancers, TNBC lacks ER, PR, and HER2 expression, making it unresponsive to endocrine therapy or HER2-targeted agents. For patients with metastatic TNBC, chemotherapy has long remained the mainstay of treatment. However, advances in molecular diagnostics have deepened the understanding of TNBC heterogeneity[18-20], leading to its classification into distinct molecular subgroups, including basal-like 1 and 2, luminal androgen receptor (LAR), and mesenchymal subtypes[21, 22].

Beyond conventional chemotherapy, novel targeted therapies have been developed to address specific TNBC subgroups. PARP inhibitors have shown efficacy in tumors with homologous recombination deficiency, particularly in patients harboring BRCA mutations. Antibody-drug conjugates (ADCs) represent another promising approach, allowing selective delivery of cytotoxic agents to cancer cells expressing specific surface antigens[23]. Additionally, therapeutic strategies targeting the PI3K-AKT and MAPK signaling pathways are currently under investigation for their potential role in TNBC treatment. Despite these advances, the vast molecular diversity within TNBC has posed a significant challenge, and many of these novel treatment options have yet to demonstrate sufficient clinical impact in routine practice.

doi:10.6342/NTU202504448

Over the past decade, immunotherapy has revolutionized oncology, providing a breakthrough for cancers with limited targeted treatment options, such as small cell lung cancer, melanoma, and EGFR wild-type non-small cell lung cancer. TNBC, known for its immunogenic properties, has also become a key focus for immunotherapy research. Studies have revealed that the intrinsic molecular subtypes of TNBC are linked to distinct tumor microenvironment characteristics, influencing immune responses to treatment[24]. In particular, tumor-infiltrating lymphocytes (TILs) in the stromal region have been identified as prognostic markers in TNBC, further highlighting the role of the immune system in disease progression[25].

In the era of immunotherapy, immune checkpoint inhibitors (ICIs) have emerged as a promising approach for TNBC treatment. However, initial results in unselected TNBC populations were modest—monotherapy with the PD-L1 inhibitor atezolizumab demonstrated a response rate of only 24% in advanced TNBC patients[26]. Similarly, the KEYNOTE-086 trial indicated that pembrolizumab provided clinical benefit only to a small subset of patients with PD-L1-positive TNBC[27]. Nevertheless, PD-L1 negativity does not necessarily preclude the potential benefits of ICIs. Emerging evidence suggests that combining ICIs with other anticancer therapies may enhance treatment response by increasing tumor antigenicity and promoting immune activation[28]. In particular, combining chemotherapy with immunotherapy has yielded promising results in metastatic TNBC, leading to improved clinical outcomes[29]. Ongoing research continues to explore additional combination strategies, including the integration of radiotherapy, targeted agents, and novel immune-modulating approaches to further enhance the efficacy of immunotherapy in TNBC.

1.4 ROLE OF RADIOTHERAPY IN BREAST CANCER

Radiotherapy is a cornerstone of cancer treatment and plays a critical role in the management of solid tumors. It is estimated that approximately 50% of all cancer patients undergo radiotherapy at some

doi:10.6342/NTU202504448

point during their disease course, either as a definitive, adjuvant, neoadjuvant, or palliative treatment modality[30]. The therapeutic efficacy of radiotherapy is primarily attributed to ionizing radiation-induced DNA damage, which disrupts cellular function and ultimately leads to tumor cell death. Mechanistically, radiation exerts its cytotoxic effects by inducing cell cycle arrest in the G2/M phase, thereby increasing tumor cell sensitivity to apoptotic and mitotic catastrophe pathways, which are the predominant mechanisms of radiation-induced cell death[31, 32].

In breast cancer treatment, radiotherapy is widely utilized across different disease stages and molecular subtypes. Following primary surgery, adjuvant radiotherapy is considered a standard of care, reducing the risk of local recurrence and improving long-term disease control[10]. However, the role of radiotherapy is being re-evaluated in the context of modern systemic therapies. The increasing use of targeted therapies, endocrine treatments, immune checkpoint inhibitors (ICIs), and chemotherapy advancements has led to improved systemic disease control, raising questions about whether extensive radiotherapy, particularly regional nodal irradiation (RNI) and internal mammary node irradiation (IMN-RT), provides additional benefits.

As previously mentioned, immunotherapy becomes the hope of cancer treatment. High-dose ionizing radiation is known for its immunogenic properties, acting as an in situ "tumor vaccine" that enhances anti-tumor immunity. It promotes the release of tumor-associated antigens, primes the adaptive immune system, and induces chemokine secretion to recruit tumor-specific cytotoxic T lymphocytes (CTLs). Additionally, radiation increases the production of IFNγ and TNF, which further stimulate immune responses, and enhances the abscopal effect, where localized radiation leads to tumor regression outside the irradiated area[33-36]. These immunomodulatory effects are even more pronounced when combined with immune checkpoint inhibitors (ICIs).

Radiation also reshapes the tumor microenvironment (TME) through multiple mechanisms, fostering interactions with various anti-cancer therapies[35]. However, these synergies remain

doi:10.6342/NTU202504448

incompletely understood. Clinically, the PEMBRO-RT trial, a phase II randomized study, demonstrated that stereotactic body radiotherapy (SBRT) combined with pembrolizumab improved overall response rates (ORR), progression-free survival (PFS), and potentially overall survival (OS)[37].

In breast cancer, the combination of SBRT and immunotherapy has also been explored. Ho *et al*. conducted an early phase II trial evaluating pembrolizumab with hypofractionated radiotherapy in metastatic TNBC, reporting an overall response rate of 17.6%[38]. Notably, among patients assessed at week 13 post-treatment, three achieved a complete response outside the radiation field, suggesting a strong abscopal effect. While these findings highlight the potential of immunotherapy in TNBC, the absence of a reliable biomarker remains a challenge in predicting response. Combining immunotherapy with other immunogenic treatments may offer a more effective strategy for improving clinical outcomes.

Despite these advantages, radiation resistance and toxicity remain key challenges, necessitating ongoing research into radiotherapy optimization, radiosensitizers, and combination strategies with systemic therapies to maximize treatment efficacy while minimizing adverse effects.

doi:10.6342/NTU202504448

1.5 ROLE CDK4/6 INHIBITORS IN BREAST CANCER

1.5.1 MECHANISM OF CDK4/6 INHIBITORS

Cyclin-dependent kinases 4 and 6 (CDK4/6) play a pivotal role in cell cycle regulation, acting as essential drivers of cell cycle progression from the G1 to S phase. Their activity is tightly controlled by both positive regulators, such as cyclins D1/D2/D3, and negative regulators, including tumor suppressors like p16INK4A, encoded by CDKN2A. In response to mitogenic signals, cyclin D–CDK4/6 complexes phosphorylate the retinoblastoma protein (Rb), releasing E2F transcription factors and enabling cell cycle progression. Aberrations in this pathway are frequently observed in various solid malignancies, making CDK4/6 an attractive therapeutic target[39-41].

The development of selective CDK4/6 inhibitors, including ribociclib, palbociclib, and abemaciclib, has revolutionized breast cancer treatment. These inhibitors directly target the cyclin D–CDK4/6–p16–Rb pathway, effectively halting tumor cell proliferation by preventing Rb phosphorylation and subsequent cell cycle progression. Moreover, CDK4/6 activity is intricately linked to ER signaling, providing a biological rationale for dual inhibition strategies[42].

The CDK4/6–cyclin D axis has been shown to play a crucial role in breast tumorigenesis, as demonstrated in preclinical models[43, 44]. Cyclin D1 overexpression is frequently observed in breast cancer tissues, particularly in ER-positive tumors[45], and is associated with hormone receptor positivity[46].

1.5.2 ANTITUMOR EFFECT OF CDK4/6 INHIBITORS

Preclinical studies have demonstrated synergistic effects between CDK4/6 inhibitors and anti-estrogen therapy, effectively blocking the CDK4/6–cyclin D axis and suppressing tumor growth[47]. Among these inhibitors, palbociclib has been extensively studied and has demonstrated significant

doi:10.6342/NTU202504448

clinical benefit. In combination with letrozole, palbociclib has been shown to prolong PFS and OS in patients with advanced ER-positive, HER2-negative breast cancer, leading to its approval as a first-line treatment for this patient population[8, 13].

Beyond metastatic disease, CDK4/6 inhibitors have also been explored in the neoadjuvant setting. The addition of palbociclib to letrozole significantly enhanced the suppression of malignant cell proliferation, as indicated by decreased Ki-67 levels in primary ER-positive breast cancer[13, 48]. Recent randomized trials have confirmed the efficacy of CDK4/6 inhibitors in the adjuvant setting. The NATALEE trial[49] demonstrated that ribociclib combined with an aromatase inhibitor improved disease control in patients with HR-positive, HER2-negative stage II or III early breast cancer. Similarly, the monarchE trial[50] showed that abemaciclib combined with endocrine therapy significantly improved invasive disease-free survival in patients with HR-positive, HER2-negative, node-positive breast cancer. These findings highlight the expanding role of CDK4/6 inhibitors in the adjuvant treatment of early-stage breast cancer, paving the way for future therapeutic advancements.

Other than hormone-positive breast cancer, preclinical evidence suggests that CDK4/6 inhibitors also exhibit activity in non-luminal cell lines[51, 52]. However, due to the frequent loss of Rb protein, TNBC patients have traditionally been considered poor candidates for CDK inhibition. Interestingly, TNBC has shown high sensitivity to CDK inhibition both *in vitro*[53] and *in vivo*, with one preclinical study demonstrating that a CDK2/9 inhibitor in combination with eribulin was effective against TNBC[54]. These findings suggest that additional, yet unidentified, factors related to TNBC proliferation and cell cycle progression may exist.

One such factor was recently identified in a study showing that death effector domain-containing protein (DEDD) is overexpressed in more than 60% of TNBC cases, where it drives a mitogen-independent G1/S cell cycle transition. DEDD upregulation was found to enhance cyclin D1 expression,

doi:10.6342/NTU202504448

and TNBCs with DEDD overexpression exhibited a DEDD-dependent vulnerability to combined treatment with a CDK4/6 inhibitor and an EGFR inhibitor, both in vitro and in vivo[55].

An incidental clinical finding further supports the potential role of cell cycle inhibition in TNBC treatment. In a randomized phase II trial, Tan *et al.* compared Trilaciclib, a CDK4/6 inhibitor, plus chemotherapy versus chemotherapy alone in patients with metastatic TNBC[56]. The primary hypothesis was that CDK4/6 inhibition could protect bone marrow during chemotherapy due to its effects on the cell cycle. Although the study did not meet its primary endpoint, it unexpectedly demonstrated significantly improved PFS and OS in patients receiving Trilaciclib with chemotherapy compared to chemotherapy alone. While the precise mechanism of CDK4/6 inhibition in TNBC remains unclear, these promising clinical findings warrant further investigation.

1.5.3 CDK4/6 INHIBITORS IN IMMUNE MODULATION

CDK4/6 inhibitors not only induce tumor cell cycle arrest but also enhance anti-tumor immunity. Early studies demonstrated that CDK4 and CDK6, along with their associated cyclins, play a crucial role in the proliferation of both myeloid[57] and lymphoid lineage immune cells[58]. Additionally, cell cycle arrest can activate the senescence-associated secretory phenotype (SASP) in certain cancer cells, leading to the recruitment of innate immune cells[59].

Goel *et al.* reported that CDK4/6 inhibitors induce tumor cells to express endogenous retroviral elements[60], triggering the production of type III interferons, which in turn enhance tumor antigen presentation. Moreover, CDK4/6 inhibitors significantly suppress the proliferation of regulatory T cells (Tregs), potentially due to reduced activity of the E2F target, DNA methyltransferase 1 (DNMT1). As a result, CDK4/6 inhibition enhances the anti-tumor effects of cytotoxic T cells. Deng *et al.* further demonstrated that CDK4/6 inhibitors enhance anti-tumor T-cell activity[61], in part by derepressing

doi:10.6342/NTU202504448

NFAT family proteins. Although CDK4/6 inhibition reduces the overall T-cell population, it increases the abundance of TILs.

PD-L1, a key immune inhibitory signal, is a potential biomarker for ICIs. Zhang *et al*. discovered a link between CDK4/6 activity and PD-L1 protein stability, revealing that PD-L1 expression fluctuates throughout the cell cycle[62]. Inhibition or depletion of cyclin D and CDK4 led to increased PD-L1 levels in breast cancer cells, regardless of Rb status. This finding suggests a potential rationale for combining CDK4/6 inhibitors with ICIs. However, some animal studies reported downregulation of PD-1 and CTLA-4 co-inhibitory markers in $CD4^+$ and $CD8^+$ T cells[61], indicating that the role of CDK4/6 inhibitors in immune checkpoint regulation remains controversial. Nonetheless, preclinical models have demonstrated promising anti-tumor effects when combining CDK4/6 inhibitors with ICIs[63]. The summary of current evidences in mechanisms how CDK4/6 inhibitors regulated immune system, through the effect on tumor itself or impact on tumor microenvironment was described in previous review[64, 65].

CDK4/6 inhibitors have also shown immune-regulatory effects in clinical trials. The neoMONARCH phase II neoadjuvant trial[66] in HR-positive, HER2-negative breast cancer demonstrated that abemaciclib, either alone or in combination with anastrozole, significantly reduced Ki67 expression and led to a radiographic tumor response. However, this study found no increase in TILs following abemaciclib treatment. Gene expression profiling using RNA-seq in a subset of patients revealed upregulation of inflammatory and T cell–related pathways in tumors treated with abemaciclib plus anastrozole. These emerging clinical findings suggest a potential role for CDK4/6 inhibitors in immune modulation, warranting further investigation.

1.6 FIND OUT THE BEST TREATMENT COCKTAIL IN BREAST CANCER

doi:10.6342/NTU202504448

From the clinical results of immunotherapy in TNBC, CD4/6 inhibitors alone or with letrozole in HR positive breast cancer, one thing is clear that the single treatment strategy is not enough for breast cancer control, especially in subtype of TNBC, in which huge inter-patient, and intra-tumoral heterogeneity make it impossible to have a single best solution for all.

After the success of CDK 4/6 inhibitor with anti-estrogen, other combination treatment was also investigated. PI3K-akt-mTOR pathway was also known to regulate CDK4/6-cyclin complex and PI3K inhibitor was reported to have synergistic effect with CDK 4/6 inhibitor in ER positive breast cancer[67]. Another combination inhibition of STAT3 and PARP were shown to significantly increase cell death in the palbociclib resistant breast cancer cells[68]. The correlation between CDK4/6 inhibition and the immune reaction of tumor microenvironment were mentioned as above. PI3K inhibitors were not only synergistic with CDK4/6 inhibitors, but also regulated immune response together. Teo *et al*. reported combined CDK4/6 and PI3Ka inhibition increase T-cell activation and reduces immunosuppressive cell[69].

The combination of radiotherapy and CDK4/6 inhibitors were proposed in many kinds of solid cancer. Synergistic effect of radiotherapy with CDK4/6 inhibitors were reported in several cancer models like hepatocellular carcinoma, esophageal cancer, KRAS-mutant lung cancer, head and neck squamous cell carcinoma, and brain cancers including atypical teratoid rhabdoid tumor (ATRT) and glioblastoma[70-74]. However, there are scarce data addressing interaction between radiotherapy and CDK4/6 inhibition in ER+, HER2- breast cancer. As mentioned above, radiotherapy is the standard of care in the adjuvant treatment for early breast cancer[10] and plays an important role in treating metastatic cancer patients. Besides, CDK4/6 inhibitors are most commonly used in ER+, HER2- breast cancer clinically. Currently, only few case reports and retrospective studies showing the feasibility and potential benefit of combining CDK4/6 inhibitors and radiotherapy in breast cancer patients [75, 76].

doi:10.6342/NTU202504448

This doctoral thesis aims to explore strategies for optimizing breast cancer treatment by investigating the role of radiotherapy in the era of modern systemic therapy, including chemotherapy and targeted therapy, with a particular focus on reassessing the impact of extended regional nodal irradiation in locally advanced breast cancer. Additionally, it examines the synergistic effects of combining radiotherapy with CDK4/6 inhibitors in luminal breast cancer, uncovering the underlying mechanisms that may enhance therapeutic efficacy. Furthermore, this study evaluates the immune-modulatory effects of both radiotherapy and CDK4/6 inhibitors and investigates whether their combination can enhance the effectiveness of immunotherapy in TNBC mouse models.

By addressing these key aspects, this research provides valuable insights into how radiotherapy, CDK4/6 inhibitors, and immunotherapy can be effectively integrated into clinical practice. A deeper understanding of their interactions could facilitate the development of more rational combination strategies, ultimately improving treatment efficacy, disease control, and patient outcomes. These findings may serve as a foundation for future clinical trials, guiding the optimal use of these therapies in both luminal breast cancer and TNBC to maximize therapeutic benefits.

doi:10.6342/NTU202504448

CHAPTER 2. ROLE OF RADIOTHERAPY FOR EARLY BREAST CANCER IN THE ERA OF MORDERN SYSTEMIC TREATMENT

2.1 INTRODUCTION

As described in Chapter 1, radiotherapy plays an important role in early breast cancer in adjuvant setting which improved local control and cancer specific survival for nodal positive patinets. Regional nodal irradiation reduced recurrence risk in breast cancer patients with positive lymph nodes (LNs), particularly when combined with chest wall irradiation after modified radical mastectomy[77, 78]. The Early Breast Cancer Trialists' Collaborative Group meta-analysis confirmed that postmastectomy radiotherapy (PMRT), which includes both chest wall irradiation and RNI, offers substantial benefits for patients with positive axillary LNs[79]. As breast-conserving surgery (BCS) has become the standard surgical approach, RNI is also recommended for high-risk BCS patients to improve disease control.

Key clinical trials have provided strong evidence supporting the effectiveness of RNI. The MA-20 trial demonstrated that RNI, targeting the medial supraclavicular fossa (SCF), internal mammary chain (IMN), and high axillary LNs, significantly improved 10-year disease-free survival (DFS) (82.0% vs. 77.0%; HR = 0.76; $p = 0.01$) and distant metastasis-free survival (DMFS) (86.3% vs. 82.4%; HR = 0.76; $p = 0.03$) in patients with positive or high-risk negative LNs undergoing BCS[80]. Similarly, the EORTC 22922/10925 trial reported that RNI reduced 15-year breast cancer-related mortality (16.0% vs. 19.8%; $p = 0.0055$)[81]. Despite these proven benefits, the optimal extent of LN irradiation remains a subject of debate.

The inclusion of IMN irradiation in RNI has been particularly controversial. Both the MA-20 and EORTC 22922/10925 trials incorporated IMN-RT as part of their treatment approach, yet its survival benefit has been debated for decades[82, 83]. A large Danish population-based study[84], DBCG-IMN,

doi:10.6342/NTU202504448

found that IMN-RT improved overall survival (60.1% vs. 55.4% at 15 years; $p = 0.007$), lowered distant metastasis rates (35.6% vs. 38.6%; $p = 0.04$), and reduced breast cancer mortality (31.7% vs. 33.9%; $p = 0.05$). However, prospective randomized controlled trials, including the French trial and the Korean KROG-0806 trial, did not demonstrate a statistically significant benefit in DFS or OS for patients receiving IMN-RT[85, 86]. These conflicting results continue to fuel debate over the routine use of IMN-RT as part of RNI.

Another unresolved question is the role of axillary LN irradiation (ALRT), which has not been consistently included in RNI trials. The AMAROS trial, which compared axillary nodal dissection (ALND) and ALRT, demonstrated that ALRT could replace ALND in patients with LN-positive early-stage breast cancer undergoing BCS or mastectomy[87]. However, whether ALRT offers additional benefits for patients who have already undergone ALND remains unknown. Further research is needed to determine whether ALRT improves clinical outcomes in high-risk patients following ALND.

In this chapter, we aimed to discover the role of radiotherapy in nodal early breast cancer for which especillay focused on the impact of these treatment fields of RT in the context of modern systemic treatments including adequate hormone therapy, taxane-based chemotherapy regimens, and targeted therapy against HER2.

2.2 MATERIALS AND METHODS

2.2.1 PATIENTS

This study included patients with localized breast cancer diagnosed between July 2008 and April 2014 who underwent primary surgery followed by adjuvant systemic therapy and RNI as part of their adjuvant radiotherapy. The RNI field covered the SCF, with or without inclusion of the axillary lymph nodes or internal mammary nodes. Patients who had received neoadjuvant systemic therapy were excluded.

doi:10.6342/NTU202504448

A total of 512 patients met the eligibility criteria and were included in the analysis. Data on patient demographics (age, histological type, tumor grade, and pathological stage) were collected, along with treatment details, such as surgical approach for the breast and axilla, number of LNs removed, specific RNI targets, and types of adjuvant systemic therapy received.

2.2.2 TECHNIQUE OF RADIOTHERAPY

All patients in this study underwent computed tomography (CT)-based planning followed by standard fractionated radiation therapy, delivering 50 Gy across 25 sessions to the affected breast or chest wall, as well as the regional lymphatic areas. Those who had a lumpectomy received an additional tumor bed boost of 10–16 Gy, administered at 2 Gy per fraction, to enhance local disease control.

All individuals received radiation to the SCF, with 78 undergoing ALRT and 20 receiving IMN-RT. The radiation approach utilized either three-dimensional conformal techniques (3D-CRT) or forward-planned field-in-field (FIF) intensity modulation, optimizing dose distribution. Notably, inverse-planned IMRT or volumetric-modulated arc therapy (VMAT) was not employed in this study.

These treatment modalities were chosen to ensure precise targeting of the lymphatic regions while minimizing radiation exposure to adjacent healthy structures, thereby balancing therapeutic efficacy and safety.

2.2.3 RESPONSE EVALUATION AND STATISTICAL ANALYSIS

In this study, locoregional recurrence-free survival (LRFS) was defined as the duration from the initiation of RT to the occurrence of locoregional failure or death. Disease-free survival was measured from the start of RT to the first documented event of locoregional recurrence, distant metastasis, or death from any cause, whichever occurred first. Overall survival was determined as the time from the

doi:10.6342/NTU202504448

beginning of RT to death from any cause. Both DFS and OS calculations were anchored to the start of RT.

To evaluate survival outcomes, the Kaplan–Meier method was utilized, with differences in survival curves assessed using log-rank tests. A Cox proportional hazards regression model was applied to estimate hazard ratios and assess the impact of various clinical factors on survival.

To minimize potential confounding bias and achieve balanced comparison groups, propensity score matching (PSM) was performed. Patients who underwent IMN-RT were matched 1:1 with those who did not receive IMN-RT, based on key clinical and pathological factors, including tumor (T) stage, nodal (N) stage, histologic grade, and molecular subtypes. Nearest-neighbor matching without replacement was implemented using a caliper width of 0.2, ensuring closely matched baseline characteristics. This process resulted in 17 matched pairs, which were subsequently analyzed for treatment-related differences.

All statistical analyses were conducted using IBM SPSS Statistics (version 24.0; IBM Corp., Armonk, NY), with two-sided *p*-values below 0.05 considered statistically significant. The integration of these rigorous statistical methodologies helped enhance the reliability of the findings and account for potential biases in treatment selection.

2.3 RESULTS

2.3.1 CLINICAL CHARACTERISTICS OF PATIENTS

Between 2009 and 2014, a total of 512 patients who met the eligibility criteria were included in this analysis. The median age at diagnosis was 51 years, with a range spanning from 26 to 88 years. The majority of cases (88.5%) were diagnosed as invasive ductal carcinoma, making it the predominant histological subtype.

doi:10.6342/NTU202504448

Based on ERand HER2 status, patients were categorized into four molecular subtypes: ER-positive/HER2-negative (65.8%, 337 patients), ER-positive/HER2-positive (12.3%), ER-negative/HER2-positive (10.0%), and ER-negative/HER2-negative (triple-negative breast cancer, TNBC) (11.9%). Regarding disease stage, 31.2% (160 patients) were diagnosed with early-stage disease (T1-2, N0-1), while the remaining 68.8% (352 patients) had locally advanced disease (T3-4 or N2-3).

Surgical treatment varied within the cohort, with 228 patients (44.5%) undergoing partial mastectomy, while 284 (55.5%) underwent total mastectomy. Regardless of the surgical approach, 92.4% (473 patients) underwent ALND, with a median of 19 lymph nodes removed.

Regarding systemic therapy, nearly all patients (95.9%, 491 patients) received adjuvant chemotherapy, with the majority (441 patients) receiving taxane-based regimens that included anthracyclines. All HER2-positive patients were treated with anti-HER2 therapy, and 97.5% of ER-positive patients received endocrine therapy.

In terms of regional nodal irradiation, all patients underwent supraclavicular fossa radiotherapy (SCF-RT). Additionally, 78 patients (15.2%) received ALRT, and 20 patients (3.9%) received IMN-RT. These comprehensive patient characteristics, including demographic, pathological, and treatment details, are summarized in **Table 2-1**.

doi:10.6342/NTU202504448

Table 2-1 Patient and Treatment characteristics, N=512

Patient characteristics	N (%)	Treatment characteristics	N (%)
Histology		Breast Surgery Type	
IDC	453 (88.5)	Partial mastectomy	228 (44.5)
ILC	38 (7.4)	Total mastectomy	284 (55.5)
Mucinous	6 (1.2)		
Metaplastic	5 (1.0)		
Others	10 (2.0)		
Molecular Subtypes		Axilla Surgery Type	
ER positive / HER-2 negative	337 (65.8)	SLND	39 (7.6)
ER positive / HER-2 positive	63 (12.3)	ALND	473 (92.4)
ER negative / HER-2 positive	51 (10.0)	Median LND number	19
ER negative / HER-2 negative	61 (11.9)	Median positive LN number	4
Grade		Adjuvant Chemotherapy	
I	65 (12.7)	No	21 (4.1)
II	219 (42.8)	Yes	491 (95.9)
III	192 (37.5)	Taxane use	441 (89.8)***
N/A	36 (7.0)	Adriamycin use	480 (97.8)
Pathological T stage		Anti HER-2 treatment*	
0	6 (1.2)	Yes	116 (22.7) $
1	123 (24.0)	No	396 (39.6)
2	255 (49.8)		
3	105 (20.5)		
4	10 (2.0)		
X (cannot be assessed)	13 (2.5)		
Pathological N stage		Adjuvant hormone therapy**	
0	13 (2.5)	Yes	390 (76.2)
1	187 (36.5)	No	122 (23.8)
2	193 (37.7)		
3	119 (23.2)		
Age		Additional regional RT	
<40	63 (12.3)	Axilla RT	78 (15.2)
40-60	349 (68.2)	IMN RT	20 (3.9)
>60	100 (19.5)		
Median age	51		
Risk group		Margin status	
Early stage	160 (31.2)	Negative	457 (89.3)
Locally advanced	352 (68.8)	Positive	23 (4.5)
		N/A	32 (6.2)

Abbreviations: N, numbers; N/A, not available; IDC, invasive ducal carcinoma; ILC, invasive lobular carcinoma; SLND, sentinel lymph node dissection; LND, lymph node dissection;
* All HER-2 positive patients received anti HER-2 treatment
** 97.5% of ER+ patients received any hormone therapy
*** Taxane and Adriamycin use % was calculated from patients received chemotherapy
$ The total of 116 patients includes two initially HER2 2+ patients who received anti-HER2 treatment but were later confirmed as HER2-negative by FISH and discontinued treatment.

doi:10.6342/NTU202504448

2.3.2 CLINICAL OUTCOMES AND PROGNOTISC FACTORS

Between 2009 a With a median follow-up duration of 121.1 months (95% confidence interval [CI]: 26.6 to 161.8 months), the 10-year LRFS, DFS, and OS rates were 83.1%, 75.5%, and 87.9%, respectively. Survival outcomes differed among molecular subtypes, with differences observed in DFS ($p = 0.036$) and OS ($p = 0.006$), while LRFS did not show statistically significant variation ($p = 0.061$), as shown in **Figure 2-1**.

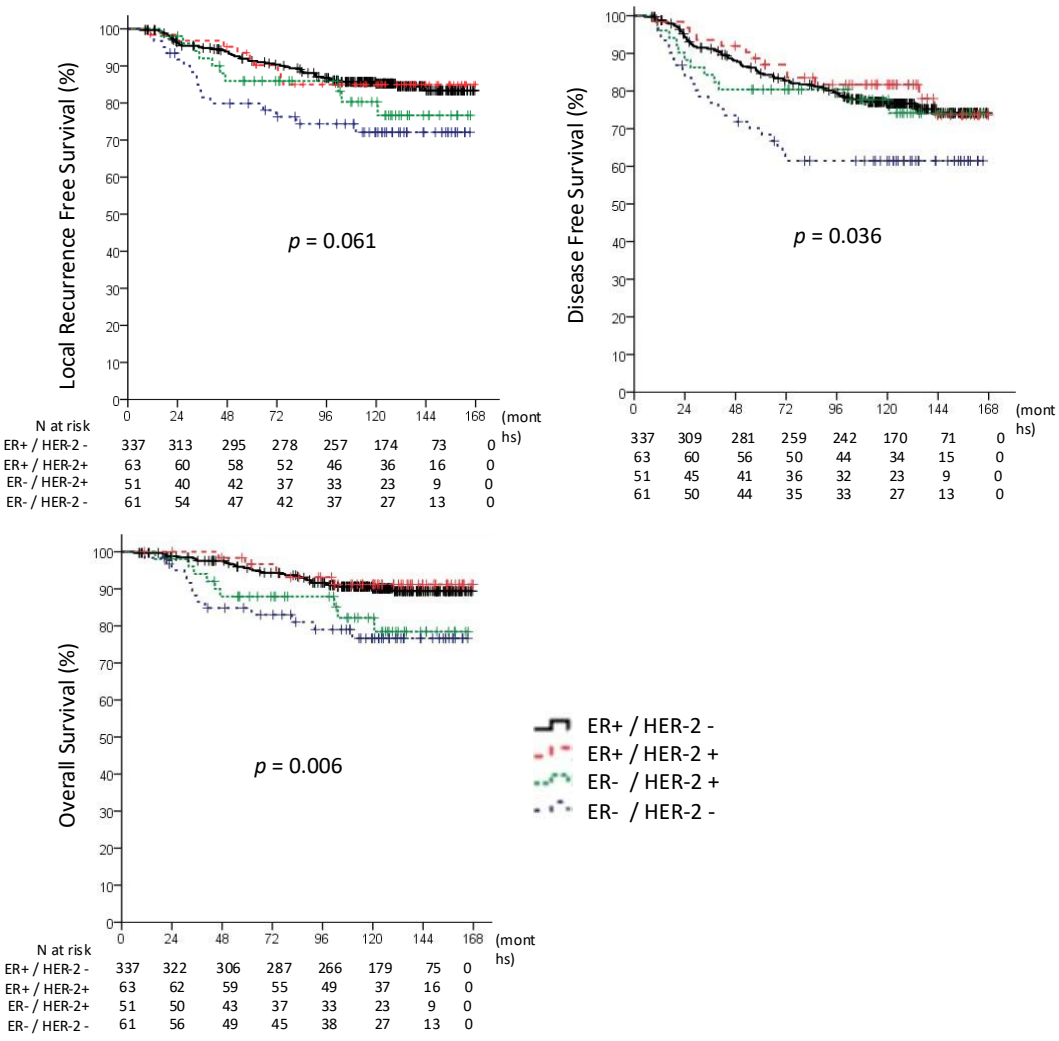

Figure 2-1 Locoregional recurrence-free survival, disease-free survival, and overall survival for patients with different molecular subtypes.

Among the subtypes, ER-negative/HER2-negative (TNBC) patients had the poorest outcomes, with 10-year LRFS, DFS, and OS rates of 72.1%, 61.4%, and 76.6%, respectively. Conversely, ER-

doi:10.6342/NTU202504448

positive/HER2-negative patients demonstrated the most favorable survival, with corresponding rates of 85.2% (LRFS), 81.7% (DFS), and 90.1% (OS). Patients in the ER-positive/HER2-positive and ER-negative/HER2-positive groups, both of whom received anti-HER2 therapy, had comparable 10-year outcomes (LRFS: 85.0% vs. 80.3%, DFS: 81.7% vs. 77.7%, and OS: 91.2% vs. 82.2%, respectively). There were no statistically significant differences in pathological T stage (p = 0.812) or N stage (p = 0.161) across the molecular subtypes (**Table 2-2**, and **Table 2-3**).

Table 2-2 Distribution of T stage among all molecular subtypes

	Molecular Subtypes N (% of pT stage among each subtypes)				
T stage	ER+/HER2-	ER+/HER2+	ER-/HER2+	ER-/HER2-	Total
pT0	2 (0.6)	2 (3.2)	1 (2.0)	1 (1.6)	6 (1.2)
pT1	78 (23.1)	13 (20.6)	16 (31.4)	16 (26.2)	123 (24.0)
pT2	170 (50.4)	30 (47.6)	26 (51.0)	29 (47.5)	255 (49.8)
pT3	73 (27.1)	15 (23.8)	5 (9.8)	12 (19.7)	105 (20.5)
pT4	6 (1.8)	1 (1.6)	1 (2.0)	2 (3.3)	10 (2.0)
pTx	8 (2.4)	2 (3.2)	2 (3.9)	1 (1.6)	13 (2.5)
Total	337 (100.0)	63 (100.0)	51 (100.0)	61 (100.0)	512 (100.0)

The Pearson's chi-squared test P = 0.812 (two-tail)

Table 2-3 Distribution of N stage among all molecular subtypes

	Molecular Subtypes N (% of pN stage among each subtypes)				
N stage	ER+/HER2-	ER+/HER2+	ER-/HER2+	ER-/HER2-	Total
pN0	10 (3.0)	0 (0.0)	1 (2.0)	2 (3.3)	13 (2.5)
pN1	130 (38.6)	20 (31.7)	12 (23.5)	25 (41.0)	187 (36.5)
pN2	129 (38.3)	27 (42.9)	21 (41.2)	16 (26.2)	193 (37.7)
pN3	68 (20.2)	16 (25.4)	17 (33.3)	18 (29.5)	119 (23.2)
Total	337 (100.0)	63 (100.0)	51 (100.0)	61 (100.0)	512 (100.0)

The Pearson's chi-squared test P= 0.161 (two-tail)

In this study, only 20 patients (3.9%) received internal mammary node radiotherapy (IMN-RT), the majority of whom (15 patients) had pN2 or N3 disease. However, there was no significant difference in the 10-year DFS rate between those who underwent IMN-RT (78.5%) and those who did

doi:10.6342/NTU202504448

not (75.4%; $p = 0.747$). Given the limited number of patients receiving IMN-RT, we compared our cohort's characteristics with those in previous trials (**Table 2-4**).

Our study population was similar to the KROG-0806 trial[88], as both had a high proportion of T1-2 tumors (87.4% in KROG vs. 73.8% in our study) and a comparable proportion of N1 disease (41.4% vs. 36.5%). Both studies also incorporated modern systemic therapies, including taxane-based chemotherapy. By contrast, earlier trials such as the French study and EORTC 22922/10925[81] included patients from an earlier treatment era, leading to worse oncologic outcomes than those observed in more recent trials, such as MA-20[80] and KROG.

In our study, patients with early-stage disease (T1-2, N0-1) who received RNI to the SCF but not to the IMNs had 7-year and 10-year DFS rates of 85.9% and 84.2%, respectively. These results were comparable to the 10-year DFS rate (82%) reported in the MA-20 trial for patients who received SCF irradiation with IMN-RT, suggesting that IMN-RT may not provide a substantial additional benefit in this subgroup.

doi:10.6342/NTU202504448

Table 2-4 Comparison of Major Investigations Addressing Internal Mammary Nodes Irradiation and Current Study

	French Trial	EORTC 22922	MA20 (Ref. 4)	DBCG-IMN	KROG-0806	Current Study
Enrollment date	1991-1997	1996-2004	2000-2007	2003-2007	2008-2020	2008-2014
Number of Patients	1334	4004	1832	3089	735	512
Patient criteria	MRM with pN+ or central/medial tumor	BCS or mastectomy, central/medial primary tumor N0/+, lateral tumor with N+ Exclude cT4, N3	BCS only; N+ or N- with high risk factor Exclude cT4, N2-3	BCS or mastectomy, pN+	BCS or mastectomy with ALND, pN+	BCS or mastectomy, pN+ or T3N0
Intervention	PMRT with SCF/axilla +/- IMN RT	Breast/CW RT +/- RNI (IMN, SCF)	Breast RT +/- RNI (IMN, SCF, high axilla)	Right side: RNI + IMN RT Left side: RNI, no IMN RT	Breast/CW RT + RNI (SCF) + /- IMN RT	Breast/CW RT + RNI (SCF +/- Axilla RT) +/- IMN RT
Patient characteristics						
T1-2 percentage	85%	95%	99%	94%	87.4%	73.8%
N0-1 percentage	N0 25%, N1 44%	N0 44%, N1 43%	N0 9.7%, N1 85%	No N0 pts, N1 59%	No N0 pts, N1 41.4%	N0 2.5%, N1 36.5%
ER+ percentage	50%	29% hormone therapy	75%	80%	71.3%	78.1%
chemotherapy	61%	25%	91%	18%	98.9%	95.9%
Taxane use percentage	Not reported	Not reported	25%	Not reported	95.6%	89.8%
Central Medial lesion	64%	Not reported	38%	40%	41.6%	45.7%
HER-2 positive percentage	Not reported Not reported	Not reported Not reported	Not reported Not reported	Not reported Not reported	22.3% 22.2%	22.3% 22.7%

doi:10.6342/NTU202504448

HER-2 targeted therapy						
Intervention / Control						
OS	10-yr 62.6% / 59.3%	15-yr 73.1% / 70.9%	10-yr 82.8% / 81.8%	15-yr 60.1% / 55.4%*	7-yr 89.4% / 82.2%	10-yr 94.1% / 87.3%
DFS	10-yr 53.2% / 49.9%	15-yr 60.8% / 59.9%	10-yr 82.0% / 77.0%*	Not reported	7-yr 85.3% / 81.9%	10-yr 78.5% / 75.4%
Breast cancer mortality	Not reported	15-yr 16.0% / 19.8%*	10-yr 10.3% / 12.3%	15-yr 31.7% / 33.9%*	7-yr 8.4% / 10.8%	10-yr 5.9% / 10.5%
DMFS	Not reported	15-yr 70.0% / 68.2%	10-yr 86.3% / 82.4%*	15-yr DM 35.6%/38.6%*	7-yr 85.8% / 83.2%	10-yr 83.8% / 78.1%
LRR (event percentage)	9.2% / 9.8%	8.3% / 9.5%	4.3 % / 6.8%*	Not reported	2.2% / 4.3%	10% / 7.5%
Toxicity (Intervention Control)	No difference in Gr 3/4 toxicity or cardiac event	Lung fibrosis 5.1/2.3% Cardiac fibrosis 2.0/1.1% Heart disease 8.6/7.2%	>Gr 2Lung 0.4/0.3% >Gr 2 Heart 0.4/0.4% Lymphedema 8.4/4.5% Telangiectasia 6.9/4.3% Fibrosis 4.1/2.0%	Cardiac death 0.6% in both groups.	Arm edema 24.0/22.3% Cardiac event 2.2/1.3% Tissue fibrosis 1.4/1.3% Pneumonitis 6.5/3.3%	8% have lymph edema after RT.
Subgroup analysis	Medial/central tumors and pN+ benefit more from IMNRT in OS	No special subgroups benefit more from RNI	ER negative pts received RNI had better OS than control group	Neither medial or lateral lesions benefit from IMN RT more	Medial/central group have DFS, DMFS, and breast cancer mortality benefit	No special subgroups benefit more from IMNRT

Abbreviations: N, nodal status; N/A, ER, estrogen receptor; RNI, regional nodal irradiation, IMN, internal mammary node; SCF, supraclavicular fossa; PMRT, post mastectomy radiotherapy; CW, chest wall; BCS, breast conservative surgery; ALND, axillary lymph node dissection; LND, lymph node dissection; RT; radiotherapy; IMN, internal mammary nodes; RT, radiotherapy; OS, overall survival; DFS, disease free survival; DMFS, distant metastasis free survival; LRR, local regional recurrence. * Statistically significant.

* All HER-2 positive patients in the current study received anti HER-2 treatment

doi:10.6342/NTU202504448

Additionally, this study cohort demonstrated similarities with the KROG-0806 trial, particularly in patient characteristics. The proportion of T1-2 tumors was 87.4% in KROG and 73.8% in this study, while the percentage of N1 disease was 41.4% and 36.5%, respectively. Both studies predominantly involved Asian populations and incorporated modern systemic therapies, with a high prevalence of taxane-based chemotherapy (95.6% in KROG vs. 89.8% in this study). The 7-year DFS rates in the KROG-0806 trial (85.3% vs. 81.9% for IMN-RT vs. no IMN-RT) were also consistent with the 10-year DFS outcomes observed in this study (78.5% vs. 75.4%), suggesting a comparable disease trajectory in both cohorts.

To further examine the potential impact of IMN-RT while addressing the small sample size and potential confounders, a propensity score matching (PSM) analysis was conducted. Patients who underwent IMN-RT were matched with those who did not, based on tumor (T) stage, nodal (N) stage, histologic grade, and molecular subtype, yielding 17 patient pairs with well-balanced baseline characteristics. In this matched cohort, the 10-year LRFS rates were 79.0% for the IMN-RT group and 93.8% for those without IMN-RT ($p = 0.308$), while the 10-year DFS rates were 74.3% and 86.5%, respectively ($p = 0.388$) (**Figure 2-2**). These findings indicated no statistically significant differences in LRFS or DFS between the two groups, aligning with the results of the overall cohort analysis.

While PSM analysis helps minimize confounding and enhances the reliability of the comparison, the small sample size of the matched cohort limits the statistical power of the findings. Thus, further

doi:10.6342/NTU202504448

validation through larger prospective studies is necessary to draw definitive conclusions regarding the role of IMN-RT in regional nodal irradiation strategies.

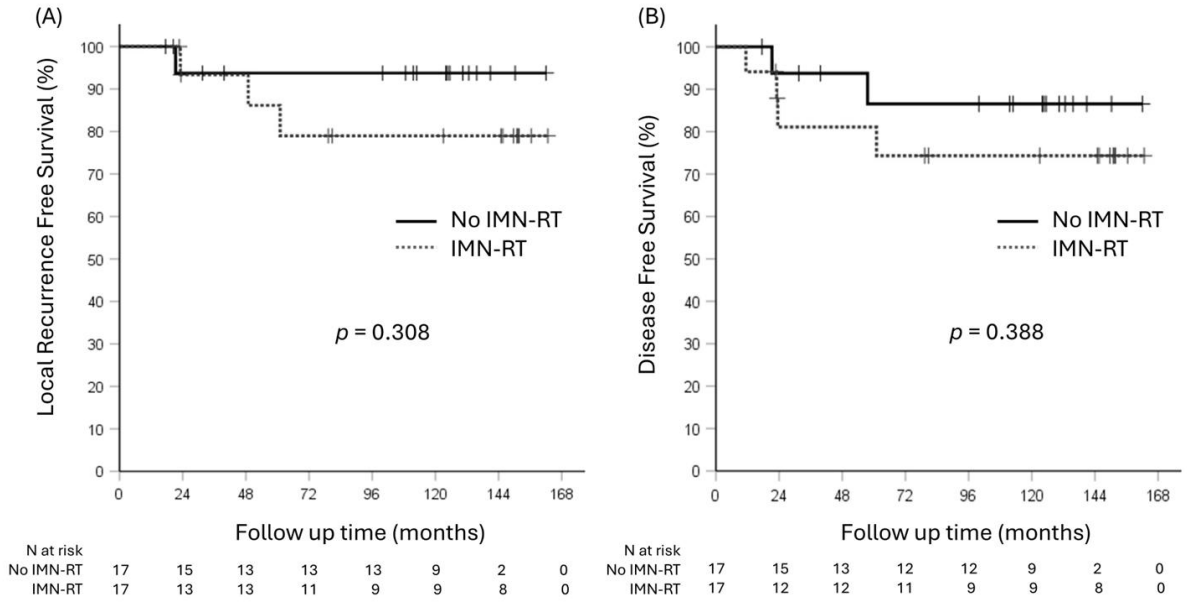

Figure 2-2 (A) Locoregional recurrence-free survival and (B) disease-free survival among patients who underwent internal mammary node radiotherapy (IMN-RT) compared to those who did not in propensity score mathching.

2.3.3 CLINICAL OUTCOMES FOR PATIENTS WHO RECEIVED ALRT

In our institutional approach, ALRT in combination with SCF-RT was typically administered to patients with pathological N3 disease or those deemed to have a high recurrence risk. Overall, patients who received ALRT in addition to SCF-RT exhibited a lower 10-year DFS rate compared to those who did not (66.1% vs. 77.2%; $p = 0.035$). This disparity may be attributed to differences in nodal burden, as among the 78 patients who underwent ALRT, 70 (89.7%) had pathological N3 disease. To

doi:10.6342/NTU202504448

ensure a more accurate comparison with fewer confounding factors, the analysis was refined to focus on pathological N3 patients, who comprised the majority of the ALRT group. Within this subgroup, the 10-year LRFS and DFS rates were similar between those who received ALRT and those who did not (LRFS: 67% vs. 81.7%, $p = 0.153$; DFS: 62.3% vs. 64.9%, $p = 0.789$; **Figure 2-3**).

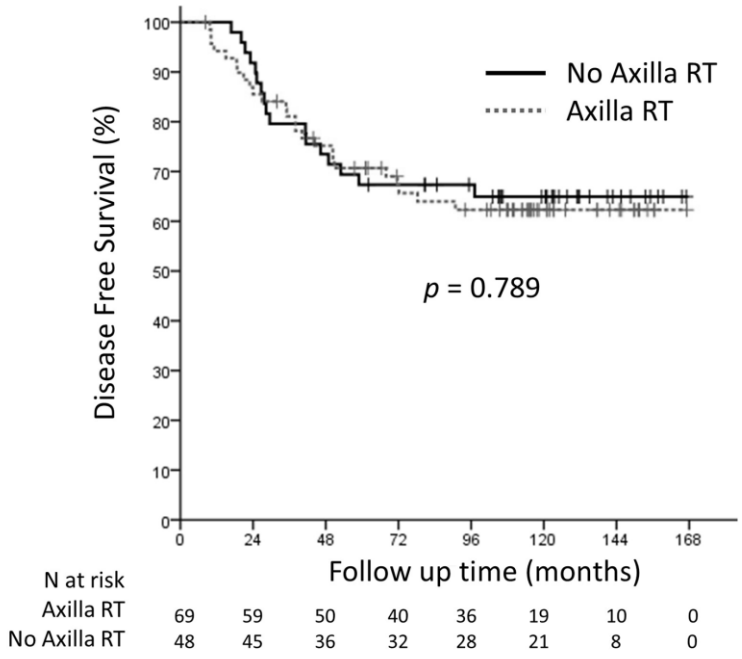

Figure 2-3 Disease-free survival for patients with pathological N3 status who underwent axillary radiotherapy or not.

A subgroup analysis of DFS within the pathological N3 cohort suggested a potential benefit of ALRT in ER-positive patients (HR = 0.662; 95% CI = 0.311–1.408) but not in ER-negative patients, where ALRT appeared to be associated with poorer DFS (HR = 2.958; 95% CI = 0.832–10.523). However, due to the low event rate in the ER-negative group, these findings did not achieve statistical significance. Notably, patients with ER-negative/HER2-negative (TNBC) disease derived no benefit

doi:10.6342/NTU202504448

from ALRT, and in fact, ALRT was linked to a worse DFS outcome (HR = 5.324; 95% CI = 1.104–25.684). The subgroup analysis was shown in **Figure 2-4**.

To further explore the effect of ALRT on DFS, univariate and multivariate analyses were conducted, adjusting for tumor grade, pathological T and N stage, surgical approach, molecular

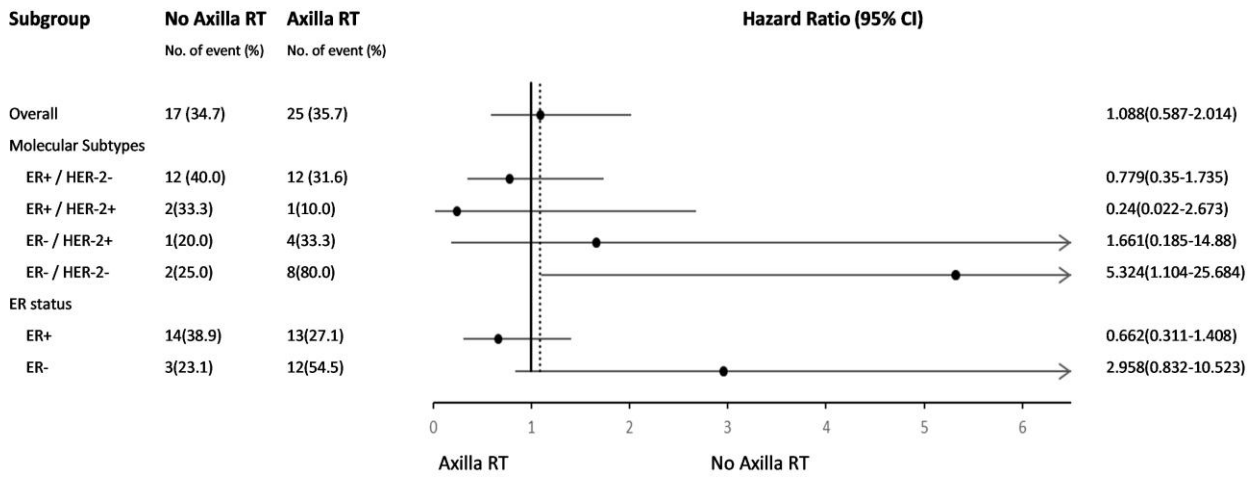

Figure 2-4 Subgroup analysis of DFS in patients with pathological N3 disease, comparing those who received axillary radiotherapy (ALRT) versus those who did not.

subtype, and systemic treatment. The univariate analysis (Table 3) identified several factors correlated with worse DFS, including grade III tumors (p = 0.003), higher pathological N stage (p = 0.002), mastectomy (p = 0.007), ALRT administration (p = 0.037), locally advanced disease (p = 0.004), and ER-negative/HER2-negative status (p = 0.007). However, multivariate analysis (Table 3) revealed that ALRT was not an independent predictor of DFS when adjusted for these variables (HR = 1.060; 95% CI = 0.578–1.944; p = 0.850). The subgroup analysiss

doi:10.6342/NTU202504448

Interestingly, tumor grade III remained the only significant factor influencing DFS in multivariate analysis (HR = 2.320; 95% CI = 1.107–4.862; p = 0.026), underscoring its strong impact on prognosis. Additionally, ER-negative/HER2-negative disease was associated with poorer DFS (HR = 1.454; 95% CI = 0.874–2.419; p = 0.150), reinforcing the aggressive nature of this subtype, regardless of ALRT use. These findings further suggest that ALRT may have a limited role in improving outcomes for high-risk patients, particularly those with biologically aggressive tumor subtypes, highlighting the need for alternative treatment strategies in this population.

2.4 DISCUSSION

This retrospective study evaluated the long-term clinical outcomes of breast cancer patients who underwent RNI, with a median follow-up of 10 years. Our findings revealed variations in survival based on molecular subtypes, with ER-negative/HER2-negative (TNBC) patients exhibiting the poorest survival rates. Additionally, early-stage lymph node-positive breast cancer patients who did not receive IMN-RT had outcomes comparable to those reported in previous trials that included IMN-RT[80, 86]. Furthermore, the DFS of patients with extensive LN involvement (pN3 disease) was assessed based on the use of ALRT. Our analysis indicated that ALRT did not improve DFS, and stratification by molecular subtype suggested that ER-positive patients might benefit more from ALRT than those with ER-negative disease.

doi:10.6342/NTU202504448

The management of breast cancer has undergone significant changes with the growing understanding of molecular subtypes and targeted treatment approaches[19]. However, major RNI trials[80, 81, 89, 90] were conducted before the widespread adoption of modern systemic therapy, limiting their ability to assess the impact of biological subtypes on radiation outcomes. A large cohort study demonstrated that molecular classification serves as a predictor for locoregional recurrence[6], while previous research found inferior survival in TNBC and HER2-enriched subtypes compared to luminal breast cancer[91]. Consistent with these observations, our study found that patients with TNBC had the lowest LRFS, DFS, and OS. Meanwhile, patients with HER2-positive disease who received anti-HER2 therapy achieved survival rates comparable to those with ER-positive/HER2-negative breast cancer. This aligns with findings by Tseng *et al*.[91], who reported that HER2-positive patients treated with trastuzumab had lower 5-year locoregional recurrence rates than those with luminal A and B breast cancer. These results underscore the transformative impact of targeted therapy on HER2-positive disease, though further studies are needed to evaluate whether adjuvant radiotherapy can be optimized based on systemic treatment response.

The IMN-RT debate remains unresolved, despite decades of research[82]. Proponents argue that clinical trials demonstrating the benefits of RNI[80, 87] included IMN-RT in their treatment plans[83]. However, critics highlight that postmastectomy RT trials, including MA-20 and EORTC 22922/10925, demonstrated the benefits of RNI, particularly SCF-RT, but not the direct benefits of IMN-RT. Furthermore, studies specifically evaluating IMN-RT[85, 86] failed to show a statistically significant

doi:10.6342/NTU202504448

advantage. The potential for radiation-induced toxicity also raises concerns regarding IMN-RT. While the MA-20 trial reported no significant increase in grade 2 cardiac or pulmonary toxicity, the EORTC 22922/10925 trial found higher rates of lung and heart fibrosis in patients receiving RNI. Similarly, the KROG trial reported a higher incidence of radiation pneumonitis in the IMN-RT group, reinforcing the delicate risk-benefit balance in determining its use for early-stage LN-positive breast cancer.

The interpretation of IMN-RT outcomes is further influenced by systemic therapy advancements and follow-up duration. The French and KROG trials[85, 86] suffered from limitations such as suboptimal systemic therapy or insufficient follow-up, leading to inconclusive results regarding IMN-RT efficacy. Our study, conducted in the era of modern systemic treatments, fills this gap. Nearly all patients received hormone therapy, anthracycline- and taxane-based chemotherapy, and HER2-targeted therapy (**Table 2-1**). Evidence from the early 2000s demonstrated that taxane-based chemotherapy improved 5-year DFS and OS by 5% and 3%, respectively, while trastuzumab significantly enhanced DFS and OS in HER2-positive patients in the BCIRG-006 trial[92]. However, RNI's role in the modern treatment landscape remains unclear. At our institution, IMN-RT is rarely administered unless IMN involvement is confirmed. Among the 20 patients who received IMN-RT, DFS was not significantly different from those who did not undergo IMN-RT, even after propensity score matching. Importantly, patients in our study who did not receive IMN-RT achieved DFS rates comparable to historical cohorts that did receive IMN-RT (**Table 2-4**). This suggests that IMN-RT

doi:10.6342/NTU202504448

may not be necessary for early-stage LN-positive patients receiving optimal systemic therapy. Since no trials have demonstrated an OS benefit of IMN-RT, it may be reasonable to omit IMN-RT in carefully selected patients without compromising long-term disease control.

Another key aspect of this study is ALRT, which was not routinely included in early RNI trials. In the EORTC 22922/10925 trial, ALRT was only administered if fewer than 10 LNs were removed or if more than three nodes were positive. The AMAROS trial remains the only randomized study comparing ALRT to ALND, showing comparable efficacy[93]. However, patients receiving both ALND and ALRT experienced significantly higher lymphedema rates compared to those undergoing ALND or ALRT alone (5-year rates: 58.3% vs. 24.5% vs. 11.9%).

Unlike prior studies, this analysis specifically assessed the role of ALRT in pN3 disease, where over half of patients received ALRT. However, ALRT did not improve LRFS, DFS, or OS. Subgroup analysis suggested worse DFS in ER-negative/HER2-negative patients who received ALRT, though the low event rate prevented statistical significance. This should be interpreted cautiously, as it does not conclusively indicate harm. Conversely, ER-positive patients showed a trend toward improved DFS with ALRT, suggesting that hormone receptor-positive disease may respond better to locoregional therapy. This aligns with the hypothesis that ER-positive tumors, which typically exhibit slower progression, may benefit from more aggressive local interventions. Tseng *et al*.[91] previously reported that luminal A and B subtypes had lower locoregional recurrence rates after PMRT compared

doi:10.6342/NTU202504448

to TNBC, supporting the idea that RNI may be more beneficial in hormone receptor-positive cancers. Based on this and our findings, we hypothesize that ER-positive/N3-stage patients may benefit more from RNI (including SCF-RT and ALRT) by achieving longer locoregional control. The KROG-0806 trial, which included a comparable population, did not specify ALRT rates, limiting the ability to directly assess its contribution to survival. Moving forward, careful selection of patients for ALRT should consider nodal burden, surgical approach, and tumor biology.

This study has several limitations, including selection bias and its retrospective nature, which may limit its ability to fully address the role of RNI, particularly IMN-RT and ALRT. Most patients in this cohort received SCF-RT as part of RNI, and their clinical outcomes were similar to those in the MA-20 trial, where both SCF-RT and IMN-RT were used. This may be attributed to the widespread use of modern systemic therapies, including taxane-based regimens and HER2-targeting agents. While this study did not incorporate progesterone receptor status or Ki-67 index, it identified ER-negative/HER2-negative disease as a significant predictor of poor survival. Future research should explore personalized radiation approaches based on molecular subtypes and genetic markers[94] to refine systemic therapy and optimize radiotherapy strategies.

2.5 SUMMARY

This study demonstrated that SCF-RT alone provided comparable outcomes to historical RNI (SCF-RT plus IMN-RT) cohorts, aligning with findings from the KROG-0806 trial. These results

doi:10.6342/NTU202504448

suggest that IMN-RT may be safely omitted in early-stage LN-positive patients receiving modern systemic therapy. Additionally, ALRT did not improve outcomes in ER-negative/pN3 patients, indicating that more intensive systemic therapy may be preferable to extensive radiotherapy fields in high-risk cases.

doi:10.6342/NTU202504448

CHAPTER 3. RADIOSENSITIZING EFFECTS OF CDK4/6 INHIBITORS IN HORMONE POSITIVE AND HER2-NEGATIVE BREAST CANCER

3.1 INTRODUCTION

In Chapter 2, we understood the role of radiotherapy in breast cancer, and the RT impact seems to be higher in ER+/HER2- breast cancer. Although this type of breast cancer is associated with a relatively favorable prognosis. However, patients with luminal-type breast cancer are known to have a higher risk of late recurrence[12].

The cyclin-dependent kinases 4 and 6 (CDK4/6) are essential regulators of cell cycle progression, governed by cyclin D1/D2/D3 and inhibited by tumor suppressors such as p16INK4A as described in Chapter 1. When activated, the cyclin D–CDK4/6 complex phosphorylates the Rb leading to the release of E2F transcription factors, which in turn facilitate cell cycle transition from the G1 to S phase. Dysregulation of this pathway has been implicated in multiple solid tumors, making CDK4/6 inhibition an attractive therapeutic strategy[39-41]. In preclinical models, the CDK4/6-cyclin D axis has been found to play a pivotal role in breast tumorigenesis, with cyclin D1 overexpression frequently observed in breast cancer and linked to ER positivity[43, 44].

The clinical success of CDK4/6 inhibitors in combination with endocrine therapy exemplifies the potential of targeted combination treatments[14]. Palbociclib, when paired with letrozole, has

doi:10.6342/NTU202504448

demonstrated a significant OS benefit in patients with ER+, HER2- advanced breast cancer[13]. Other CDK4/6 inhibitors, including ribociclib and abemaciclib, have also achieved remarkable results in ER+, HER2- breast cancer[50]. A study by Hortobagyi *et al*. found that patients receiving ribociclib plus letrozole had a longer median OS compared to those receiving a placebo plus letrozole (63.9 months vs. 51.4 months, $P = 0.008$)[95]. Similarly, the monarchE trial demonstrated a superior 4-year invasive disease-free survival (IDFS) rate in patients treated with abemaciclib plus endocrine therapy versus endocrine therapy alone (85.8% vs. 79.4%, $P < 0.0001$) for node-positive, HR-positive, HER2-negative early breast cancer. Notably, in this trial, adjuvant RT preceded abemaciclib treatment, but the safety and efficacy of concurrent RT and abemaciclib were not assessed.

The rationale of combining RT with CDK4/6 inhibitors have been described in Chapter 1. This chapter aims to assess whether CDK4/6 inhibitors can sensitize HR-positive, HER2-negative breast cancer cells to RT using both in vitro and in vivo models. Additionally, we seek to elucidate the molecular mechanisms underlying this combination therapy, providing insights that may support its clinical application and expand treatment options for this subtype of breast cancer.

3.2 MATERILS AND METHODS

3.2.1 BREAST CANCER CELL LINES AND CULTURE CONDITIONS

To examine whether CDK4/6 inhibitors enhance radiosensitivity, we utilized HR-positive, HER2-negative breast adenocarcinoma cell lines, MCF-7 and T-47D. These cell lines were obtained

doi:10.6342/NTU202504448

from the American Type Culture Collection (ATCC) (MCF-7: HTB-22™, T-47D: HTB-133™). The HR-positive, HER2-negative status of both cell lines was confirmed (Supplementary Materials). Cells were maintained under standard culture conditions at 37°C with 5% CO_2. MCF-7 cells were grown in Dulbecco's Modified Eagle Medium (DMEM), whereas T-47D cells were cultured in Roswell Park Memorial Institute (RPMI) 1640 medium (Gibco).

3.2.2 CDK4/6 INHIBITORS AND IONIZAING RADIATION

Ribociclib (Med Chem Express, catalog no. HY-15777A) and palbociclib (Sigma, catalog no. PZ0199) were prepared in 100% dimethyl sulfoxide (DMSO) at an initial concentration of 10 mmol/L for functional and radiosensitivity assessments. Ionizing radiation (IR) was administered using a Cs137 irradiator at a dose rate of 3 Gy/min.

3.2.3 COLONOGENIC ASSAY

To determine radiosensitivity, MCF-7 and T-47D cells were seeded at 2000 cells per well in six-well plates. One hour before irradiation, cells were treated with ribociclib or palbociclib. The radiation doses ranged from 0 to 4 Gy, and the culture medium was left unchanged until the end of the experiment. After 7–14 days, colonies consisting of ≥50 cells were counted under an inverted phase-contrast microscope (100× magnification). The combination index (CI) was calculated using the Chou–Talalay method[96].

3.2.4 FLOW CYTOMETRY

doi:10.6342/NTU202504448

To evaluate apoptotic cell death, MCF-7 and T-47D cells were treated with various doses of rand CDK4/6 inhibitors (ribociclib or palbociclib). After 24 hours, cells were harvested, washed with cold PBS, and resuspended in Annexin V binding buffer (BD Biosciences, San Diego, CA, USA).

Cells were then stained with FITC-conjugated Annexin V (cat. 556547, BD Biosciences) and propidium iodide (PI) (cat. 556463, BD Biosciences) according to the manufacturer's instructions. The staining reaction was performed at room temperature in the dark for 15 minutes, followed by immediate analysis using an LSR II flow cytometer (BD Biosciences, San Diego, CA, USA).

To differentiate early apoptotic (Annexin V+/PI−), late apoptotic (Annexin V+/PI+), necrotic (Annexin V−/PI+), and viable (Annexin V−/PI−) cells, quadrant gating was set using unstained controls and single-stained compensation controls. FlowJo 10.1 software (Ashland, OR, USA) was used for data processing and analysis. Each experiment was performed in triplicate to ensure reproducibility..

3.2.5 CELL PROLIFERATION ASSAY

Cells were seeded into 96-well plates at a density of 1000 cells per well in 100 μL of medium, followed by treatment with varying concentrations of ribociclib or palbociclib. After 72 hours, cell proliferation was assessed using the CellTiter 96® Aqueous Non-Radioactive Cell Proliferation Assay (Promega, Madison, WI, USA). Absorbance was measured at 450 nm using a microplate reader, and the half-maximal inhibitory concentrations (IC50) were determined.

doi:10.6342/NTU202504448

3.2.6 IMMUNOFLUORESCENCE STAINING

Breast cancer cells were plated onto chamber slides (#30104, SPL Life Sciences, South Korea) and subjected to different treatment regimens. After fixation with 3.7% paraformaldehyde for 8 minutes, cells were blocked with 3% bovine serum albumin (BSA) containing 0.3% Triton X-100 at room temperature for 60 minutes. Primary antibodies against γH2AX (#9718, Cell Signaling Technology) and 53BP1 (ab172580, Abcam, UK) were incubated overnight at 4°C. Following secondary antibody incubation with Alexa Fluor 488-conjugated antibody, DAPI (#40043, Biotium, USA) was used for nuclear staining. Cells were mounted with fluorescent mounting medium (FMH030, ScyTek Laboratories, USA) and analyzed using a fluorescence microscope (IX71, Olympus, Tokyo, Japan).

3.2.7 WESTERN BLOT ANALYSIS

Protein lysates were prepared from MCF-7 and T-47D cells following treatment with RT alone, CDK4/6 inhibitors alone, or their combination. Proteins were extracted using Mammalian Protein Extraction Reagent (M-PER, Pierce, Rockford, IL, USA) and separated using 10% SDS-PAGE gel electrophoresis. The separated proteins were transferred onto nitrocellulose membranes (Novex, San Diego, CA, USA) and blocked overnight using Tris-buffered saline with 0.1% Tween (TBST) and 5% nonfat dry milk. After incubation with primary antibodies (listed in **Table 3-1**), blots were developed using peroxidase-conjugated secondary antibodies and visualized using an enhanced

doi:10.6342/NTU202504448

chemiluminescence (ECL) detection system (Boehringer Mannheim, Germany). Each western blot experiment was repeated three times to confirm reproducibility.

3.2.8 NF-κB ACTIVITY ASSAY

To assess NF-κB p65 DNA-binding activity, nuclear extracts were prepared from MCF-7 and T-47D cells treated with control, RT, ribociclib or palbociclib alone, or their combination. The NF-κB p65 transcription factor assay kit (ab133112, Abcam, USA) was used according to the manufacturer's protocol. Briefly, nuclear extracts were added to the wells and incubated for 1 hour or overnight, followed by washing and primary NF-κB antibody incubation. After additional washing steps, samples were treated with an HRP-conjugated secondary antibody, and color development was achieved using a developing solution incubated for 15–45 minutes. The reaction was stopped using a stop solution, and absorbance was measured using a microplate reader.

3.2.9 IN VIVO MOUSE MODEL

Female BALB/cAnN.Cg-Foxn1nu/CrlNarl nude mice (5–6 weeks old) were purchased from BioLASCO Taiwan Co., Ltd. All animal procedures were approved by the Institutional Animal Care and Use Committee (IACUC) of National Taiwan University College of Medicine and College of Public Health (IACUC No. 20210366). Mice were implanted with 17β-estradiol pellets (0.72 mg/pellet, 60-day release, Innovative Research of America) to enhance breast cancer cell engraftment[97].

doi:10.6342/NTU202504448

For tumor implantation, MCF-7 cells were mixed with Matrigel and injected orthotopically (100 μL of 1×10^7 cells/mL per mouse). Tumor dimensions were measured using calipers, and volumes were calculated using the formula:

$$\text{Tumor volume} = \pi/6 \times L \times W \times H$$

where L = length, W = width, and H = height. When tumors reached approximately 100 mm^3, mice were randomly assigned to four groups: control, ribociclib alone, RT alone, and combination therapy (ribociclib + RT). Radiation (2 Gy per session, total 6 Gy) was delivered every other day using a Cs137 irradiator, and ribociclib was administered orally (200 mg/kg daily, days 1–5). RT was performed 2 hours after ribociclib administration.

3.2.10 IMMUNOHISTOCHEMISTRY STAINING

Tumor specimens were washed with 1X PBS, fixed in 4% formaldehyde, and embedded in paraffin. Sections were cut at 6-μm thickness, deparaffinized, and incubated with primary antibodies, including p-NF-κB p65 (ab86299, Abcam), p-ERK (#4376S, Cell Signaling Technology), and c-Myc (SC-40, Santa Cruz Biotechnology, USA). Visualization was performed using the indirect immunoperoxidase method as per the manufacturer's protocol.

3.2.11 STATISTICAL ANALYSIS

doi:10.6342/NTU202504448

All quantitative data were presented as mean ± standard error of the mean (SEM). The statistical test used for each dataset is specified in the corresponding figure legend. A p-value < 0.05 was considered statistically significant, with p-values represented as follows: $P < 0.05$, $P < 0.01$, $P < 0.001$. Statistical analyses were conducted using GraphPad Prism software (version 9.0.0, GraphPad Software, Inc.), which was also used for data visualization.

doi:10.6342/NTU202504448

Table 3-1 Key resources

REAGENT or RESOURCE	SOURCE	IDENTIFIER
ribociclib	Med Chem Express	Cat#: HY-15777A
palbociclib	Sigma	Cat#: PZ0199
17β-extradiol pellet	Innovative Research of America	0.72 mg/pellet, 60-day release
Antibodies		
γH2AX	Cell Signaling	Cat#: 9718
53BP1	Abcam	Cat#: ab172580
DAPI	Biotium	Cat#: 40043
DNA-PKcs	Cell Signaling	Cat#: 4602S
p-DNA-PKcs	Cell Signaling	Cat#: 68716S
ERK	Cell Signaling	Cat#: 9102S
p-ERK	Cell Signaling	Cat#: 4376S
c-Myc	Santa Cruz Biotechnology	Cat#: SC-40
RB	Cell Signaling	Cat#: 9309S
p-RB	Cell Signaling	Cat#: 8516S
cleaved caspase 3	Cell Signaling	Cat#: 9664S
ATM	Cell Signaling	Cat#: 2873S
p-ATM	Cell Signaling	Cat#: 13050S
Rad-51	Cell Signaling	Cat#: 8875
vinculin	Cell Signaling	Cat#: 13901
p-NF-κB p65	Abcam	Cat#: ab86299
Critical commercial assays		
CellTiter 96® Aqueous Non-Radioactive Cell Proliferation Assay	Promega	
NF-κB p65 transcription factor assay kit	Abcam	Cat#: ab133112
Experimental models: Cell lines and mice		
MCF-7	ATCC	ATCC® HTB-22™
T-47D	ATCC	ATCC® HTB-133™
BALB/cAnN.Cg-Foxn1nu/CrlNarl mice	BioLASCO Taiwan Co., Ltd.	
Software and algorithms		
GraphPad Prism	GraphPad Software, Inc	version 9.0.0
Biorender.com	Biorender.com	
Other		
Cs137 irradiator	In House	
Fluorescent microscope	In House	IX71, Olympus

doi:10.6342/NTU202504448

3.3 RESULTS

3.3.1 CDK4/6 INHIBITORS SENSITIZE HR-POSITIVE, HER2-NEGATIVE BREAST CANCER CELL TO RADIOTHERAPY

To examine whether CDK4/6 inhibitors enhance radiosensitivity, we utilized mouse HR-positive, HER2-negative breast adenocarcinoma cell lines, MCF-7 (ATCC® HTB-22™) and T-47D (ATCC® HTB-133™) in this experiment. These two cell lines both are ER positive and HER2 negative, presenting luminal type breast cancer behaviors.

To confirm the molecular subtype of MCF-7 and T-47D as hormone receptor-positive and HER2-negative, we conducted a comparative analysis using well-characterized breast cancer cell lines with distinct receptor profiles. The ER-negative, triple-negative cell line MDA-MB-231 (ATCC HTB-26™) and two HER2-overexpressing lines, ZR-75-30 (ATCC CRL-1504™) and SK-BR-3 (ATCC HTB-30™), were included for reference. As illustrated in **Figure 3-1**, MCF-7 and T-47D cells demonstrated positive ER expression, while MDA-MB-231 lacked ER expression. Furthermore, HER2 was not detected in MCF-7 and T-47D, in contrast to its strong expression in ZR-75-30 and SK-BR-3, confirming the HR-positive/HER2-negative phenotype of MCF-7 and T-47D cell lines.

doi:10.6342/NTU202504448

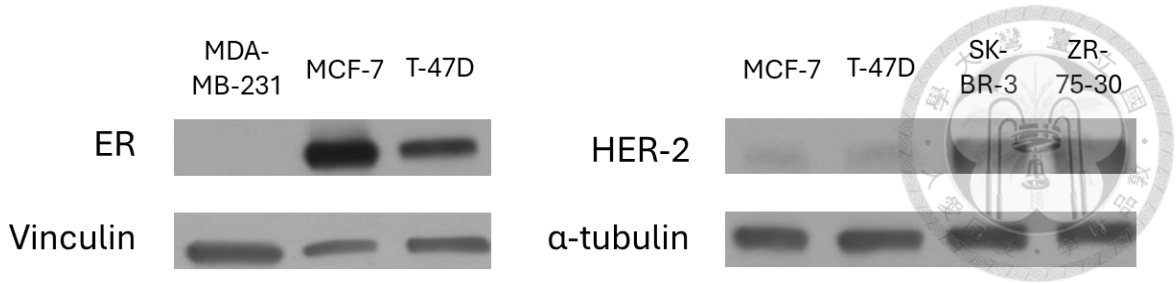

Figure 3-1 Verification of HR positivity and HER2 negativity using western blotting.

The selection of MCF-7 and T-47D cell lines for this study was based on several key considerations. First, both cell lines serve as well-established models of luminal-type breast cancer, characterized by HR positivity and HER2 negativity. Second, ribociclib and palbociclib—two clinically approved CDK4/6 inhibitors—are commonly used in the treatment of this breast cancer subtype and have demonstrated prolonged survival benefits with manageable toxicity in clinical trials[8, 95]. Third, the therapeutic impact of these inhibitors as single agents in HR-positive breast cancer models is well-supported by preclinical and clinical evidence[47, 98]. Finally, utilizing MCF-7 and T-47D allows us to closely model the clinical context and investigate whether CDK4/6 inhibition can potentiate the effects of radiotherapy in HR-positive, HER2-negative breast cancer.

We determined the half-maximal inhibitory concentrations (IC50) of ribociclib and palbociclib in these two cell lines using MTT assay. For MCF-7, the IC50 values were 17.09 μM for ribociclib and 2.33 μM for palbociclib, while for T-47D, the respective IC50 values were 26.12 μM and 34.22 μM. The dose–response curves illustrating the effects of both CDK4/6 inhibitors on these cell lines are presented in **Figure 3-2**.

doi:10.6342/NTU202504448

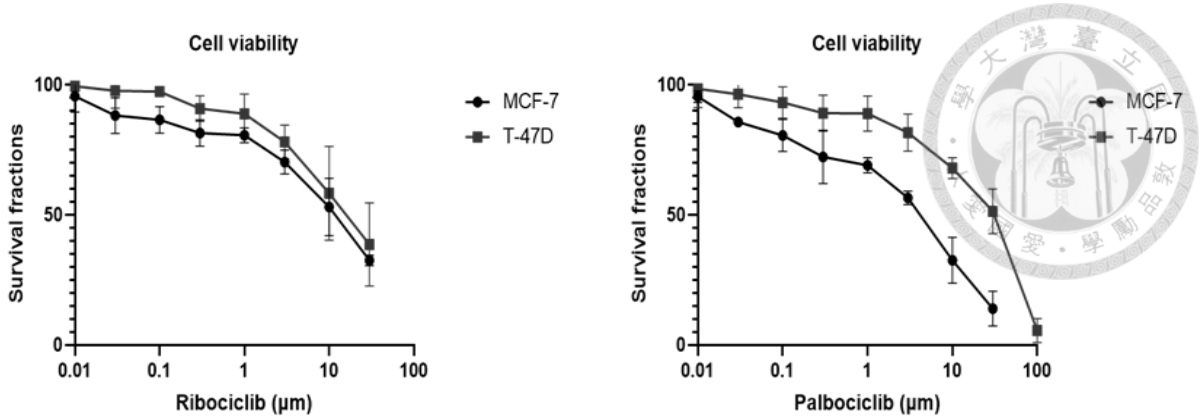

Figure 3-2 The concentration-response curves for the CDK4/6 inhibitors ribociclib and palbociclib in MCF-7 and T-47D cell lines.

To examine potential off-target effects on non-malignant cells, we included MCF-10A, a non-tumorigenic mammary epithelial cell line (ATCC CRL-10317™), as a model for normal breast tissue. Western blot analysis revealed that CDK4 expression was lower in MCF-10A compared to the cancer cell lines MCF-7 and T-47D (**Figure 3-3**). We then performed MTT assays to evaluate the cytotoxic effects of ribociclib and palbociclib (30 μM each) across the three cell types. Results showed a greater reduction in cell viability in MCF-7 and T-47D than in MCF-10A, indicating a selective antiproliferative effect of these inhibitors on malignant cells (**Figure 3-4**). Together, these data suggest that ribociclib and palbociclib preferentially inhibit tumor cell proliferation, with limited toxicity to normal breast epithelial cells, supporting their therapeutic safety profile in breast cancer management.

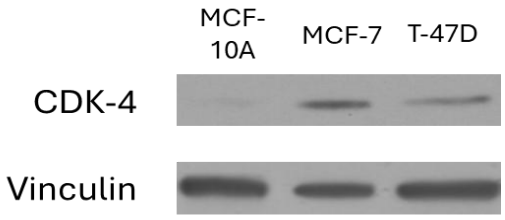

Figure 3-3 Western blot analysis of CDK4 expression in the MCF-10A, MCF-7, and T-47D cell lines

doi:10.6342/NTU202504448

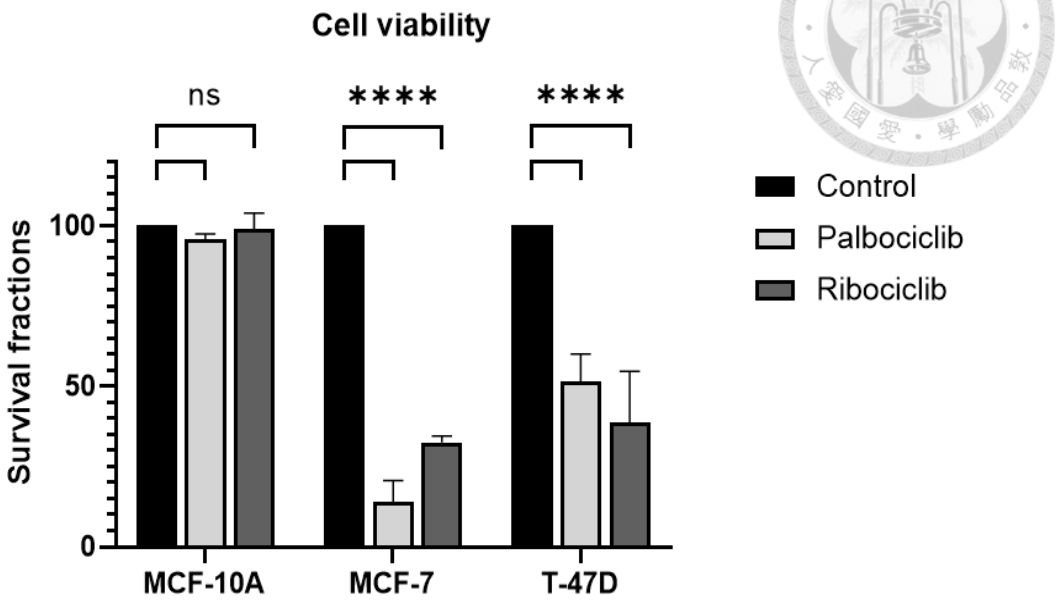

Figure 3-4 Cell viability was assessed with MTT assay for MCF-10A, MCF-7, and T-47D cell lines treated with control, palbociclib 30 μM or ribociclib 30 μM. ns, no significance. **** $P < 0.0001$.

To assess whether CDK4/6 blockade enhances radiosensitivity, we conducted clonogenic survival assays. Cells were pretreated for 1 hour with escalating concentrations of ribociclib (0, 50, 100, 200 nM) or palbociclib (0, 15, 30, 60 nM) before exposure to ionizing radiation (0, 1, 2, or 4 Gy). A significant synergistic reduction in colony formation was observed when CDK4/6 inhibitors were combined with RT in both cell lines (**Figure 3-5**). Survival curves were fitted using the linear-quadratic model via non-linear regression analysis, clearly demonstrating a dose-dependent radiosensitization effect. The combination index (CI), calculated to evaluate drug–RT interaction, was consistently <1 across all treatment groups, indicating synergy ($P < 0.01$; **Figure 3-6**).

doi:10.6342/NTU202504448

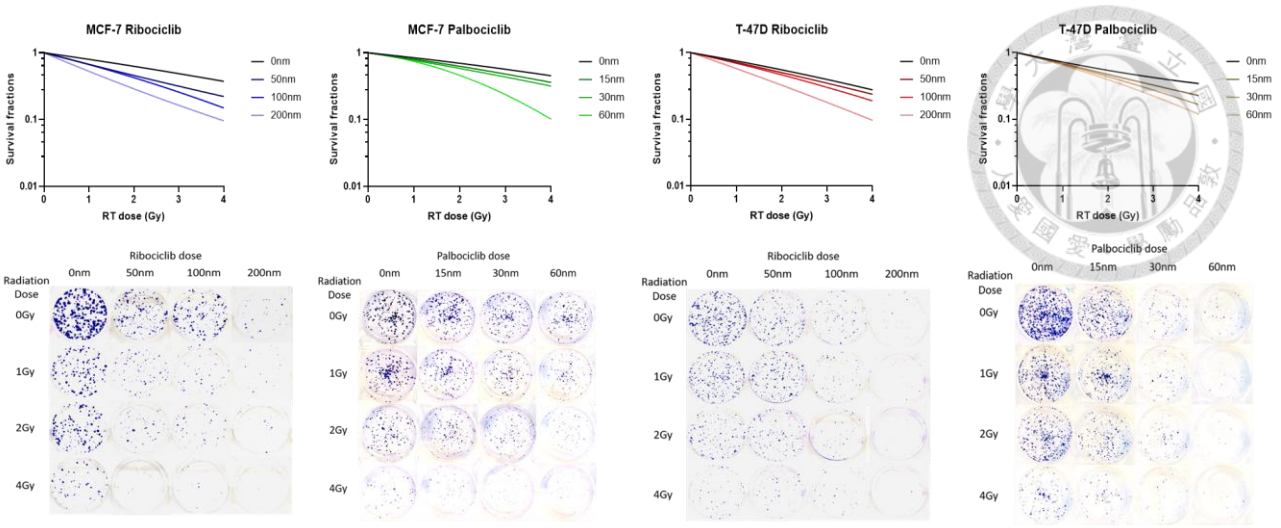

Figure 3-5 Cell survival evaluated via clonogenic assay for MCF-7 and T-47D cell lines treated with ribociclib or palbociclib followed by radiation.

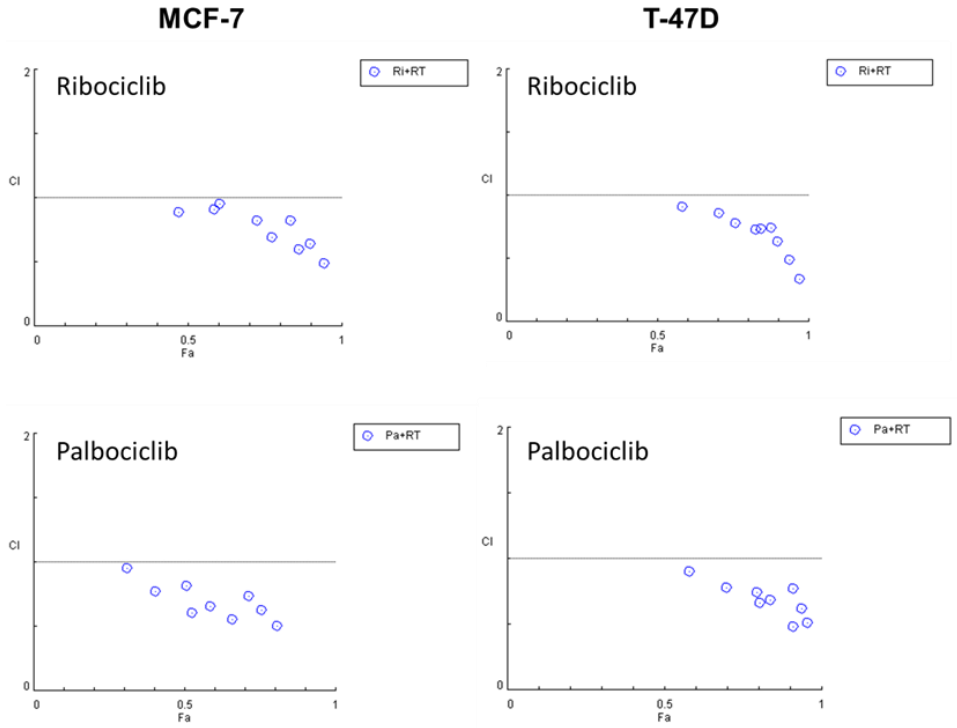

Figure 3-6. The combination index of both MCF-7 and T-47D treated with ribociclib or palbociclib with RT.

doi:10.6342/NTU202504448

3.3.2 IMPACT OF CDK4/6 INHIBITION COMBINED WITH RT ON CELL CYCLE PROGRESSION

As described in previous chapters, CDK4/6 inhibitors target the cyclin D–CDK4/6–p16–Rb pathway, effectively inhibiting tumor cell proliferation by preventing Rb phosphorylation and subsequent cell cycle progression. To verify the expression of Rb protein and its phosphorylated form (p-Rb) in our HR-positive, HER2-negative breast cancer models, we performed Western blot analysis on MCF-7 and T-47D cells. Both cell lines exhibited detectable levels of Rb and p-Rb under basal conditions. Following treatment with ribociclib (50 nM) or palbociclib (30 nM), a marked reduction in p-Rb expression was observed, while total RB levels remained unaffected (**Figure 3-7**). Interestingly, radiation alone induced upregulation of p-Rb, an effect that was subsequently reversed by co-treatment with either CDK4/6 inhibitor.

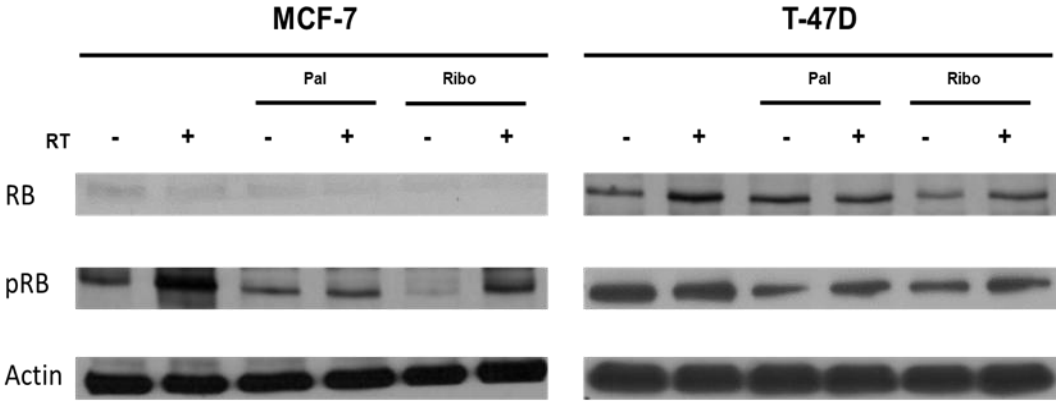

Figure 3-7 Rb and p-Rb protein expression under treatment with radiotherapy (RT) 0/4 Gy, palbociclib 0/30 nM or ribociclib 0/50 nM.

doi:10.6342/NTU202504448

Following the promising results observed in the clonogenic survival assays, we next explored the cellular mechanisms underlying the enhanced treatment effect by examining cell cycle distribution and apoptotic response. Flow cytometry was used to analyze cell cycle progression under various treatment conditions. T-47D cells exposed to ionizing radiation alone showed a notable accumulation in the G2/M phase, consistent with the known role of RT in halting cells prior to mitosis. In contrast, treatment with CDK4/6 inhibitors alone led to a marked increase in G1 phase cells, indicating effective cell cycle arrest at the G1 checkpoint, a hallmark of CDK4/6 inhibition.

Interestingly, the combination of CDK4/6 inhibition with radiotherapy induced cell cycle arrest at both G1 and G2/M phases, suggesting a synergistic effect on disrupting cell cycle progression compared to control or single treatments (**Figure 3-8**). Notably, varying the concentration of CDK4/6 inhibitors did not significantly alter the distribution of cell populations across phases, indicating that even lower doses were sufficient to exert their cell cycle–modulating effects in combination with RT.

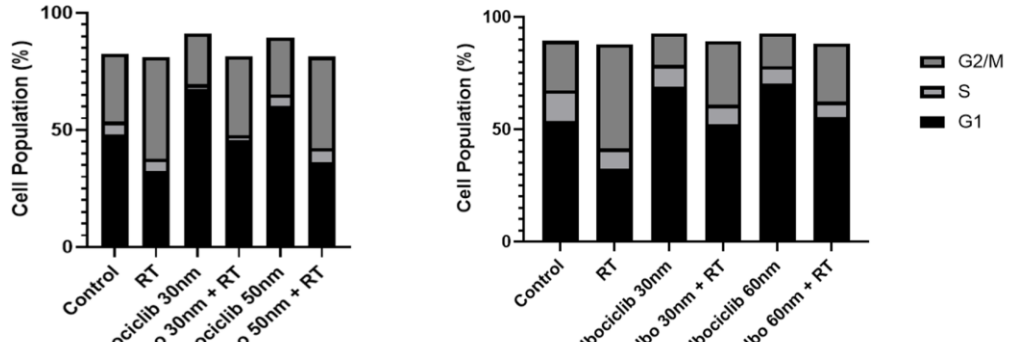

Figure 3-8 Cell cycle analysis of T-47D cells treated with radiation 4Gy and two different doses of Palbociclib or 50nm Ribociclib 1hr prior to radiation.

doi:10.6342/NTU202504448

3.3.3 IMPACT OF CDK4/6 INHIBITIOR AND RADIATION SEUQENCE ON CELL SURVIVAL

To evaluate whether the treatment sequence influences the efficacy of combining CDK4/6 inhibitors with radiotherapy, we performed a clonogenic survival assay using MCF-7 cells under three different administration schedules. In Sequence 1, cells were treated with ribociclib (0, 25, or 50 nM) on day 1, followed by ionizing radiation (0, 1, or 2 Gy) on day 2, allowing a 24-hour interval. In Sequence 2, ribociclib was administered 1 hour prior to RT, representing the concurrent approach used throughout the rest of the study. In Sequence 3, RT was delivered on day 1, followed by ribociclib treatment on day 2, also with a 24-hour gap. The colony formation assay condition was described previously.

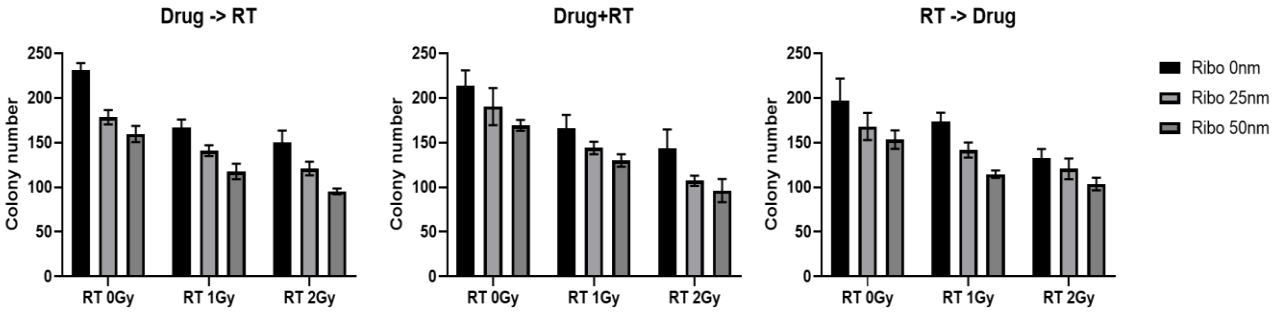

Figure 3-9 Effect of treatment sequence on clonogenic survival in MCF-7 cells treated with ribociclib and RT.

As shown in **Figure 3-9**, the sequence of administration did not significantly impact clonogenic survival, regardless of the ribociclib dose or radiation exposure. MCF-7 cells were treated with ribociclib (0, 25, or 50 nM) and exposed to ionizing radiation (0, 1, or 2 Gy) following three different

doi:10.6342/NTU202504448

treatment schedules: Sequence 1 – ribociclib administered 24 hours prior to RT; Sequence 2 – ribociclib given 1 hour before RT (concurrent treatment); Sequence 3 – RT delivered 24 hours before ribociclib treatment. Surviving fractions were measured using a colony formation assay. These findings indicate that the timing of drug and radiation delivery has minimal effect on the overall radiosensitizing outcome in this model. Consequently, Sequence 2 (pretreatment with CDK4/6 inhibitor 1 hour before RT) was adopted as the standard protocol for all subsequent experiments in this study.

3.3.4 EFFECT OF CDK4/6 INHIBITORS COMBINED WITH RT ON DNA DOUBLE STRAND BREAKS AND REPAIR AND THE IMPACT ON CELLULAR APOPTOSIS

Radiotherapy is a well-established inducer of DNA double-strand breaks (DSBs), which can lead to genomic instability and cancer cell death[32]. To assess the extent of DNA damage and repair under different treatment conditions, we performed immunofluorescence staining for γH2AX and 53BP1, two key markers associated with early DNA damage response and DSB repair[33,34].

MCF-7 and T-47D cells were treated with 4 Gy of ionizing radiation in the presence or absence of palbociclib (50 nM) or ribociclib (30 nM). Immunofluorescence was conducted 24 hours post-treatment to quantify nuclear foci formation of γH2AX and 53BP1.

doi:10.6342/NTU202504448

Treatment with either CDK4/6 inhibitor alone significantly increased the number of γH2AX and 53BP1 foci in both cell lines compared to untreated controls, suggesting that CDK4/6 inhibition impairs DNA repair or induces replication stress. Exposure to radiation alone also resulted in a marked increase in both markers, consistent with known RT-induced DNA damage. Importantly, combining CDK4/6 inhibitors with RT further enhanced DNA damage, as evidenced by a significantly greater number of γH2AX foci in MCF-7 (palbociclib: $P = 0.0105$; ribociclib: $P = 0.0085$) and T-47D cells (palbociclib: $P = 0.0265$; ribociclib: $P = 0.0189$) compared to RT alone. A similar pattern was observed for 53BP1, with combination treatment significantly increasing foci numbers in MCF-7 (palbociclib: $P = 0.0015$; ribociclib: $P = 0.0124$) and T-47D (palbociclib: $P = 0.0071$; ribociclib: $P = 0.0389$) cells. The summarized results were shown in **Figure 3-10**.These results suggest that CDK4/6 inhibitors potentiate RT-induced DNA damage by impairing the DNA repair response, providing a mechanistic rationale for the observed radiosensitization effect in HR-positive, HER2-negative breast cancer cells.

doi:10.6342/NTU202504448

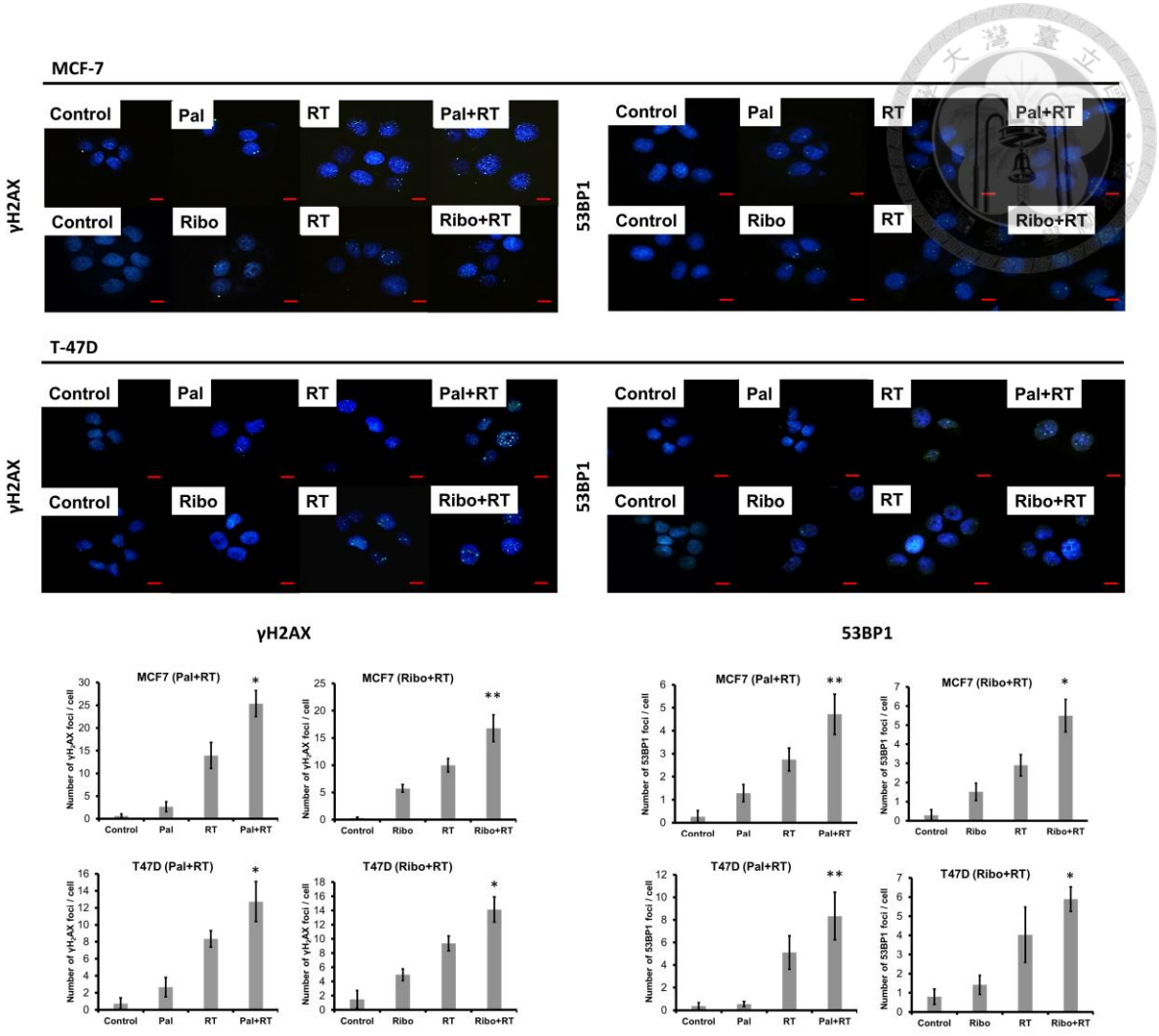

Figure 3-10 MCF-7 and T-47D cells were treated with or without palbociclib (30 nM) or ribociclib (50 nM) in combination with 4 Gy RT. After 24 hours, cells were fixed and stained for γH2AX and 53BP1 foci. Nuclei were counterstained with DAPI, and foci were visualized using confocal microscopy. * $P < 0.05$; ** $P < 0.01$. Scale bar = 10 μm.

To investigate whether the radiosensitizing effect of CDK4/6 inhibitors is associated with impaired DNA double-strand break (DSB) repair, we analyzed the expression of key DNA repair proteins—ATM, phosphorylated ATM (p-ATM), Rad51, DNA-PKcs, and phosphorylated DNA-PKcs (p-DNA-PKcs)—in MCF-7 and T-47D cells following treatment with radiotherapy (RT) alone or in combination with palbociclib or ribociclib. As expected, RT alone led to a marked upregulation of p-

doi:10.6342/NTU202504448

ATM, Rad51, and p-DNA-PKcs, indicating activation of the DNA repair machinery (**Figure 3-11**). Interestingly, both CDK4/6 inhibitors as single agents suppressed the expression of these proteins, suggesting a basal inhibition of DSB repair pathways.

More notably, when cells were pretreated with palbociclib or ribociclib one hour before RT, we observed a significant reduction in p-ATM, Rad51, and p-DNA-PKcs levels compared to RT alone. This implies that CDK4/6 inhibition compromises RT-induced activation of DNA repair signaling, thereby enhancing radiation sensitivity in HR-positive, HER2-negative breast cancer cells.

To assess whether these treatments also affected apoptotic signaling, we examined the expression of cleaved caspase-3, a key marker of apoptosis. RT alone increased cleaved caspase-3 levels in both cell lines, consistent with RT-induced apoptotic cell death. However, both palbociclib and ribociclib, when used alone, reduced cleaved caspase-3 expression, suggesting that CDK4/6 inhibitors predominantly exert cytostatic rather than pro-apoptotic effects. Intriguingly, the combined treatment with RT and CDK4/6 inhibitors further reduced cleaved caspase-3 levels compared to RT alone, reinforcing the idea that radiosensitization is primarily mediated through interference with DNA repair mechanisms, rather than by promoting apoptosis (**Figure 3-11)**.

doi:10.6342/NTU202504448

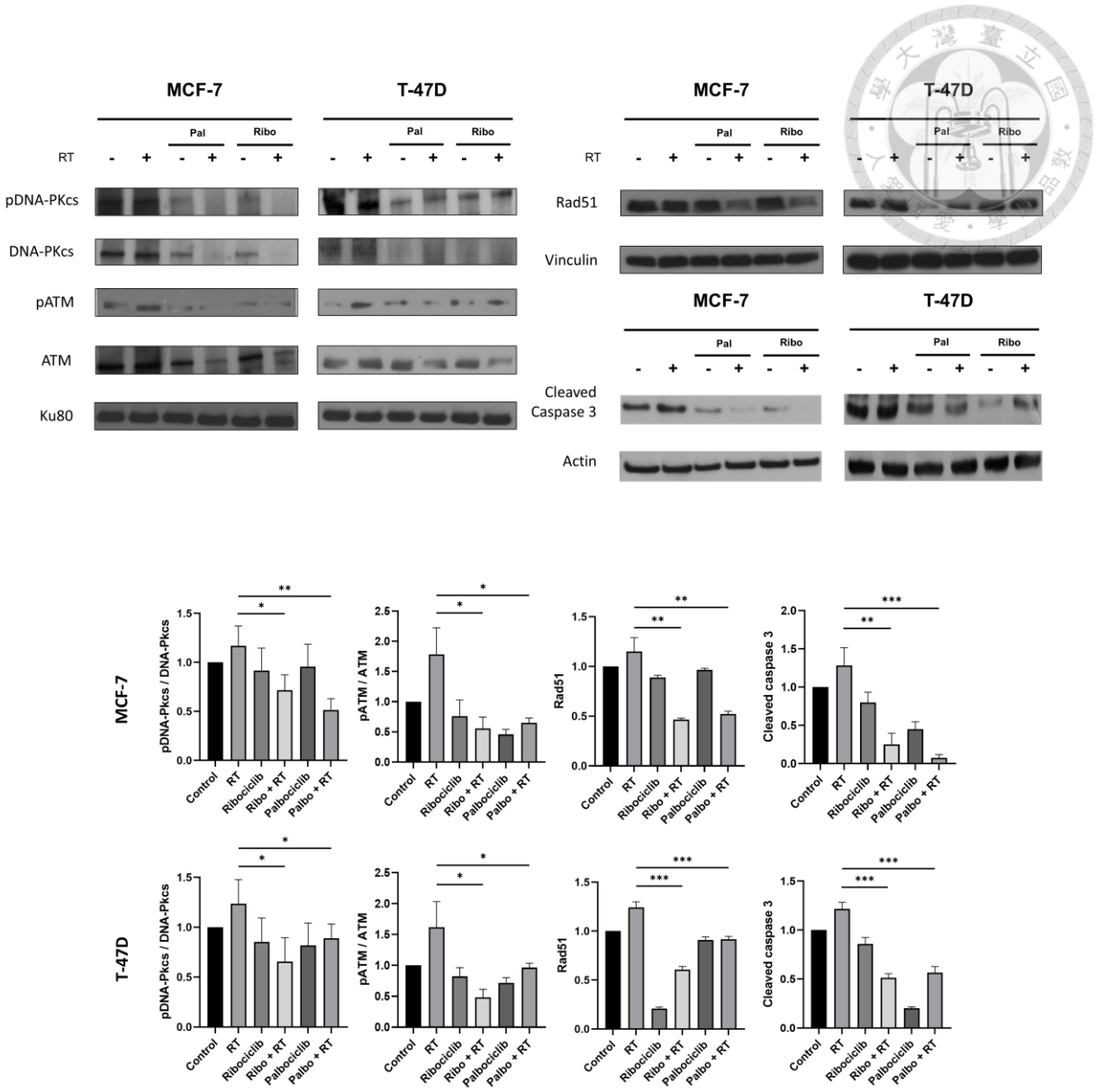

Figure 3-11 Western blot for DNA-PKcs, phosphorylated DNA-PKcs (p-DNA-PKcs), ATM, phosphorylated ATM (p-ATM), Rad51 and cleaved Caspase 3. *$P < 0.05$; **$P < 0.01$; **$P < 0.001$.

Annexin V/propidium iodide (PI) staining was performed to assess the impact of CDK4/6 inhibitors and RT on apoptosis. We compared apoptosis levels across different treatment groups, including CDK4/6 inhibitor monotherapy, RT alone, and combination therapy. Although distinct changes in cell cycle distribution were observed, none of the treatments led to a significant increase

doi:10.6342/NTU202504448

in apoptosis (**Figure 3-12**). These results suggest that the reduction in clonogenic survival is not mediated by enhanced apoptotic activity. This finding is consistent with cleaved caspase-3 data, further supporting that the synergistic effect of CDK4/6 inhibitors and RT does not occur through the induction of apoptosis.

This result aligns with previous studies reporting that CDK4/6 inhibitors primarily exert cytostatic effects, inducing G1 phase arrest without triggering substantial apoptosis. Our data reinforce the notion that the radiosensitizing effect of CDK4/6 blockade is likely mediated through cell cycle disruption rather than apoptosis induction.

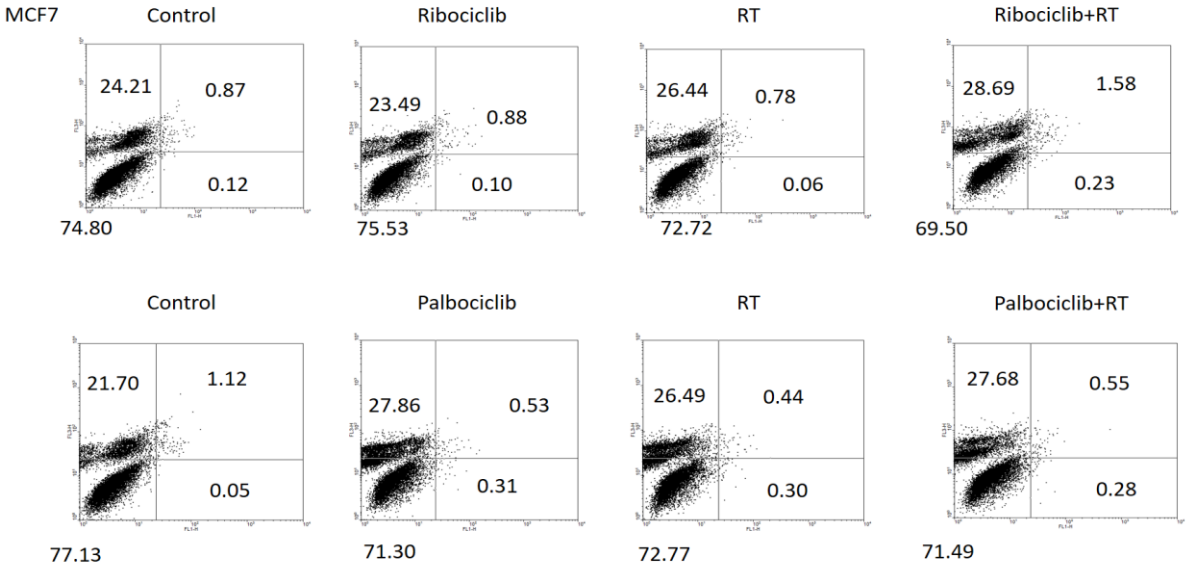

Figure 3-12 Apoptosis analysis Annexin-PI stain. MCF-7 cells were treated with radiation 0Gy or 2Gy, Palbociclib 0 or 30nm. There is no significant change of apoptosis level at any treatment condition.

doi:10.6342/NTU202504448

3.3.5 CDK4/6 INHIBITORS ATTENUATE ERK AND NF-κB/C-MYC PATHWAYS

Beyond inducing cytotoxic effects,rt also triggers cellular stress responses that can activate pro-survival pathways, notably the NF-κB signaling cascade. Activation of NF-κB has been associated with increased resistance to RT by promoting cell survival and inhibiting apoptosis[99]. One of the key downstream effectors of NF-κB, the transcription factor c-Myc, is frequently overexpressed in various cancers, including breast cancer, where it plays a critical role in regulating cell growth, proliferation, and survival[100]. Our previous findings also demonstrated that the MAPK/ERK pathway contributes to enhanced migration and invasion in HR-positive, HER2-negative breast cancer cell lines, which may underlie the poor prognosis associated with this subtype[101]. Moreover, evidence from several studies indicates that ERK signaling activated by RT contributes to the development of radioresistance in cancer cells [102, 103].

To determine the effects of CDK4/6 inhibitors on these pro-survival signaling pathways, we examined the expression of phosphorylated ERK (p-ERK) and c-Myc following RT with or without palbociclib or ribociclib. Western blot analysis revealed that RT alone (4 Gy) markedly increased the levels of p-ERK and c-Myc at 24 hours post-treatment in both MCF-7 and T-47D cells. While treatment with palbociclib or ribociclib as single agents reduced p-ERK levels in MCF-7 cells, no significant change was observed in T-47D cells. However, combining either CDK4/6 inhibitor with

doi:10.6342/NTU202504448

RT significantly suppressed p-ERK expression in both cell lines compared to RT alone (**Figure 3-13**). Similarly, both palbociclib and ribociclib led to decreased expression of c-Myc in MCF-7 and T-47D cells. Notably, combination treatment with CDK4/6 inhibitors and RT resulted in a more pronounced reduction in c-Myc levels than RT alone (**Figure 3-13**), suggesting an additive or synergistic effect in disrupting NF-κB/c-Myc-mediated survival signaling.

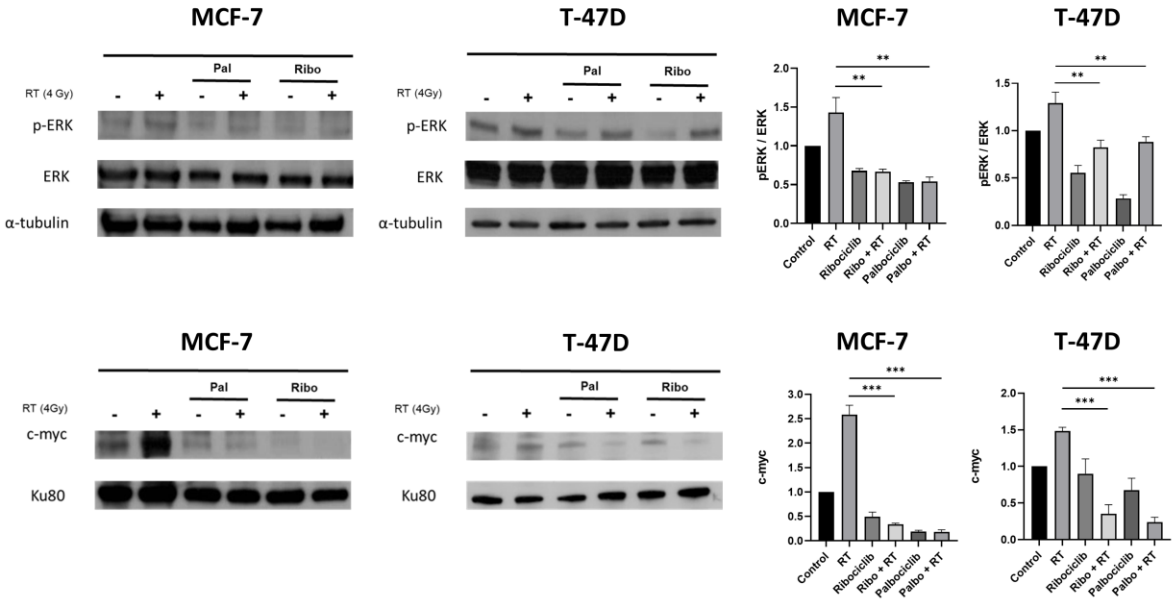

Figure 3-13 Western blot analysis of p-ERK, ERK c-myc in MCF-7 and T-47D cells treated with palbociclib (30 nM) or ribociclib (50 nM), with or without RT (4 Gy). *P < 0.05; **P < 0.01; ***P < 0.001.

To further assess NF-κB activity, we evaluated its transcriptional activation. As expected, RT increased NF-κB transcriptional activity in both cell lines. In contrast, treatment with palbociclib or ribociclib alone led to reduced NF-κB activity. When combined with RT, both inhibitors significantly

doi:10.6342/NTU202504448

suppressed NF-κB activation compared to RT alone in MCF-7 ($P < 0.001$) and T-47D ($P < 0.01$) cells (**Figure 3-14**). These results indicate that CDK4/6 inhibitors may enhance the efficacy of RT not only by impairing DNA repair but also by inhibiting compensatory pro-survival pathways such as NF-κB and its downstream effectors.

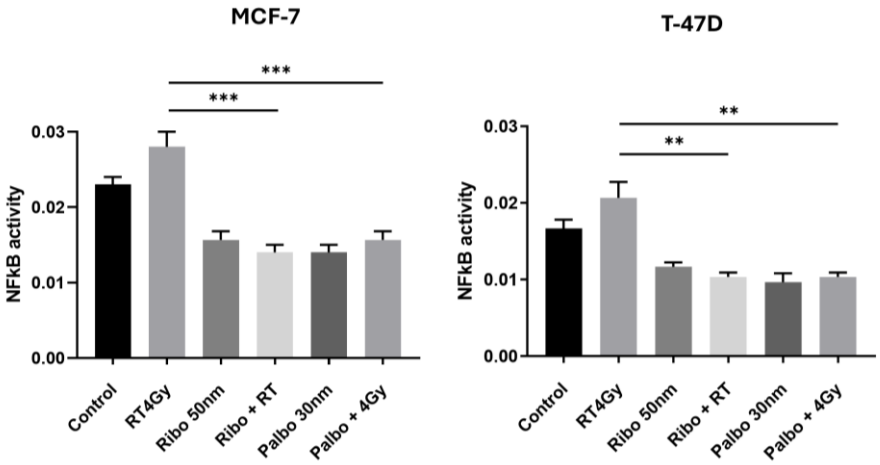

Figure 3-14 NF-κB p65 transcriptional activity assay across control, RT, CDK4/6 inhibitor monotherapy, and combination treatment groups. *P < 0.05; **P < 0.01; ***P < 0.001.

3.3.6 SYNERGISTIC ANTITUMOR EFFECT OF CDK4/6 INHIBITORS AND RT IN VIVO

To investigate the *in vivo* antitumor efficacy of CDK4/6 inhibitors in combination with RT, we employed an orthotopic xenograft model using MCF-7 breast cancer cells. As illustrated in **Figure 3-15**, female BALB/cAnN.Cg-Foxn1nu/CrlNarl nude mice bearing orthotopic MCF-7 tumors were divided into four groups (n = 6 per group): control, RT alone (2 Gy every other day, total 6 Gy),

doi:10.6342/NTU202504448

ribociclib alone (200 mg/kg/day, days 1–5), and ribociclib combined with RT. Tumor volumes were measured over time to evaluate therapeutic responses.

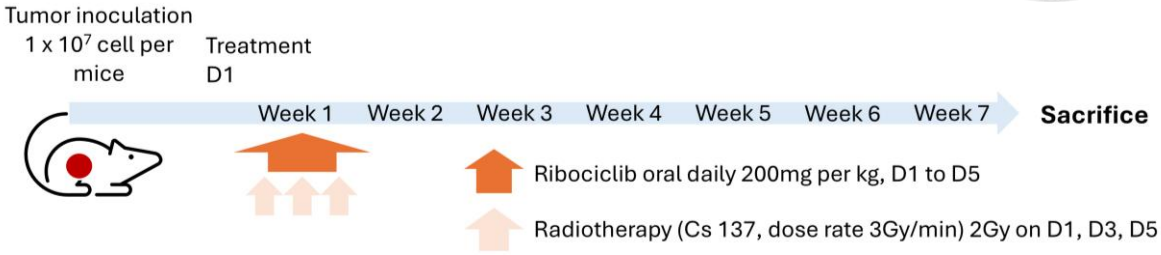

Figure 3-15 MCF-7 mouse model treatment schedule.

As shown in **Figure 3-16**, the combination of ribociclib and RT produced a pronounced antitumor effect, significantly suppressing tumor growth compared to any monotherapy or the untreated control group ($P < 0.0001$). After 43 days, tumors in the combination group demonstrated a volume reduction of 93% and 88% relative to the ribociclib-only and RT-only groups, respectively, underscoring a strong synergistic effect. Throughout the course of treatment, all regimens—including the combination—were well tolerated, with no apparent toxicity. Body weight remained stable across all groups, indicating preserved general health and the absence of treatment-related systemic toxicity (**Figure 3-16**).

doi:10.6342/NTU202504448

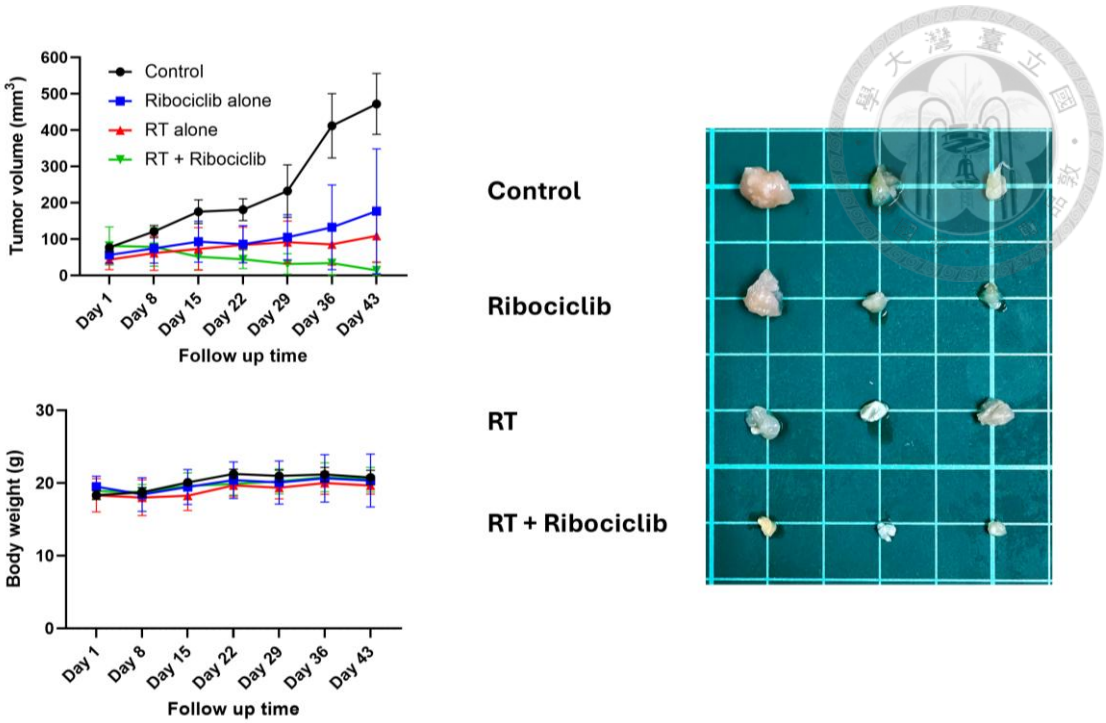

Figure 3-16 MCF-7 xenograft tumor volume, excised tumors and body weight

To confimr the molecular mechanisms underlying this synergistic effect, we analyzed tumor tissues collected on day 43 for expression of NF-κB pathway components and p-ERK, a key downstream effector of the MAPK signaling cascade. Immunohistochemistry staining (**Figure 3-17**) revealed a notable downregulation of phosphorylated NF-κB p65, c-Myc, and p-ERK in tumors from the combination treatment group compared to controls. These in vivo findings are consistent with our in vitro data, supporting the conclusion that CDK4/6 inhibitors enhance RT sensitivity by suppressing the NF-κB/c-Myc axis and ERK-mediated proliferative signaling.

doi:10.6342/NTU202504448

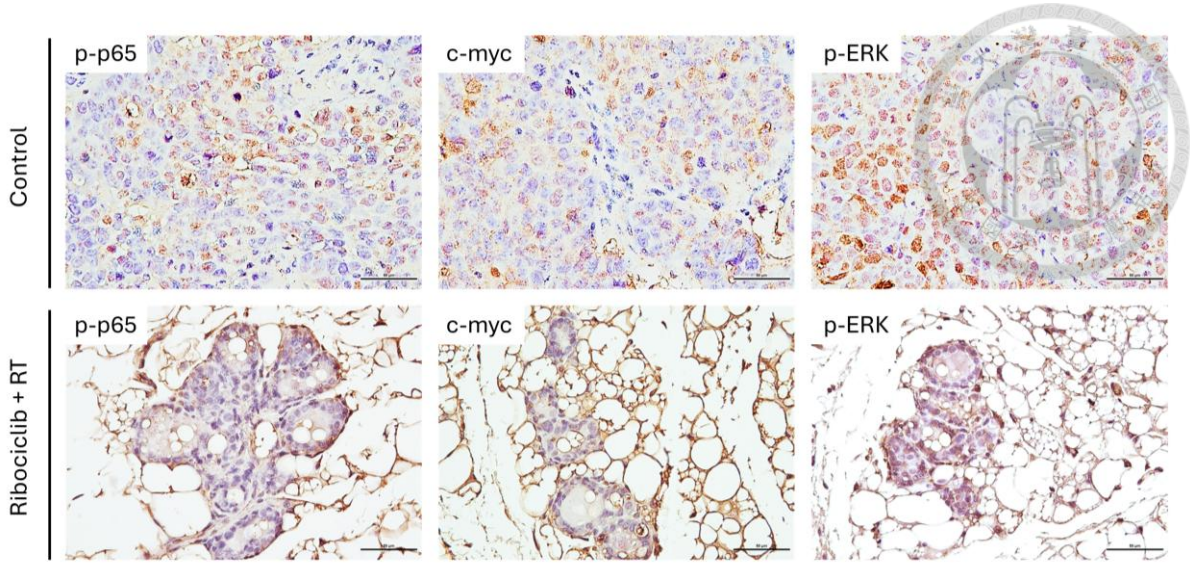

Figure 3-17 Immunohistochemical staining was performed on resected tumors for phospho-NF-κB p65, c-Myc, and phospho-ERK

To assess the potential for organ-specific toxicity associated with CDK4/6 inhibitors in combination with RT, we conducted a safety evaluation using the same nude mouse model described above Mice were treated with control, ribociclib alone, palbociclib alone, RT alone, or combination therapies (ribociclib + RT or palbociclib + RT). Liver and kidney function were evaluated by measuring serum alanine aminotransferase (ALT) and creatinine levels. As shown in **Figure 3-18**, there were no significant differences in ALT or creatinine between treatment and control groups, indicating preserved hepatic and renal function.

doi:10.6342/NTU202504448

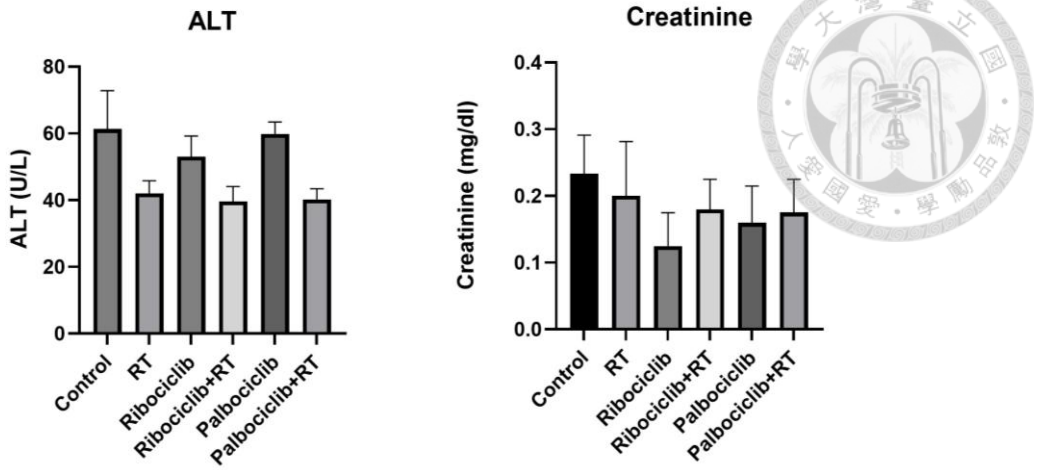

Figure 3-18 Serum alanine aminotransferase (ALT) and creatinine from MCF-7 xenograft model.

Additionally, histopathological examination of major organs—including lung, liver, and intestinal tissues—was performed using hematoxylin and eosin (H&E) staining. Representative images in **Figure 3-19** show no observable tissue damage or abnormalities in any of the treated groups. Across all treatment groups, liver tissues exhibited intact hepatic architecture without signs of radiation-

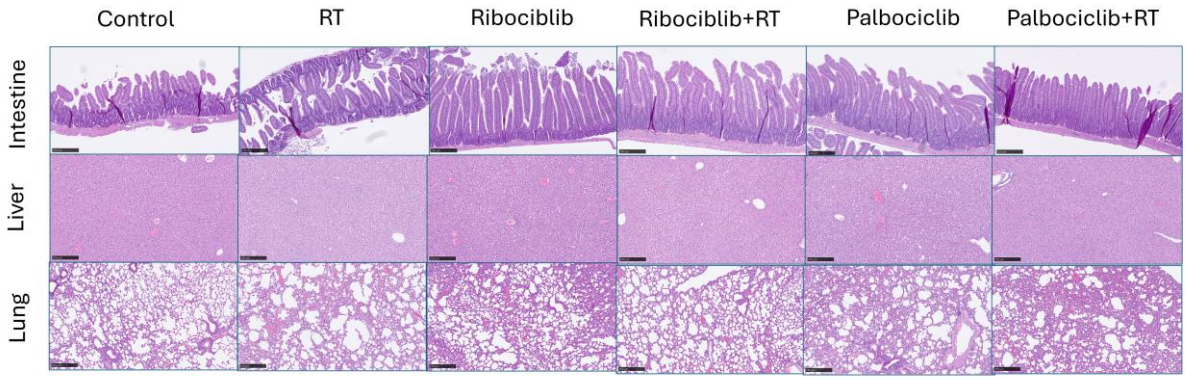

Figure 3-19 Histological assessment of major organs following treatment. Hematoxylin and eosin (H&E) staining of intestine, liver, and lung tissues from mice treated with control, ribociclib alone, palbociclib alone, RT alone, ribociclib + RT, or palbociclib + RT. Images were captured at 100× magnification.

doi:10.6342/NTU202504448

induced injury, such as hepatocyte necrosis or inflammation. Lung tissues maintained normal alveolar structure, with no evidence of fibrosis, pneumonitis, or other radiation-associated damage. Similarly, intestinal tissues showed preserved villous morphology and epithelial integrity, with no detectable mucosal injury or inflammatory response following RT or its combination with ribociclib or palbociclib. This result confirms that neither CDK4/6 inhibitors, RT, nor their combination caused detectable harm to major organs under the experimental conditions.

3.4 DISCUSSION

In this chapter, we demonstrated that CDK4/6 inhibitors—specifically ribociclib and palbociclib—potentiate the effects of RT in two Rb-proficient, HR-positive and HER2-negative breast cancer cell lines, MCF-7 and T-47D. Our results show that the radiosensitizing effect of these inhibitors is at least partially mediated by downregulating RT-activated ERK and NF-κB signaling pathways, along with promoting DNA damage accumulation through impaired DSB repair. These mechanisms were observed consistently across both cell lines. We further validated the biological significance of these findings using an *in vivo* orthotopic xenograft model, where ribociclib enhanced RT-induced tumor suppression and reduced the expression of p-ERK, p-NF-κB p65, and its downstream effector, c-Myc, in tumor tissues.

Consistent radiosensitizing effects were observed with both CDK4/6 inhibitors across the two HR+/HER2− cell lines. This aligns with previous studies in ER-positive breast cancer, which reported

doi:10.6342/NTU202504448

a synergistic interaction between CDK4/6 inhibitors and RT[104, 105]. For instance, Petroni *et al*. demonstrated improved anti-tumor responses when RT preceded palbociclib treatment, in both in vitro and in vivo models[104]. Interestingly, in our study, different treatment sequences (RT before or after CDK4/6 inhibitor exposure) had minimal impact on clonogenic survival, indicating that treatment timing may be less critical under certain experimental conditions. This observation is consistent with Pesch *et al.*[105], who reported enhanced radiation responses following short-term CDK4/6 inhibitor pretreatment

The radiosensitizing properties of CDK4/6 inhibitors have been extensively discussed in the context of their impact on DNA repair processes[106]. Radiation-induced DSBs activate a complex DNA damage response (DDR) involving multiple post-translational modifications and repair proteins. Several prior studies[70, 71, 74] have shown that CDK4/6 inhibition delays DSB repair and increases γH2AX levels, indicating persistent DNA damage after irradiation. In line with these findings, we used immunofluorescence to demonstrate sustained γH2AX and 53BP1 foci 24 hours after combined treatment with palbociclib or ribociclib and 4 Gy RT in both MCF-7 and T-47D cells.

DNA DSBs are repaired primarily via two pathways: homologous recombination (HR) and non-homologous end joining (NHEJ). Prior studies suggest that CDK4/6 inhibition can impair HR by reducing the expression of key proteins such as Rad51 and ATM[107]. However, the effects on NHEJ remain unclear. Dean *et al.* [108] reported that abemaciclib sensitized lung cancer cells by

doi:10.6342/NTU202504448

downregulating proteins involved in both HR and NHEJ, including p-ATM, p-ATR, Rad51, and p-DNA-PKcs (Ser2056). In contrast, Pesch *et al.* [105] found no significant impact of CDK4/6 inhibition on NHEJ activity in ER-positive breast cancer cells. In our study, both palbociclib and ribociclib reduced the expression of p-DNA-PKcs and p-ATM, with or without RT, suggesting that CDK4/6 inhibition compromises the function of both HR and NHEJ repair pathways. This dual impairment of DSB repair mechanisms likely contributes to increased radiosensitivity.

The role of CDK4/6 inhibitors in modulating apoptosis remains controversial. While some studies, such as Huang *et al.* [72], reported increased DNA fragmentation and apoptosis in hepatocellular carcinoma cells treated with palbociclib and RT, others like Dean *et al.* [108] described an anti-apoptotic effect marked by decreased cleaved PARP levels. Hagen *et al.* [109] offered additional nuance, showing that CDK4 knockdown enhanced RT-induced apoptosis, whereas pharmacologic inhibition with palbociclib reduced cleaved PARP expression. In our study, we observed decreased cleaved caspase-3 levels following pretreatment with low-dose palbociclib or ribociclib prior to RT, suggesting reduced apoptosis in MCF-7 and T-47D cells. This may reflect the complex regulatory effects of CDK4/6 inhibitors on apoptotic pathways, possibly influenced by their broader activity on different CDK-cyclin complexes [110].

NF-κB signaling plays a pivotal role in the survival, proliferation, and therapy resistance of HR+/HER2− breast cancer cells[111, 112]. It is well-established that NF-κB can be activated in

doi:10.6342/NTU202504448

response to cellular stress, including ionizing radiation[113], and its activation has been implicated in radioresistance by protecting tumor cells from RT-induced apoptosis[99]. In our experiments, RT increased NF-κB activity in both MCF-7 and T-47D cells, while treatment with palbociclib or ribociclib reduced this activation. Furthermore, c-Myc, a key downstream effector of NF-κB, was also downregulated in the combined treatment groups. These molecular changes were mirrored in vivo, where tumor tissues from mice receiving both ribociclib and RT showed reduced expression of p-NF-κB p65 and c-Myc.

We also found that CDK4/6 inhibitors mitigated RT-induced activation of ERK signaling in vitro and in vivo. Since ERK pathway overactivation is frequently associated with radioresistance across multiple solid tumors, including breast cancer[102], its suppression may further enhance radiosensitivity. Together, these results suggest that the radiosensitizing effects of CDK4/6 inhibitors in HR+/HER2− breast cancer may stem from both impaired DSB repair and inhibition of pro-survival signaling via NF-κB/c-Myc and ERK.

Although NF-κB inhibitors have shown promise in preclinical models[114], their clinical utility remains uncertain due to the multifaceted role of NF-κB and concerns regarding toxicity[115]. Our findings suggest that CDK4/6 inhibitors can function as indirect NF-κB and ERK pathway modulators while simultaneously enhancing DNA damage from RT—providing a multi-pronged approach to improving therapeutic outcomes in HR+/HER2− breast cancer.

doi:10.6342/NTU202504448

From a translational perspective, retrospective clinical series have reported on the safety and potential efficacy of combining RT with CDK4/6 inhibitors. For example, Figura *et al.* [116] observed favorable outcomes and tolerability in patients who received stereotactic RT for brain metastases within six months of initiating CDK4/6 inhibitor therapy. Similarly, Beddock *et al.* [117] described acceptable toxicity profiles in 30 patients treated with concurrent palbociclib and RT. In our preclinical toxicity analysis, combination therapy with ribociclib or palbociclib and RT did not impair liver or kidney function, nor did it cause histologic damage to major organs. Previous reports have even suggested a protective effect of CDK4/6 inhibitors against RT-induced intestinal injury via intestinal stem cell preservation[118]. Moreover, recent clinical studies confirm the general tolerability of CDK4/6 inhibitors when combined with RT [119, 120]. It should be noted that our safety evaluation primarily focused on organ function (liver and kidney biochemistry) and histopathological changes in major organs, but we did not investigate hematological toxicity. This is an important limitation because prior clinical studies have demonstrated that combining CDK4/6 inhibitors with other therapies can substantially increase hematological adverse events, particularly neutropenia and leukopenia[56, 121]. Therefore, future studies combining CDK4/6 inhibition with radiotherapy should incorporate comprehensive hematologic monitoring to better characterize safety profiles.

Based on the consistency between our preclinical results and emerging clinical observations, future clinical trials are warranted to evaluate the combination of CDK4/6 inhibitors with adjuvant

doi:10.6342/NTU202504448

RT in patients with early-stage, high-risk HR+/HER2− breast cancer, as well as in those with advanced or metastatic disease requiring locoregional radiation.

3.5 SUMMARY

In conclusion, this study provides strong preclinical evidence that CDK4/6 inhibitors, including palbociclib and ribociclib, not only suppress tumor cell growth but also enhance the response to radiotherapy in HR-positive, HER2-negative breast cancer. This enhanced radiosensitivity was observed both in vitro and in vivo using an orthotopic xenograft model. Mechanistically, the combination treatment attenuated radiation-induced activation of ERK and NF-κB/c-Myc signaling and disrupted key components of the DNA double-strand break repair machinery. The summary of this potential mechanism is illustrated as **Figure 3-20**. These findings support the rationale for integrating CDK4/6 inhibitors with radiotherapy as a promising therapeutic strategy, particularly in high-risk, node-positive HR+/HER2− breast cancer, and highlight the need for further clinical validation.

doi:10.6342/NTU202504448

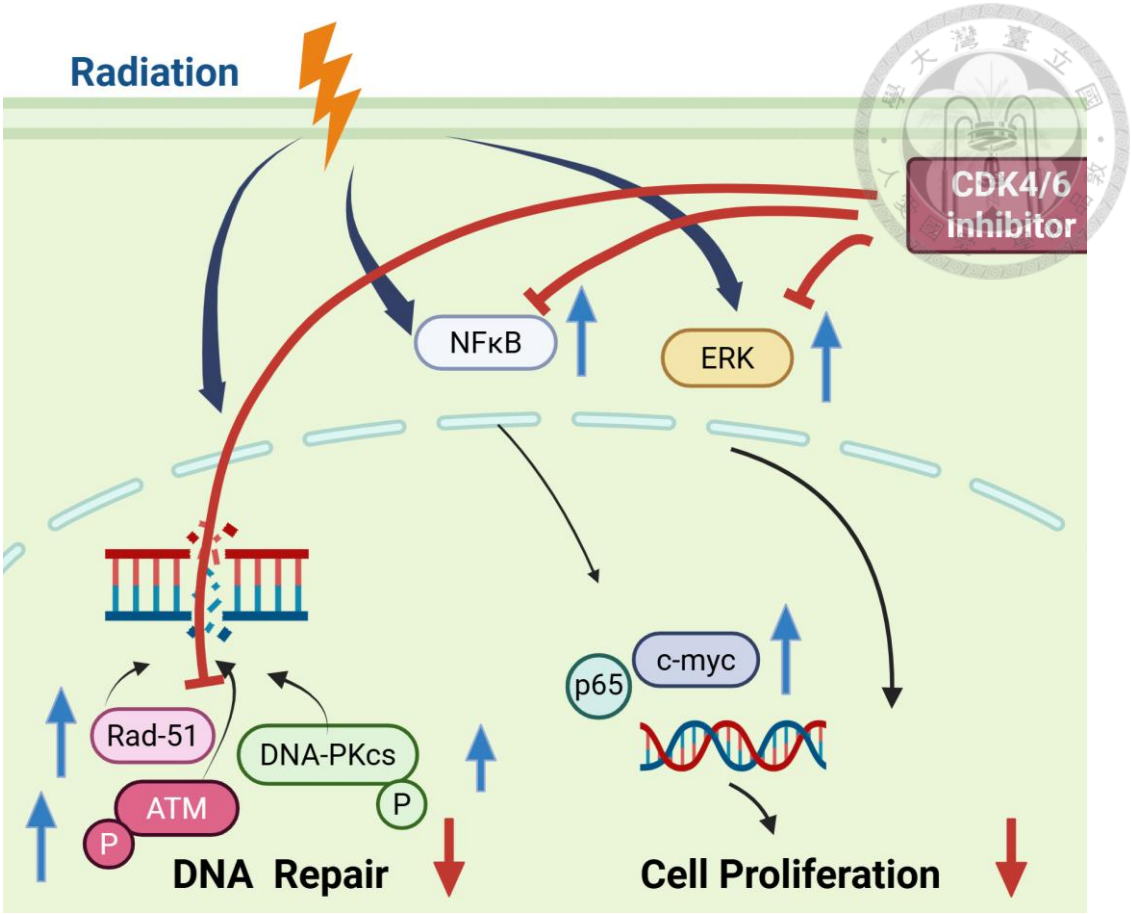

Figure 3-20 Proposed mechanisms of CDK4/6 inhibitor–mediated radiosensitization in HR-positive, HER2-negative breast cancer.

doi:10.6342/NTU202504448

CHAPTER 4. SYNERGISTIC ANTITUMOR EFFECTS OF CDK4/6 INHIBITORS, RADIOTHERAPY, AND ANTI-PD-L1 THERAPY IN TRIPLE-NEGATIVE BREAST CANCER VIA MICROENVIRONMENT REPROGRAMMING

4.1 INTRODUCTION

In previous chapters, we knew that breast cancer remains the most prevalent cancer among women globally and is classified into molecular subtypes with distinct biological behaviors and clinical outcomes. Among these, TNBC is the most aggressive and lacks targeted therapies, resulting in a poorer prognosis compared to other subtypes[3]. In our previous clinical cohort in chapter 2, TNBC patients had the worst survival outcomes, underscoring the urgent need for more effective therapeutic strategies.

Although ICIs have shown success in several malignancies, their efficacy as monotherapy in TNBC has been limited, partly due to the tumor's immunosuppressive microenvironment[24, 26]. Combination approaches, such as pairing ICIs with chemotherapy, have improved responses, as demonstrated in neoadjuvant trials with pembrolizumab[28, 122].

CDK4/6 inhibitors, originally developed to block cell cycle progression in ER-positive breast cancer, have also shown potential immunomodulatory effects. They enhance antigen presentation and promote cytotoxic T-cell infiltration[66]. While TNBC often presents with Rb pathway alterations,

doi:10.6342/NTU202504448

some TNBC subtypes retain sensitivity to CDK4/6 inhibition, as shown in both preclinical and clinical studies[53, 56].

Radiotherapy, widely used in breast cancer management, not only exerts direct cytotoxic effects but also enhances immunogenicity by releasing tumor-associated antigens and activating systemic immune responses[10, 36]. Preclinical studies suggest a synergistic interaction between RT and CDK4/6 inhibitors[71, 73], providing a rationale for triple combination approaches.

In our prior work, we demonstrated that CDK4/6 inhibitors enhance radiosensitivity in ER+/HER2− breast cancer through mechanisms involving impaired DNA damage repair and suppression of pro-survival signaling pathways. Building upon these findings, we hypothesized that CDK4/6 inhibition could also improve the efficacy of RT in TNBC, and potentially further enahcne immunotherapy effect when combined with RT.

In this chapter, we investigated whether combining CDK4/6 inhibitors, RT, and anti-PD-L1 immunotherapy could overcome resistance and improve therapeutic efficacy in TNBC. Using both the poorly immunogenic, highly metastatic 4T1 model and the relatively immunogenic EMT6 model[123-125], we aimed to evaluate the immunologic and antitumor effects of this combination strategy in immunocompetent murine models of TNBC.

4.2 MATERILS AND METHODS

doi:10.6342/NTU202504448

4.2.1 BREAST CANCER CELL LINES AND CULTURE CONDITIONS

We utilized three human and two murine TNBC cell lines, all obtained from the American Type Culture Collection (ATCC, Rockville, MD, USA). The human TNBC cell lines included MDA-MB-231 (ATCC® HTB-26™), MDA-MB-453 (ATCC® HTB-131™), and MDA-MB-468 (ATCC® HTB-132™). The murine TNBC models comprised 4T1 (ATCC® CRL-2539™) and EMT6 (ATCC® CRL-2755™). All cell lines were maintained at 37°C in a humidified atmosphere with 5% CO_2, following ATCC-recommended culture protocols. MDA-MB-453, MDA-MB-468, and 4T1 cells were cultured in RPMI-1640 medium (Gibco), MDA-MB-231 cells in Dulbecco's Modified Eagle's Medium (DMEM), and EMT6 cells in Waymouth's MB 752/1 medium.

4.2.2 DRUG AND IONIZAING IRRADIATION

This study aimed to explore the biological effects of abemaciclib, a selective CDK4/6 inhibitor, on cellular functions and its potential to enhance antitumor activity, both as a monotherapy and in combination with radiotherapy and immunotherapy. Abemaciclib was purchased from MedChemExpress (MCE, Shanghai, China) and prepared as a 10 mmol/L stock solution in 100% dimethyl sulfoxide (DMSO), then diluted to the desired concentrations for experimental use.

Ionizing radiation was administered using a Caesium-137 (Cs-137) γ-irradiator (IBL 637, CIS Bio International, Saclay, France) at an approximate dose rate of 3 Gy per minute. Whole-body irradiation was performed with the use of 5 mm lead shielding to protect non-target tissues and

doi:10.6342/NTU202504448

minimize systemic exposure. This setup allowed for localized delivery of radiation while mimicking clinically relevant RT protocols.

4.2.3 CELL PROLIFERATION ASSAY

To evaluate the antiproliferative effects of abemaciclib, five TNBC cell lines—MDA-MB-231, MDA-MB-453, MDA-MB-468, 4T1, and EMT6—were seeded into 96-well plates at a density of 1,000 cells per well in 100 μL of their respective culture media. After allowing cells to adhere overnight, they were treated with a range of abemaciclib concentrations to assess dose-dependent responses. Cell proliferation was measured 72 hours post-treatment using the CellTiter 96® AQueous One Solution Cell Proliferation Assay (Promega, Madison, WI, USA), a colorimetric method that reflects metabolic activity as an indicator of viable cell number. Absorbance was recorded at 450 nm using a multi-well microplate reader, and background values were subtracted to normalize the data. The half-maximal inhibitory concentration (IC_{50}) for abemaciclib in each cell line was calculated from the resulting dose–response curves.

4.2.4 COLONOGENIC ASSAY

Triple-negative breast cancer cell lines—MDA-MB-231, MDA-MB-453, MDA-MB-468, 4T1, and EMT6—were seeded at a density of 2,000 cells per well into six-well plates. Once adherent, cells were pretreated with varying concentrations of abemaciclib one hour prior to exposure to ionizing

doi:10.6342/NTU202504448

radiation at doses ranging from 0 to 6 Gy. Following treatment, cells were maintained in complete culture medium for the duration of the assay without media replacement.

After an incubation period of 7 to 14 days, colonies were fixed, stained, and manually counted under an inverted phase-contrast microscope at 100× magnification. A colony was defined as a discrete cluster of ≥50 cells. Clonogenic survival was used to evaluate the long-term proliferative capacity of each treatment group. To determine the degree of synergy between abemaciclib and RT, a combination index (CI) was calculated as described in 3.2.3.

4.2.5 FLOW CYTOMETRY

To evaluate PD-L1 expression on the cell surface, TNBC cell lines (MDA-MB-231, MDA-MB-453, MDA-MB-468, 4T1, and EMT6) were treated with varying doses of ionizing radiation and abemaciclib. After 24 hours, cells were harvested and stained with an anti-PD-L1 antibody (clone #13684; Cell Signaling Technology) and analyzed by flow cytometry using an LSR II cytometer (BD Biosciences, San Diego, CA, USA). This assay allowed us to assess how treatment modulates PD-L1 expression, which may have implications for immunotherapy responsiveness.

To characterize TILs, tumors derived from 4T1 orthotopic models in immunocompetent mice were harvested, mechanically dissociated, and processed into single-cell suspensions. Cells were then stained with a panel of fluorochrome-conjugated antibodies targeting immune cell surface markers, including CD45 (cat. 536709), CD4 (cat. 553051), CD8 (cat. 552877), CD11b (cat. 564985), GR-1

doi:10.6342/NTU202504448

(cat. 552093), F4/80 (cat. 565613), FoxP3 (cat. 12-5774-83), Ly6C (cat. 562737), and Ly6G (cat. 563011), all purchased from BD Biosciences or eBiosciences. An isotype control antibody (Rat IgG2a, cat. 12-4321-80, eBiosciences) was used for gating accuracy.

To exclude dead cells, we utilized the LIVE/DEAD™ Fixable Green Dead Cell Stain Kit (cat. L23101, Invitrogen, Waltham, MA). For intracellular markers such as FoxP3, cells were fixed and permeabilized using the appropriate buffers from eBiosciences, with incubation times of 30 minutes at room temperature (extended to 60 minutes for FoxP3 staining). Flow cytometric analysis was performed on the LSR II platform, and data were processed using FlowJo software version 10.1 (Tree Star, Ashland, OR, USA).

4.2.6 WESTERN BLOT ANALYSIS

To investigate protein expression profiles, MDA-MB-231, MDA-MB-453, MDA-MB-468, 4T1, and EMT6 cells were subjected to different treatments, including control (untreated), RT abemaciclib alone, or a combination of abemaciclib and RT. After treatment, total cellular proteins were extracted using the Mammalian Protein Extraction Reagent (M-PER; Pierce, Rockford, IL, USA), following the manufacturer's protocol. Equal quantities of protein from each sample were loaded and resolved on 10% SDS-PAGE gels using the Tris-glycine running buffer system. The resolved proteins were then transferred onto nitrocellulose membranes (Novex, San Diego, CA, USA). Membranes were

doi:10.6342/NTU202504448

blocked overnight at 4°C in Tris-buffered saline containing 0.1% Tween-20 (TBS-T) and 5% nonfat dry milk to prevent nonspecific binding.

For immunodetection, membranes were incubated with primary antibodies specific to total Rb (Cat# 9309S), phosphorylated Rb (p-Rb, Cat# 8516S), p-ERK (Cell Signaling, Cat# 4376S), Rad-51(Cell Signaling, Cat# 8875) and α-tubulin (loading control, Cat# 2144), all obtained from Cell Signaling Technology. After washing, membranes were incubated with species-appropriate horseradish peroxidase (HRP)-conjugated secondary antibodies. Protein bands were visualized using an enhanced chemiluminescence (ECL) detection system (Boehringer Mannheim, Germany) and captured via standard imaging methods. All experiments were performed in triplicate to confirm reproducibility and ensure experimental consistency.

4.2.7 ENZYME-LINKED IMMUNOSORBENT ASSAY (ELISA)

To evaluate systemic immune activation, serum samples collected from 4T1 tumor-bearing mice were assessed for interferon-gamma (IFN-γ) concentrations using the Quantikine™ Mouse IFN-γ ELISA kit (Cat. MIF00-1; Sigma-Aldrich), following the manufacturer's detailed protocol. All reagents were prepared according to the instructions provided. The assay was carried out by first adding the assay diluent, followed by the appropriate standards, controls, and experimental serum samples into the designated wells of the pre-coated microplate.

doi:10.6342/NTU202504448

The plates were incubated at room temperature for 2 hours to allow binding interactions. After incubation, wells were washed thoroughly to remove unbound substances. A conjugated detection antibody specific to mouse IFN-γ was then added, and plates were incubated for another 2 hours. Following another wash cycle, a chromogenic substrate solution was introduced, and the plates were kept protected from light during color development.

The reaction was terminated according to the kit instructions, and absorbance was measured at 450 nm using a calibrated microplate reader. The absorbance values were used to calculate IFN-γ concentrations in each sample by referencing a standard curve generated from the known standards included in the kit.

4.2.8 IN VIVO MOUSE MODELS

Female BALB/c mice (5–6 weeks old) were procured from the National Laboratory Animal Center (Taiwan) and housed under standard conditions. All animal procedures were reviewed and approved by the Institutional Animal Care and Use Committee of National Taiwan University (IACUC No. 20210366). For tumor implantation, each mouse was injected subcutaneously in the flank with 100 μL of either 4T1 or EMT6 cell suspension, prepared at a concentration of 1×10^5 cells/mL in sterile medium.

Tumor growth was monitored regularly, and tumor volume was estimated using caliper measurements as previously described. Once tumors reached an average size of around100 mm^3, mice

doi:10.6342/NTU202504448

were randomly assigned into eight treatment arms: (1) vehicle control (PBS for anti-PD-L1, DMSO for abemaciclib), (2) RT alone, (3) abemaciclib alone, (4) anti-PD-L1 antibody (aPD-L1) alone, (5) abemaciclib + aPD-L1, (6) abemaciclib + RT, (7) aPD-L1 + RT, and (8) triple combination of abemaciclib, aPD-L1, and RT.

Tumors were irradiated with a cesium-137 (Cs-137) gamma source at a dose of 8 Gy, delivered once per week over two consecutive weeks. Abemaciclib was administered via oral gavage at 50 mg/kg/day for two weeks, a dose previously validated for efficacy and tolerability [29]. The anti-mouse PD-L1 monoclonal antibody (clone 10F.9G2; Bio X Cell) was administered intraperitoneally at 200 μg per dose (around 10 mg/kg), three times per week, in accordance with established protocols[126]. Irradiation was performed approximately one hour following drug administration to maintain consistent timing across all relevant treatment arms[127].

Peripheral blood was collected via submandibular bleeding at three time points: baseline (prior to treatment), mid-treatment (week 2), and post-treatment (week 3), to evaluate serum IFN-γ levels as a marker of systemic immune activation. At the study endpoint, mice were euthanized, and tumors were harvested for downstream analysis. Tumor-infiltrating lymphocytes were quantified by flow cytometry, while tumor sections were processed for immunohistochemical (IHC) staining to assess immune-related and proliferation-associated markers.

4.2.9 IMMUNOHISTOCHEMISTRY STAINING

doi:10.6342/NTU202504448

Tumor tissues collected from treated mice were first gently rinsed with PBS to remove excess blood and debris. Samples were then fixed in 4% formaldehyde (Mallinckrodt Chemical Co., St. Louis, MO, USA) prepared in PBS to preserve tissue morphology and antigen integrity. Following fixation, the specimens were processed and embedded in paraffin blocks using standard histological techniques. Serial tissue sections, each 6 μm thick, were cut using a microtome and mounted on glass slides for immunohistochemical analysis.

Before antibody staining, sections were deparaffinized through graded xylene and ethanol washes, followed by rehydration in distilled water. Antigen retrieval was performed as required for specific targets. The tissue sections were then incubated with a panel of primary antibodies targeting key immune markers, including CD4 (HS-360 117, Synaptic Systems), CD8 (HS-361 003, Synaptic Systems), monocyte chemoattractant protein-1 (MCP-1, a marker of M1 macrophages; orb323291, Biorbyt), CD80 (an additional M1 macrophage marker; HPA050092, Sigma-Aldrich), iNOS (an additional M1 macrophage marker; PA3-030A, ThermoFisher) and CD206 (a marker of M2 macrophages; ab64693, Abcam).

Antibody binding was visualized using an indirect immunoperoxidase staining method, following the respective manufacturer's protocols. Positive staining was detected by chromogenic development and counterstained where appropriate to enhance tissue contrast. Slides were later

doi:10.6342/NTU202504448

examined under a light microscope for qualitative and semi-quantitative assessment of immune cell infiltration and macrophage polarization.

4.2.10 STATISTICAL ANALYSIS

All experimental procedures were independently repeated a minimum of three times to confirm the reliability and reproducibility of findings. Quantitative data are presented as the mean ± standard deviation (SD), and specific statistical tests applied to each dataset are detailed within the corresponding figure legends. A threshold of $P < 0.05$ was considered statistically significant. The levels of statistical significance are annotated in the figures as follows: $P < 0.05$ (*), $P < 0.01$ (**), $P < 0.001$ (***), and $P < 0.0001$ (****). Error bars in all graphical representations reflect SD values. All statistical evaluations and figure generation were performed using GraphPad Prism software (version 9.5.1, GraphPad Software, Inc., Windows platform).

4.3 RESULTS

4.3.1 EFFICACY AND RADIOSENSTIZATIZING POTENTIAL OF CDK4/6 INHIBITORS IN TNBC

To determine the antiproliferative potency of the CDK4/6 inhibitor abemaciclib in TNBC cell lines, we conducted cell viability assays using MDA-MB-231, MDA-MB-453, and MDA-MB-468 cells treated with a range of abemaciclib concentrations. The half-maximal inhibitory concentrations

doi:10.6342/NTU202504448

(IC_{50}) were calculated to be 12.15 μM for MDA-MB-231, 2.86 μM for MDA-MB-453, and 8.01 μM for MDA-MB-468, indicating differential sensitivity among these TNBC subtypes. Corresponding dose–response curves illustrating the viability profiles are provided in **Figure 4-1**.

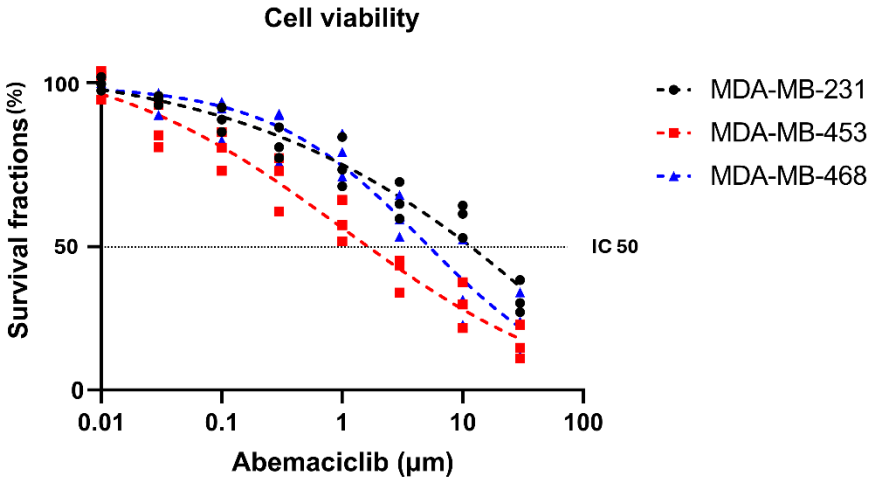

Figure 4-1 Cell viability in MDA-MB-231, MDA-MB-453, and MDA-MB-468 cell lines was assessed using a cell proliferation assay. The corresponding dose–response survival curves are shown.

The effect of abemaciclib have also been tested with clonogenic assay. We used MDA-MB-231, MDA-MB-453, and a murine TNBC cell line, 4T1 treated with different dose of abemaciclib. The result was shown in **Figure 4-2**, which demonstrated that abemaciclib alone is effective in both human and murine TNBC cell lines.

doi:10.6342/NTU202504448

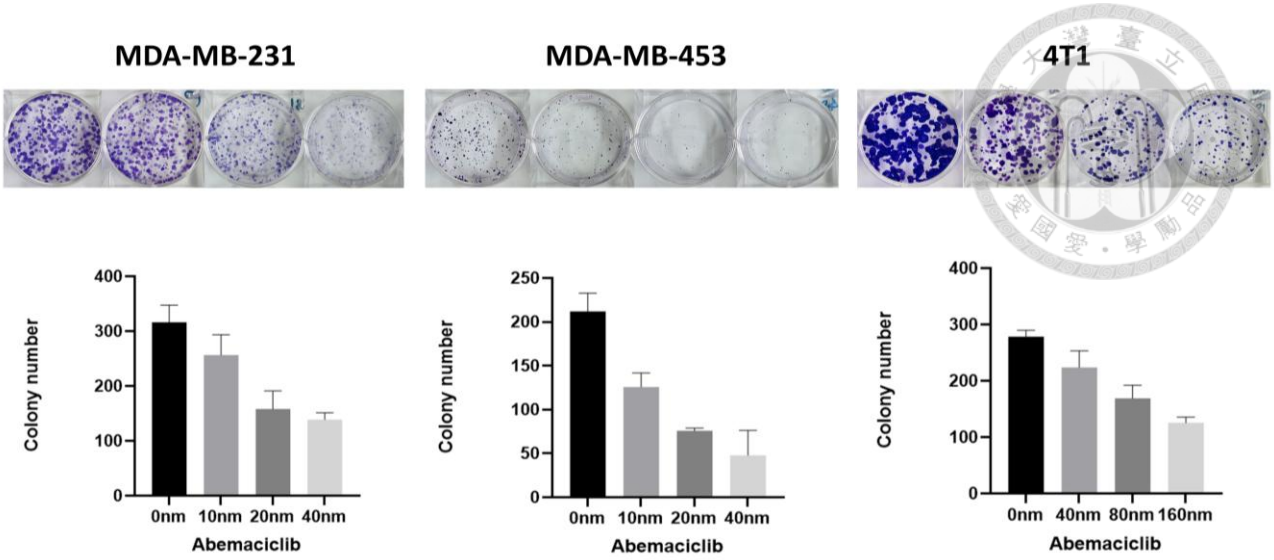

Figure 4-2 Clonogenic assay result of MDA-MB-231, MDA-MB-453, and 4T1 treated with different doses of abemaciclib.

Given that CDK4/6 promotes cell cycle progression through phosphorylation of the RB protein, which releases E2F transcription factors to initiate S phase entry[128], we next examined the expression and phosphorylation status of RB across five TNBC cell lines. Western blot analysis was performed following treatment with control, 4 Gy ionizing radiation, 50 nM abemaciclib, or their combination. Protein lysates were collected 24 hours post-treatment, and levels of total RB and p-RB were evaluated **Figure 4-3**.

doi:10.6342/NTU202504448

All five cell lines expressed detectable levels of RB protein, confirming their suitability for CDK4/6-targeted therapy. Abemaciclib treatment notably suppressed RB phosphorylation, consistent with its mechanism of action. In contrast, exposure to radiation alone did not significantly affect p-RB expression. These findings suggest that abemaciclib effectively disrupts CDK4/6-RB signaling in TNBC cells, whereas radiotherapy alone does not modulate this axis.

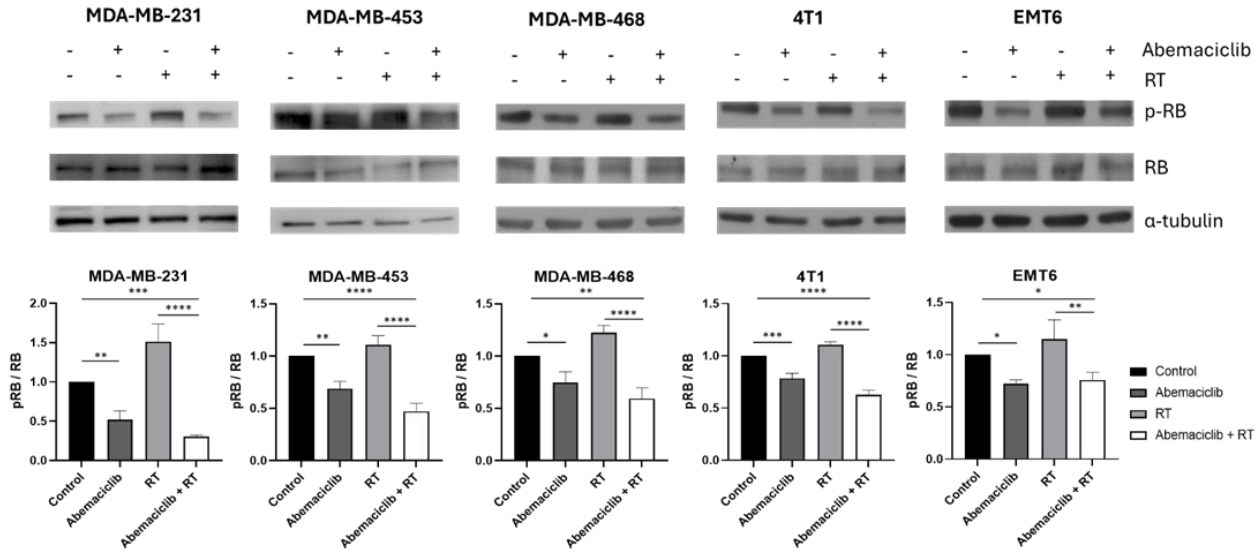

Figure 4-3 The expression of RB and p-RB in five triple-negative breast cancer cell lines treated with differential conditions of abemaciclib and RT using western blot analysis.

The radiosensitizing potential of CDK4/6 inhibitors has been previously explored in luminal breast cancer and several other tumor types[27, 129]. To investigate whether similar synergistic effects can be achieved in TNBC, we examined the ability of abemaciclib to enhance the sensitivity of TNBC cells to ionizing radiation. A clonogenic survival assay was conducted to assess long-term proliferative capacity following combination treatment.

doi:10.6342/NTU202504448

Five TNBC cell lines—MDA-MB-231, MDA-MB-453, MDA-MB-468, 4T1, and EMT6—were pretreated with increasing concentrations of abemaciclib for one hour prior to irradiation. The concentration ranges were tailored to the sensitivity of each cell line: 0–40 nM for MDA-MB-231, MDA-MB-453, and MDA-MB-468; 0–400 nM for 4T1; and 0–800 nM for EMT6. Radiation doses ranged from 0 to 4 Gy for the human cell lines and up to 6 Gy for the murine models. Abemaciclib was administered 1 h before RT. Colonies were fixed, stained, and counted after 7–14 days.

As shown in **Figure 4-4**, the combination of abemaciclib and RT produced a marked synergistic effect across all five TNBC models. This effect was dose-dependent, with higher concentrations of abemaciclib resulting in significantly reduced colony survival compared to RT alone ($P < 0.05$). Survival curves were generated using a linear-quadratic model fitted through nonlinear regression analysis, further supporting the enhanced radiosensitivity conferred by abemaciclib.

These results highlight the potential of CDK4/6 inhibition as a strategy to potentiate radiotherapy in TNBC, a subtype that typically exhibits limited responsiveness to conventional treatments.

doi:10.6342/NTU202504448

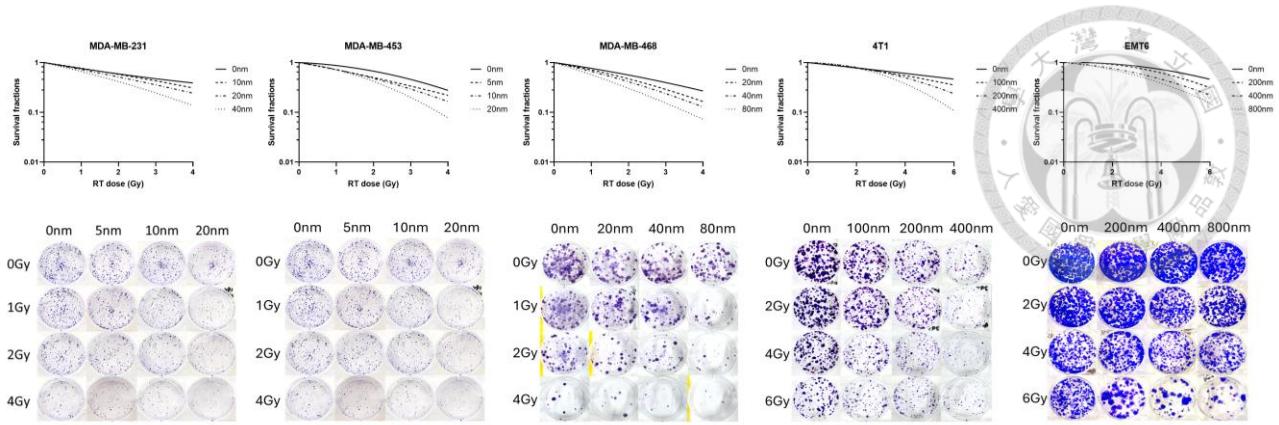

Figure 4-4 Clonogenic assay results for MDA-MB-231, MDA-MB-453, MDA-MB-468, 4T1, and EMT6 cells treated with varying doses of abemaciclib and RT.

In Chapter 3, we demonstrated that the radiosensitizing effect of CDK4/6 inhibitors was mediated, at least in part, by downregulation of radiation-induced DNA repair mechanisms and proliferation-related pathways such as phosphorylated ERK. To explore whether the synergistic effect of abemaciclib with radiation in TNBC involves similar mechanisms as observed in HR+/HER2- breast cancer cells, we examined RAD51 (a DNA double-strand break repair protein) and pERK as representative markers by western blotting in MDA-MB-231 and MDA-MB-453 TNBC cells. We found that RT increased RAD51 and pERK expression, whereas abemaciclib treatment downregulated both proteins. Although we did not investigate the entire signaling network, these findings suggest that the synergistic effect of abemaciclib and RT in TNBC cells may occur through pathways analogous to those previously identified in HR+/HER2- breast cancer. A summary of the western blotting results is shown in **Figure 4-5**.

doi:10.6342/NTU202504448

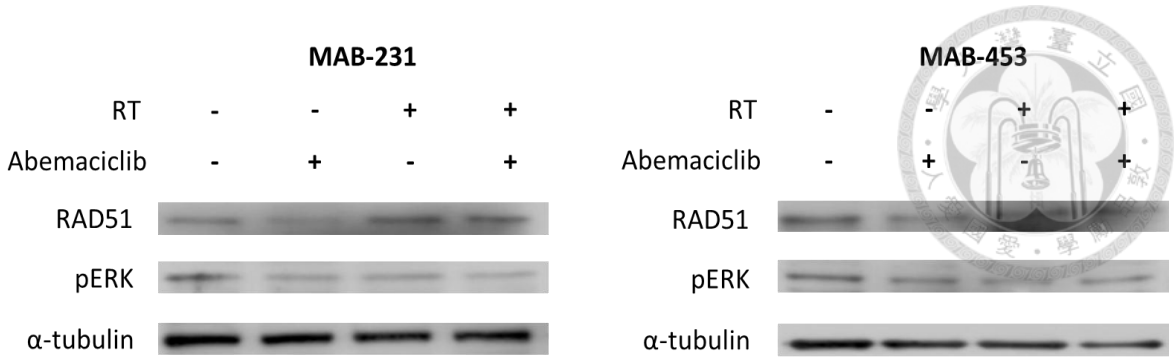

Figure 4-5 Western blot analysis of RAD51 and phosphorylated ERK (pERK) in MDA-MB-231 and MDA-MB-453 TNBC cells treated with control, RT, abemaciclib, or their combination.

4.3.2 RADIOTHERAPY MODULATES CELL SURFACE PD-L1 EXPRESSION IN TNBC CELLS

Radiotherapy and CDK4/6 inhibitors are both known to exert immunomodulatory effects, which has led to growing interest in their potential to enhance immune checkpoint blockade, particularly anti-PD-L1 therapy [38–40]. To explore this possibility, we investigated how RT and the CDK4/6 inhibitor abemaciclib—either alone or in combination—affect cell surface PD-L1 expression in TNBC models.

Five TNBC cell lines (MDA-MB-231, MDA-MB-453, MDA-MB-468, 4T1, and EMT6) were subjected to treatment with increasing doses of RT (0, 8, or 16 Gy), abemaciclib (0, 100, or 200 nM), or a combination of both. For the combination group, abemaciclib was administered one hour prior to RT (8 Gy) to mimic a clinically relevant pretreatment schedule. Flow cytometry was used to quantify surface PD-L1 expression 24 hours post-treatment.

doi:10.6342/NTU202504448

As shown in **Figure 4-6**, exposure to RT alone resulted in a dose-dependent upregulation of PD-L1 across all five cell lines, suggesting that RT may enhance tumor immune evasion by promoting PD-L1 expression. In contrast, treatment with abemaciclib alone did not significantly alter PD-L1 surface levels. When abemaciclib was combined with RT, the resulting PD-L1 expression closely resembled the effect of RT alone, with no additive or antagonistic modulation observed.

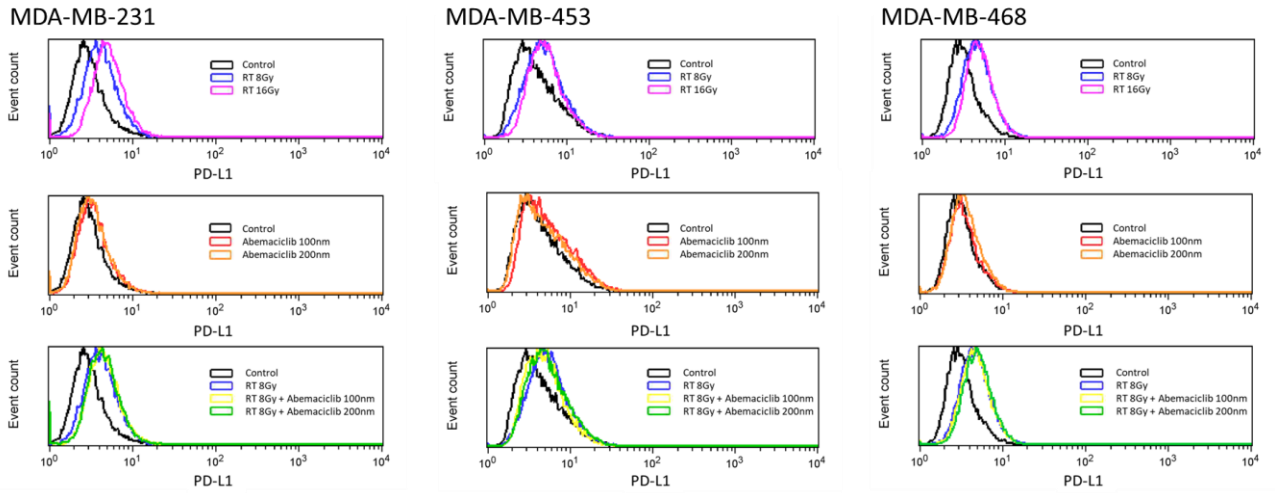

Figure 4-6 Surface PD-L1 expression in human triple negative breast cancer cell lines (in MDA-MB-231, MDA-MB-453, and MDA-MB-468) under different doses of RT and abemaciclib.

The similar finding is also shown in murine TNBC cell lines 4T1 and EMT6 as in **Figure 4-7**. The Mean fluorescence intensity (MFI) bar charts (**Figure 4-8**) quantify PD-L1 expression levels under each condition and presented as mean ± standard deviation. The difference in MFI values was assessed by an unpaired two-tailed t-test. Significance levels: * $P < 0.05$; ** $P < 0.01$; *** $P < 0.001$, **** $P < 0.0001$. These findings suggest that while RT can upregulate PD-L1 expression in TNBC cells, abemaciclib does not interfere with this process. The combination treatment does not further

doi:10.6342/NTU202504448

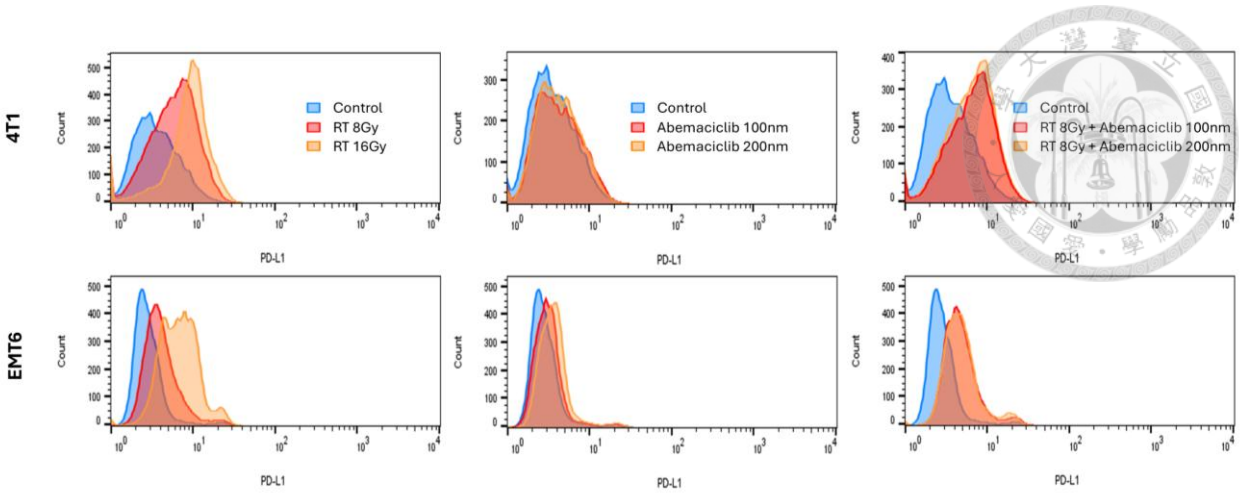

Figure 4-7 Surface PD-L1 expression in 4T1, and EMT6 cells were treated with different doses of RT (8 Gy, 16 Gy, or no RT), different doses of abemaciclib (100 nM, 200 nM, or without abemaciclib), or RT (8 Gy) in combination with abemaciclib at 100 nM or 200 nM, or without treatment.

modulate PD-L1 levels beyond what is induced by RT, indicating that the immunologic impact of CDK4/6 inhibition on PD-L1 expression is minimal in this context.

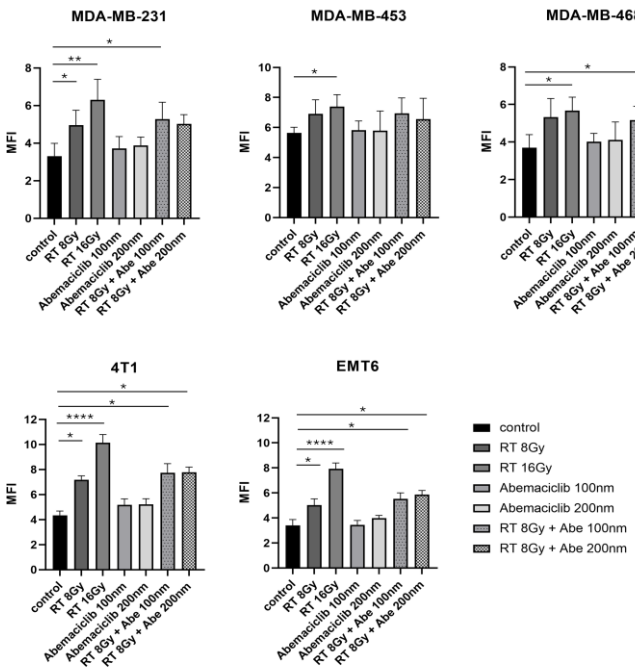

Figure 4-8 Mean fluorescence intensity of PD-L1 expression in TNBC cell lines 24 hours after different treatment combination of RT and abemaciclib.

doi:10.6342/NTU202504448

4.3.3 CDK4/6 INHIBITORS COMBINED WITH RT ENHANCES IN VIVO EFFICACY OF ANTI-PD-L1

While CDK4/6 inhibitors do not induce a strong upregulation of PD-L1 on the tumor cell surface, unlike RT, they have demonstrated immunomodulatory properties that may enhance the effectiveness of immune checkpoint blockade therapies[60, 61, 63]. High-dose RT, in particular, is well recognized for its ability to stimulate anti-tumor immunity by increasing antigen presentation, promoting immune cell infiltration, and boosting the overall response to immunotherapy[33, 36].

To investigate whether the combination of CDK4/6 inhibition, RT, and anti-PD-L1 therapy could produce a synergistic antitumor effect, we conducted in vivo experiments using two immunocompetent mouse models—4T1 and EMT6—which recapitulate the immunologic landscape of triple-negative breast cancer. Mice were randomly assigned to eight treatment groups: control, RT alone, abemaciclib alone, aPD-L1 alone, abemaciclib + aPD-L1, abemaciclib + RT, aPD-L1 + RT, and the triple combination of abemaciclib, aPD-L1, and RT. The treatment schedule and dosing strategies are illustrated in **Figure 4-9**.

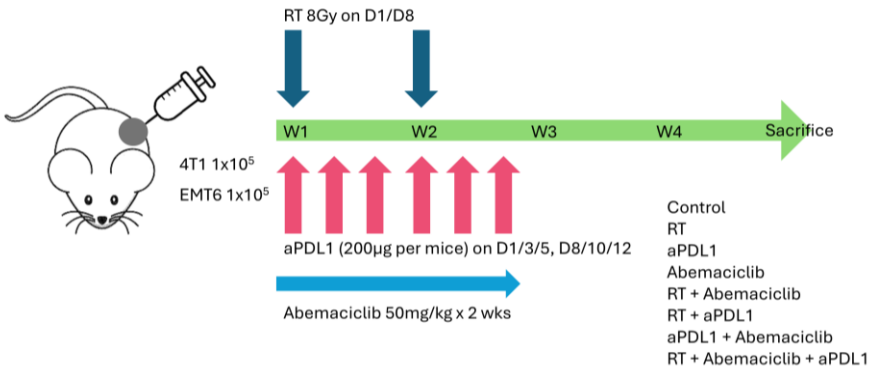

doi:10.6342/NTU202504448

Figure 4-9 The schematic diagram of the therapeutic protocol. 4T1 and EMT6 mouse models were used with female BALB/c mice for the in vivo study. Eight mice were included in each group.

Tumor volumes were measured twice weekly throughout the two-week treatment period. Body weight was monitored concurrently, and no significant weight loss or treatment-related toxicity was observed across the groups, indicating good tolerability (**Figure 4-10**). The tumor volume difference was assessed by two-way analysis of variance (ANOVA) with mixed-effect analysis. Mice were sacrificed at the study endpoint or earlier if tumor volumes reached the ethical limit (1500–2000 mm^3). Tumors were harvested, weighed, and analyzed for treatment response (**Figure 4-11**).

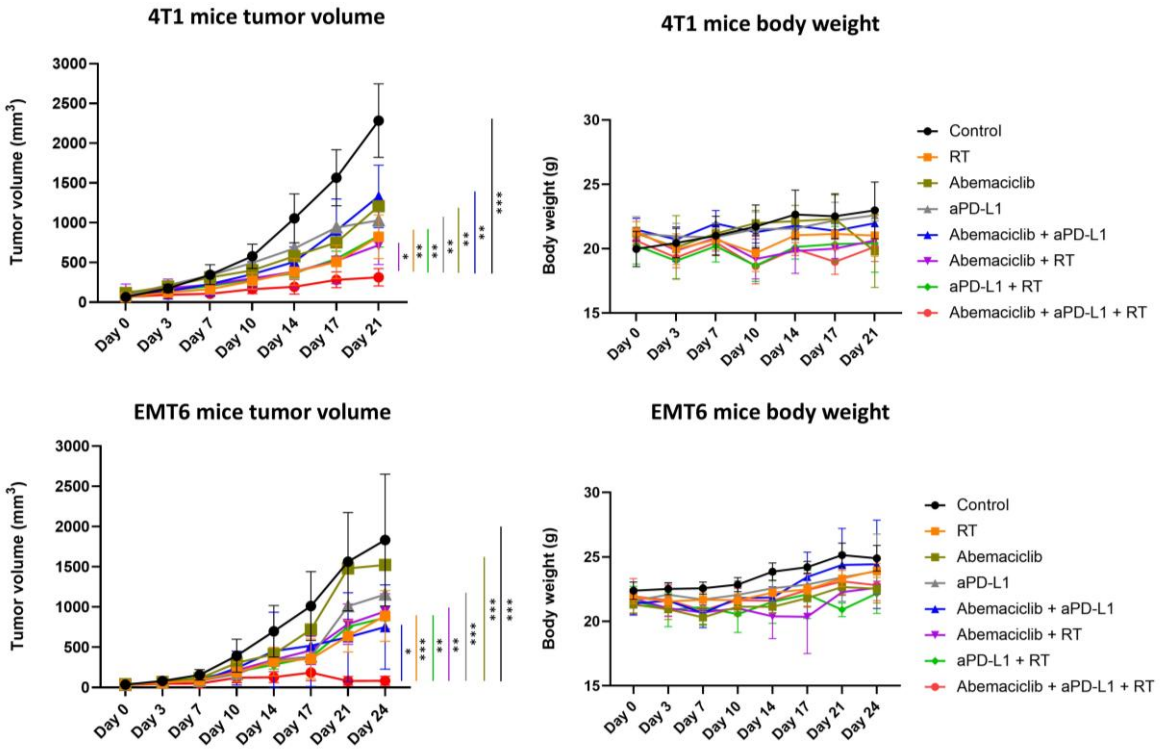

Figure 4-10 The tumor volume and body weight of the two mouse models treated with RT, abemaciclib, aPD-L1, or their dual and triple combinations.

doi:10.6342/NTU202504448

The most notable tumor suppression was observed in mice receiving the triple combination of abemaciclib, RT, and aPD-L1. This group demonstrated a significant reduction in tumor volume compared to all other treatment groups (all $P < 0.05$). In both the 4T1 and EMT6 models, tumor weights were markedly lower in the triple therapy group relative to the control group ($P < 0.001$ and $P < 0.0001$, respectively), as shown in **Figure 4-10** and **Figure 4-11**. Moreover, when compared to all single and dual therapy combinations, the triple regimen consistently produced the greatest reduction in tumor burden ($P < 0.05$), underscoring its superior antitumor efficacy.

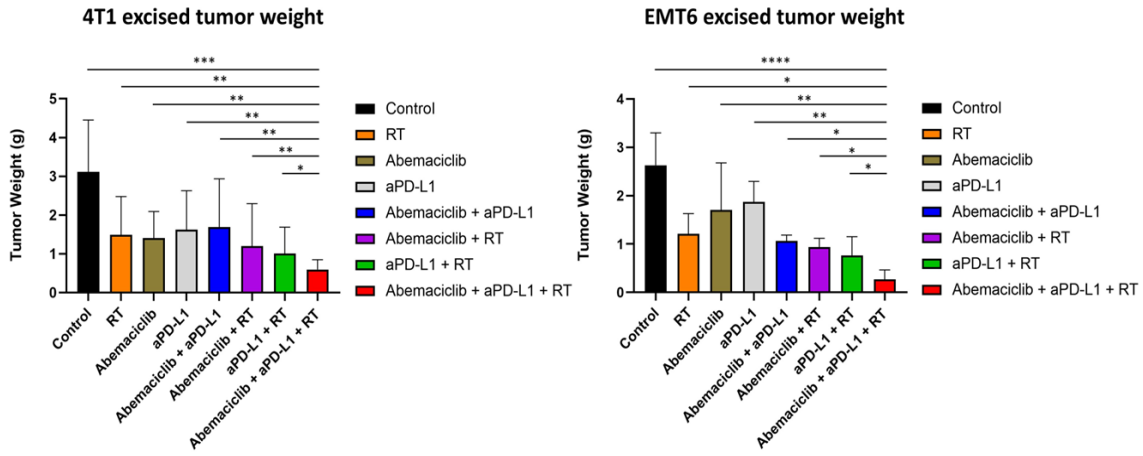

Figure 4-11 The excised tumor weight after euthanasia.

Interestingly, no significant differences in tumor control were observed among the single-agent groups (abemaciclib alone, RT alone, or aPD-L1 alone) or between any of the dual-agent combinations. These findings emphasize that the enhanced therapeutic benefit is specific to the triple combination approach, rather than additive effects from dual therapies.

doi:10.6342/NTU202504448

4.3.4 COMBINED CDK4/6 INHIBITIOR, RT, AND ANTI-PD-L1 INCREASED CIRCULATING IFN-γ

In addition to evaluating tumor growth and immune cell infiltration, we also assessed systemic immune activation by monitoring circulating cytokine levels throughout the treatment course. Interferon-gamma was chosen as a key biomarker, given its central role in orchestrating anti-tumor immunity and mediating the effects of immunotherapies. As a pro-inflammatory cytokine, IFN-γ is frequently elevated in response to immune checkpoint blockade and is associated with enhanced T-cell activation and antitumor efficacy[130]. To explore the impact of each therapeutic regimen on systemic immune responses, we quantified serum IFN-γ concentrations in the 4T1 immunocompetent mouse model.

Peripheral blood was collected at three time points—prior to treatment initiation, during active therapy (week 2), and after treatment completion (week 3) as shown in **Figure 4-12**. IFN-γ levels were measured using an ELISA. The temporal changes in circulating IFN-γ concentrations for each treatment group are illustrated in **Figure 4-13**.

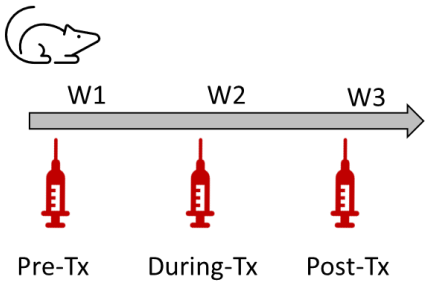

Figure 4-12 Blood sample collection time point

doi:10.6342/NTU202504448

In mice receiving vehicle control, abemaciclib monotherapy, or anti-PD-L1 alone, IFN-γ levels remained largely unchanged across all time points, indicating minimal systemic immune activation. Modest, non-significant increases in IFN-γ were observed in mice treated with RT alone, the abemaciclib + aPD-L1 combination, abemaciclib + RT, and RT + aPD-L1, suggesting a limited enhancement of immune activity with dual-modality regimens.

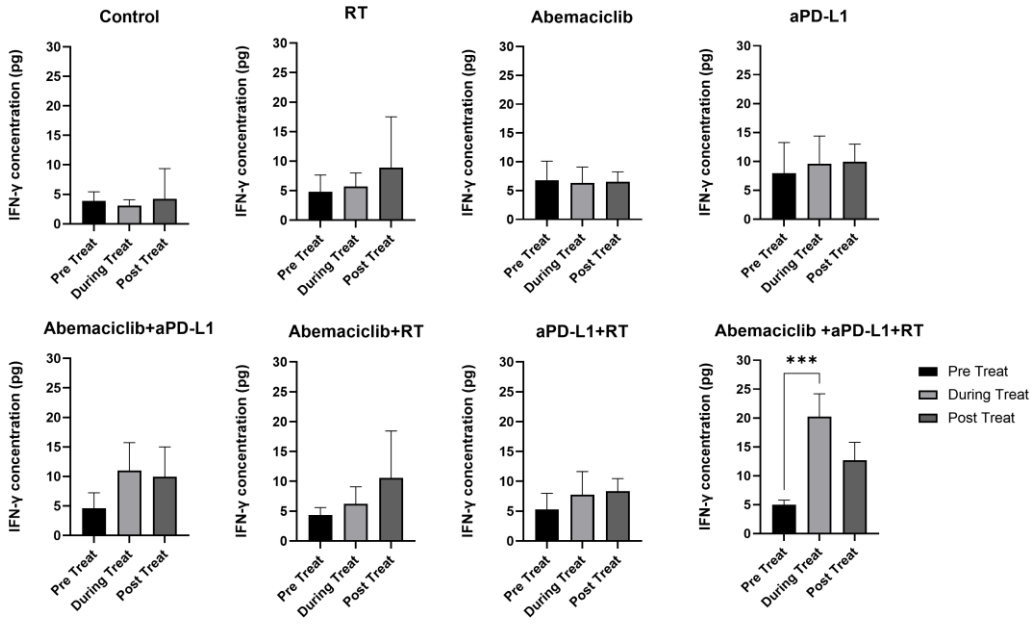

Figure 4-13 Circulating IFN-γ levels before, during, and after treatment with different combinations of RT, abemaciclib, and anti-PD-L1 antibody (aPD-L1).

In contrast, mice treated with the triple combination of abemaciclib, RT, and anti-PD-L1 antibody exhibited a robust elevation in circulating IFN-γ levels during the treatment phase, with a statistically significant increase compared to baseline ($P < 0.001$). Notably, IFN-γ levels declined

doi:10.6342/NTU202504448

following the cessation of therapy, indicating that the immune response was treatment-dependent and temporally regulated.

These findings suggest that the integration of CDK4/6 inhibition and radiotherapy significantly amplifies the immunostimulatory effects of anti-PD-L1 therapy, resulting in enhanced systemic immune activation as evidenced by increased IFN-γ production. This systemic response may contribute to the superior antitumor efficacy observed with the triple combination strategy.

4.3.5 TRIPLE COMBINATION THERAPY MODULATE TUMOR MICROENVIRONMENT

Our results indicate that the triple combination of abemaciclib, anti-PD-L1, and radiotherapy not only improves antitumor efficacy but also modulates the systemic immune response. To further investigate how this regimen alters the tumor microenvironment, we analyzed immune cell populations in tumors excised from the 4T1 model immediately after treatment (as shown in **Figure 4-14**).

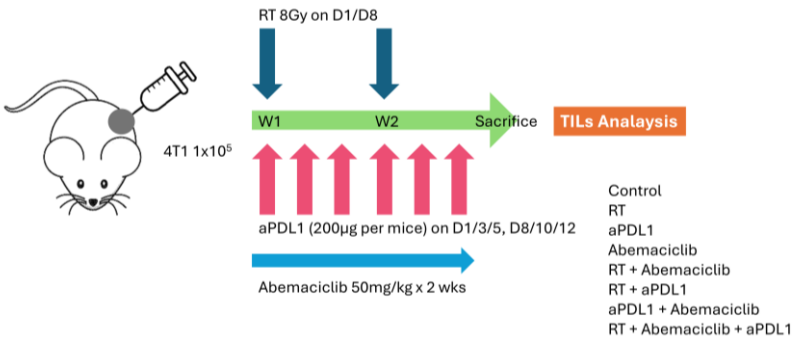

Figure 4-14 TILs were analyzed from 4T1 tumors collected on day 15 after treatment with control, RT, abemaciclib, aPD-L1, or their combinations.

doi:10.6342/NTU202504448

We characterized several TIL subsets, including $CD4^+$ and $CD8^+$ T cells, macrophages, myeloid-derived suppressor cells (MDSCs), and regulatory T cells (Tregs) with gating strategies detailed in **Figure 4-15.** The quantification result for TILs were shown in **Figure 4-16**, **4-17**, and **4-18.**

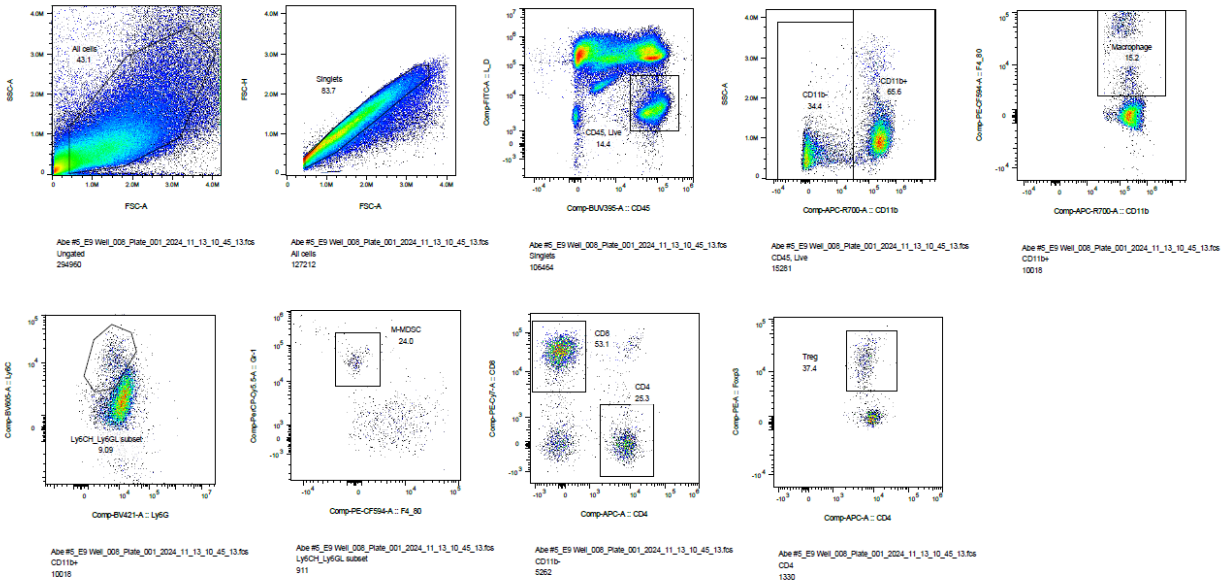

Figure 4-15 The gating strategy of tumor-infiltrating lymphocytes.

Remarkably, tumors treated with the triple therapy showed a significant increase in $CD4^+$ T cell infiltration compared to the control, as well as all single- and dual-treatment groups (**Figure 4-16**; $P < 0.0001$–$P < 0.001$). Similarly, the proportion of $CD8^+$ T cells was significantly elevated in the triple combination group relative to other treatments (**Figure 4-16**; all $P < 0.05$).

doi:10.6342/NTU202504448

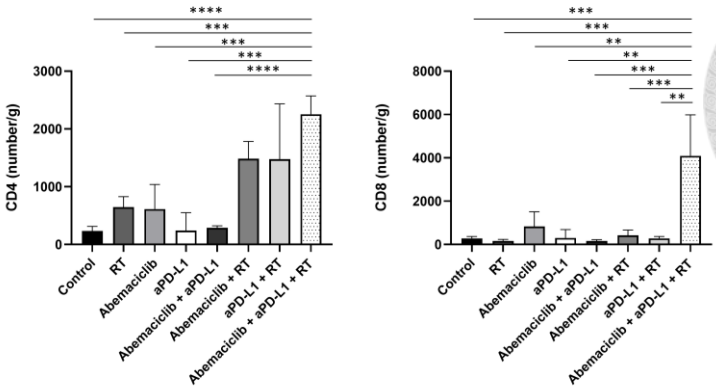

Figure 4-16 Quantification of CD4+ and CD8+ T cells from 4T1 mouse model treated with different strategies

Additionally, the number of tumor-associated macrophages was higher in the triple therapy group when compared to controls and all dual-modality arms (**Figure 4-17**; *P* ranging from < 0.05 to < 0.001). In contrast, the frequencies of Tregs, M-MDSCs, and the CD8/Treg ratio remained consistent across the different treatment conditions (**Figure 4-18**).

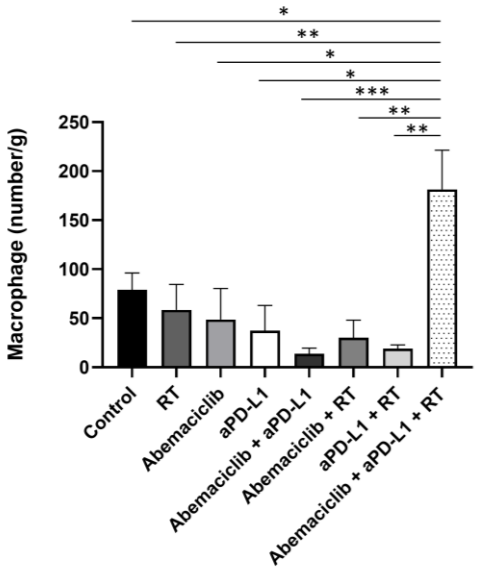

Figure 4-17 Quantification of macrophages from 4T1 mouse model treated with different strategies

doi:10.6342/NTU202504448

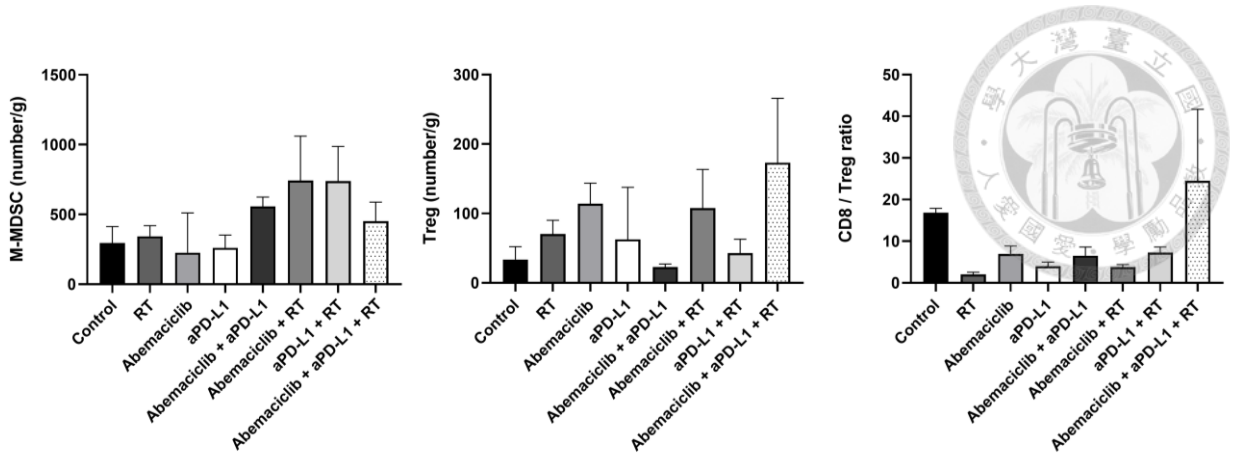

Figure 4-18 Quantification of M-MDSC, Treg and CD8/Treg ratio from 4T1 mouse model treated with different strategies

To validate these immune cell findings and further assess tumor PD-L1 expression, we performed IHC staining on tumor samples from both 4T1 and EMT6 mouse models. PD-L1 expression was significantly upregulated in tumors receiving RT alone, in combination with abemaciclib or anti-PD-L1, and in the triple combination group, relative to control tumors (**Figure 4-19**). In contrast, treatments involving abemaciclib or anti-PD-L1 alone did not alter PD-L1 levels.

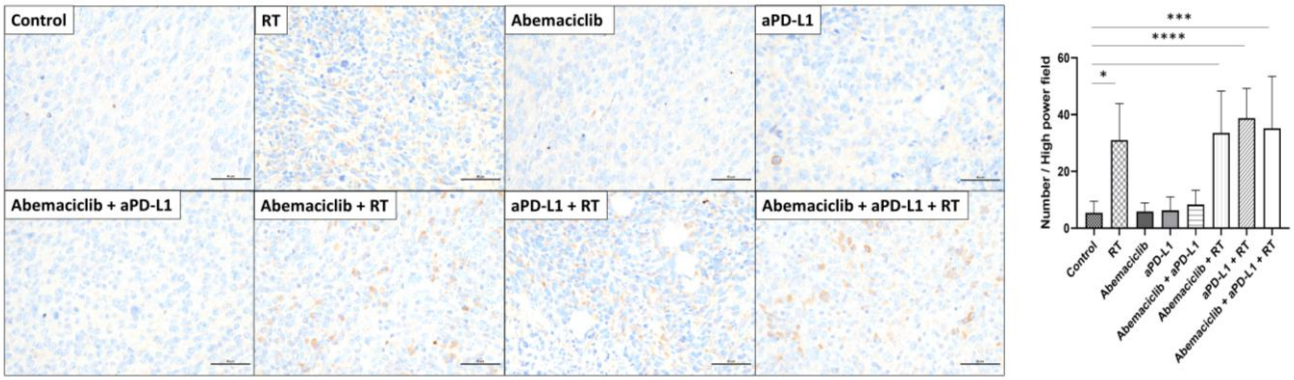

Figure 4-19 Immunohistochemical staining of PD-L1 in tumors (EMT6 immunocompetent mouse model) following treatment with abemaciclib, RT, and anti-PD-L1 antibody (aPD-L1).

doi:10.6342/NTU202504448

We aimed to further verity the TILs finding in both 4T1 and EMT6 models. Using IHC staining on the resected tumors from 4T1 and EMT6 mouse model, we confirmed that the triple treatment markedly increased both $CD4^+$ and $CD8^+$ T cell populations compared with all other groups (**Figures 4-20** and **Figure 4-21**; *P* values ranging from < 0.0001 to < 0.01). In the 4T1 mouse model, the number of $CD4^+$ T cells was significantly elevated in the triple-combination treatment group compared with all other groups. Specifically, it was higher than in the control (P < 0.01), RT alone (P < 0.0001), abemaciclib alone (P < 0.001), aPD-L1 alone (P < 0.0001), abemaciclib + aPD-L1 (P < 0.0001), abemaciclib + RT (P < 0.0001), and aPD-L1 + RT (P < 0.01) groups (**Figure 4-20**).

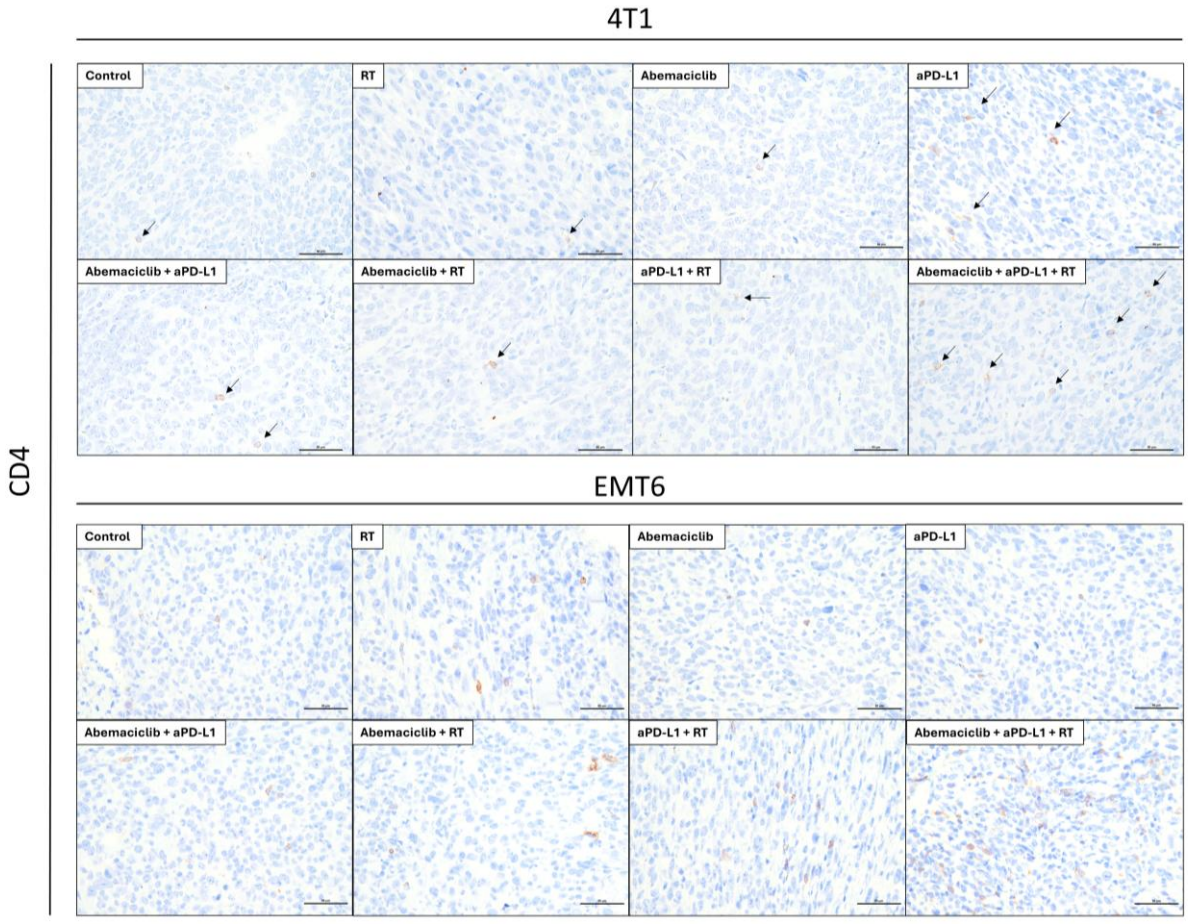

Figure 4-20 Immunohistochemical staining of CD4+ T cells in the different treatment groups

doi:10.6342/NTU202504448

Besides, the triple combination group had a significantly higher number of CD8+ T cells than the other five groups ($P < 0.0001$ compared to all other groups, **Figure 4-21**). The result from EMT6 mouse model showed similar findings.

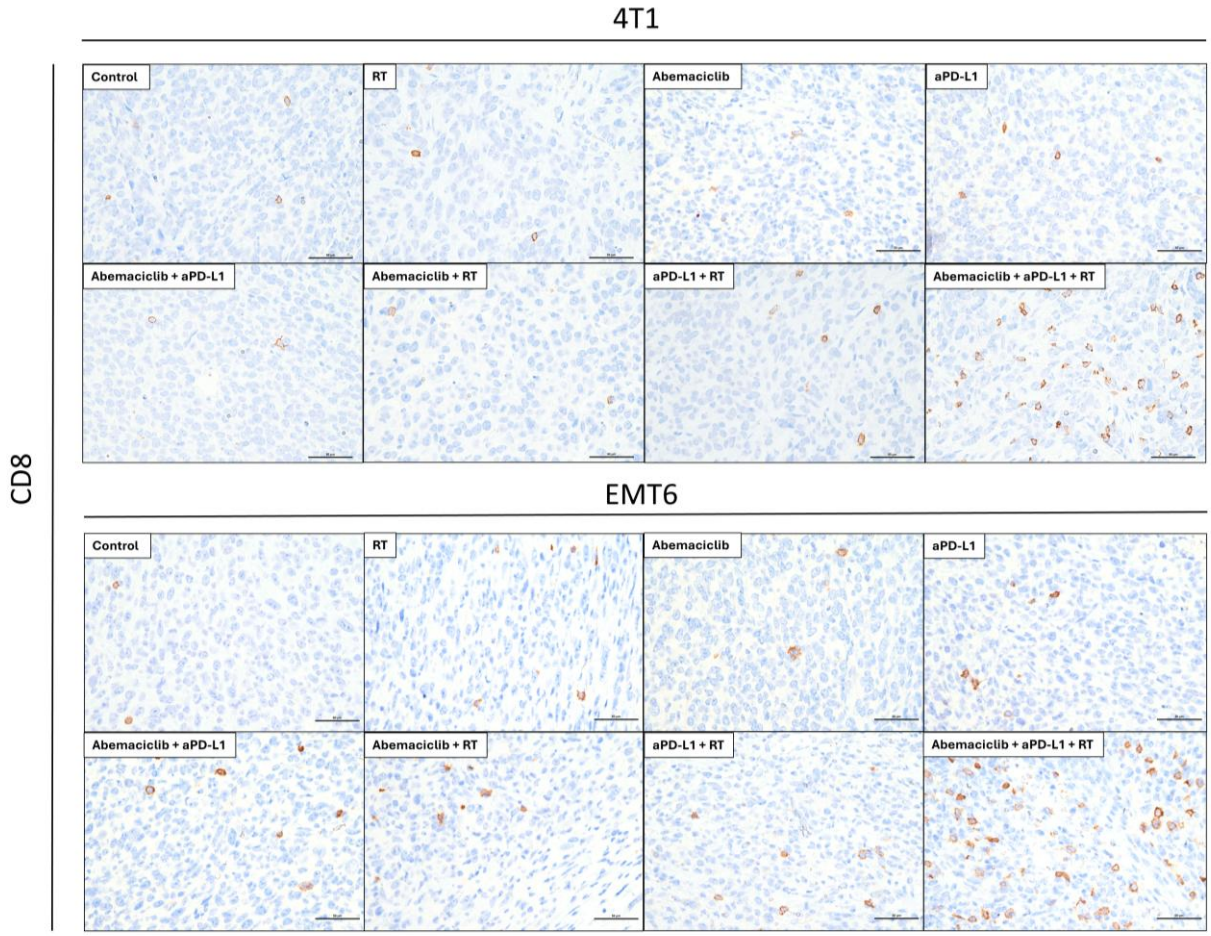

Figure 4-21 Immunohistochemical staining of CD8+ T cells in the different treatment groups

The quantification results of immunohistochemical staining for CD4+ and CD8+ T cells were shown in **Figure 4-22**.

doi:10.6342/NTU202504448

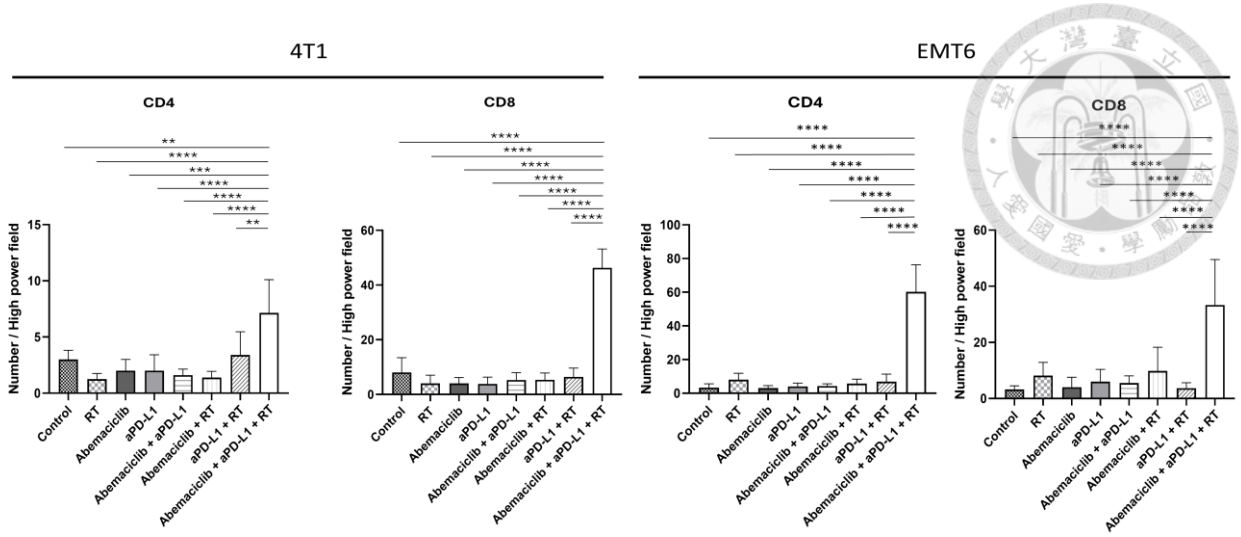

Figure 4-22 Quantification result of immmunohistochemical staining for CD4+ T cells, CD8+ T cells from both 4T1 and EMT6 models in different treatment groups

To dissect the macrophage polarization status, we assessed M1 markers (MCP-1, CD80, and iNOS) and the M2 marker (CD206). The triple therapy induced a significant rise in MCP-1+, CD80+ and iNOS+ cells while simultaneously reducing the proportion of CD206+ macrophages (**Figure 4-23**), indicating a shift toward a pro-inflammatory, immunostimulatory microenvironment.

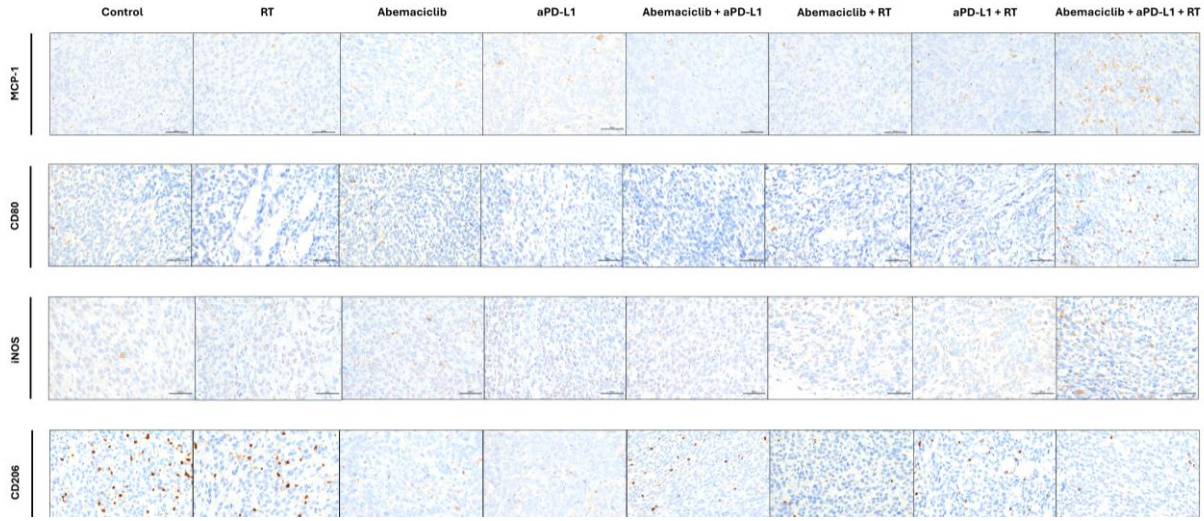

Figure 4-23 Immunohistochemical staining of MCP-1+, CD80+, iNOS+, and CD206+ cells in the different treatment groups from 4T1 mouse model resected tumors.

doi:10.6342/NTU202504448

Consistent results were observed in the EMT6 model via IHC analysis, further underscoring the robust immunomodulatory effect of the triple combination therapy in TNBC (**Figure 4-24**, $P < 0.0001$).

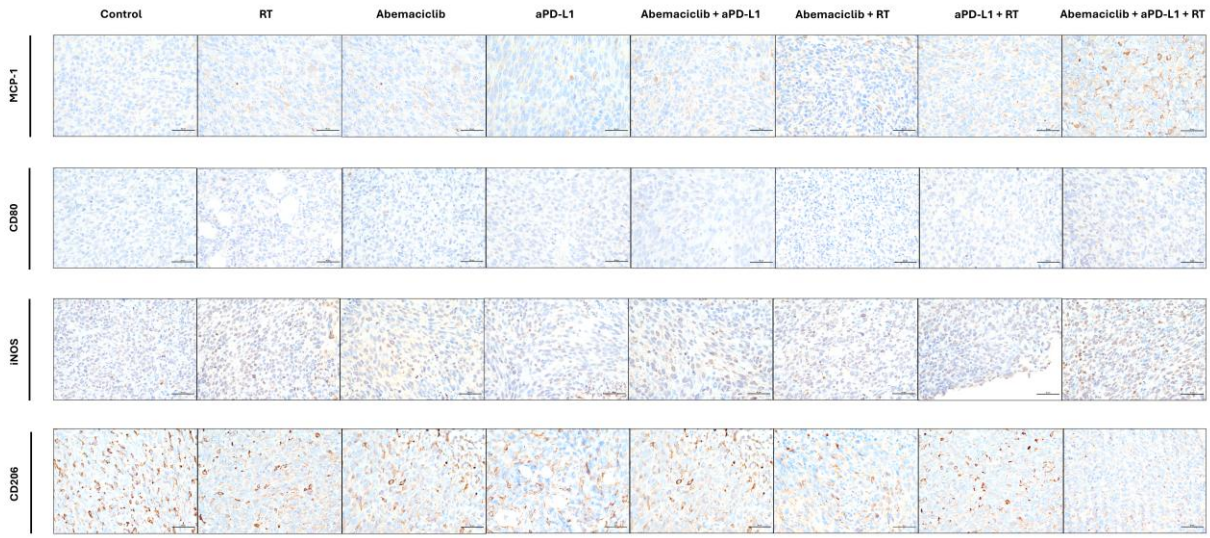

Figure 4-24 Immunohistochemical staining of MCP-1+, CD80+, iNOS+, and CD206+ cells in the different treatment groups from EMT6 mouse model resected tumors.

The quantification results of macrophage related surface markers were summarized in **Figure 4-25** which revealed a statistically significant increase in proinflammatory macrophages in the triple combination group compared to the others.

doi:10.6342/NTU202504448

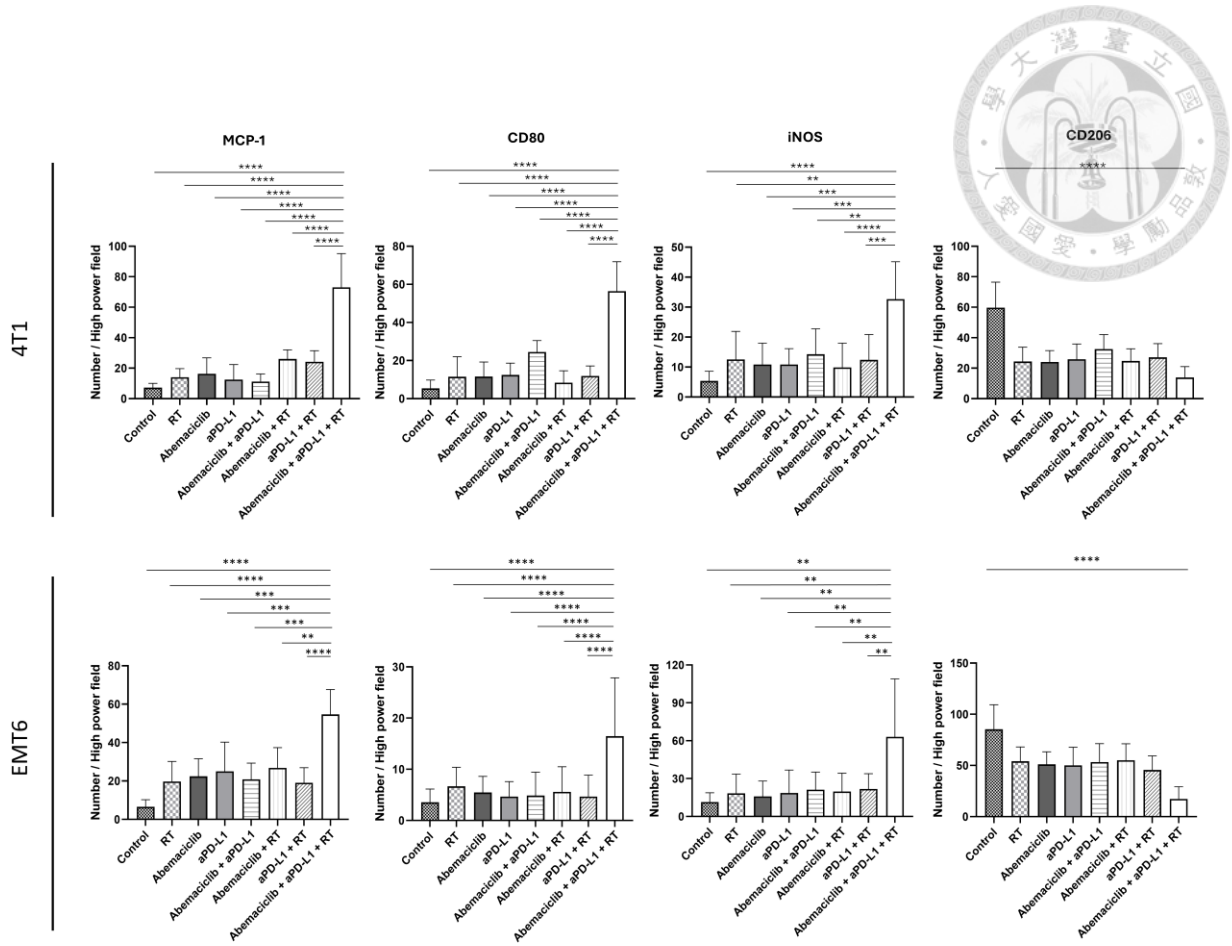

Figure 4-25 The quantification of the average number of MCP-1+, CD80+, iNOS+, and CD206+ cells within the resected tumor in the high-power field of the image for both 4T1 and EMT6 mouse models.

4.4 DISCUSSION

TNBC remains clinically challenging due to its aggressive behavior, poor prognosis, and absence of clearly defined molecular targets. Despite significant advances in precision oncology, including therapies such as PARP inhibitors and antibody-drug conjugates[23], their clinical impact on TNBC has remained limited, largely due to tumor heterogeneity.

doi:10.6342/NTU202504448

The use of CDK4/6 inhibitors in combination with endocrine therapy has proven highly effective in ER-positive breast cancer, notably with palbociclib and letrozole, now established as a first-line regimen[13]. Although RB function is critical for CDK4/6 inhibitor effectiveness, frequent RB loss in TNBC has typically been considered a limitation[131, 132]. Nevertheless, recent preclinical evidence challenges this assumption. For instance, Asghar *et al*.[53] showed differential sensitivity among TNBC cell lines to CDK4/6 inhibitors, with luminal androgen receptor-positive lines responding better than basal-like cell lines. Consistent with these findings, our study demonstrated sensitivity to abemaciclib across multiple TNBC cell lines, including MDA-MB-231, MDA-MB-453, MDA-MB-468, 4T1, and EMT6, highlighting the potential broader applicability of abemaciclib, which has demonstrated greater potency compared to other CDK4/6 inhibitors like palbociclib[133].

The synergistic effects between CDK4/6 inhibitors and RT have been well-characterized, primarily through impairment of DNA repair pathways. Previous studies consistently show delayed DNA damage repair and sustained γH2AX expression following combination therapy, underlining the importance of functional RB status in mediating this synergy[71, 106]. Our study corroborates these findings, demonstrating a robust radiosensitizing effect of abemaciclib in multiple TNBC cell lines that retain RB expression, indicating RB's critical role in this therapeutic context[134].

CDK4/6 inhibitors can profoundly modulate the tumor immune microenvironment, enhancing cytotoxic T-cell functions, antigen presentation, and activation of innate immune responses[57, 59].

doi:10.6342/NTU202504448

Prior studies have reported that CDK4/6 inhibition can increase PD-L1 expression[62], raising the possibility that combining CDK4/6 inhibitors with immune checkpoint inhibitors (ICIs) may provide therapeutic benefit. Deng et al. demonstrated in vivo that dual treatment with ICIs and CDK4/6 blockade suppressed tumor growth, supporting this approach[61]. Nevertheless, the effect of CDK4/6 inhibition on PD-L1 expression appears to be highly context-dependent. In the present study, abemaciclib did not elevate PD-L1 levels in any TNBC model tested. Across the literature, the influence of CDK4/6 inhibitors on PD-L1 expression has been variable. For example, murine 4T1 and EMT6 cells—both RB-intact with relatively high basal PD-L1—represent a context in which Shrestha et al. recently showed that CDK4/6 inhibition reduces rather than induces PD-L1, mediated by a phosphorylated RB–E2F1–SPOP signaling axis[135]. Conversely, PD-L1 upregulation is more often observed in ER-positive or RB-deficient systems, where transcriptional activation overrides SPOP-driven degradation[62]. Other experimental factors, including solvent pH, exposure duration, and metabolic acidification, may further modulate PD-L1 expression dynamics[135]. Moreover, interactions between CDK4/6 inhibitors and speckle-type POZ proteins could also underlie these divergent findings.

A methodological limitation of our work is that in-vitro PD-L1 was quantified only at a single 24-hour time point, and in-vivo PD-L1 was assessed by endpoint IHC, precluding detection of transient or delayed expression changes. Studies indicate that PD-L1 induction after therapy is time-dependent: following irradiation, tumor PD-L1 frequently peaks around 72 hours and declines

doi:10.6342/NTU202504448

by day 7, implying that single-time-point sampling can miss biologically meaningful dynamics[136]. For example, esophageal cancer models exposed to radiotherapy or chemoradiotherapy (carboplatin/paclitaxel) showed transient surface PD-L1 upregulation with a 72-hour maximum that diminished by 120–168 hours; importantly, paired clinical specimens after neoadjuvant chemoradiotherapy did not show sustained PD-L1 elevation, a finding the authors attributed to time-of-sampling effects[137]. Similar timing sensitivity has been reported for cytotoxic agents: formulations of cisplatin increased tumor PD-L1 most robustly at around 72 hours in vivo, emphasizing that drug choice and sampling window materially influence the observed PD-L1 response[138]. Taken together, these kinetics could explain why we observed RT-associated PD-L1 changes by IHC while abemaciclib did not increase PD-L1 at 24 hours in our TNBC models; a later or short-lived induction may have been missed. Future studies should incorporate multi-time-point profiling (e.g., 24, 48, 72, 120 hours, and 7 days) using flow cytometry and IHC, and consider aligning the sequencing of ICIs with known post-RT PD-L1 peaks to optimize synergy.

Clinical trials have highlighted the modest efficacy of single-agent ICIs in TNBC, underscoring the need for combination strategies[9, 29, 139]. Although chemotherapy combined with ICIs has improved outcomes, responses remain suboptimal for many patients, prompting exploration of novel combinational approaches.

doi:10.6342/NTU202504448

As noted above, both CDK4/6 inhibitors and RT have independently been shown to potentiate antitumor immunity. Several preclinical reports suggest that RT, abemaciclib, and PD-L1 blockade each relieve different checkpoints in the cancer–immunity cycle without redundancy. RT generates tumor antigens and triggers type I IFN/STING signaling, but it also induces PD-L1 expression and attracts immunosuppressive myeloid populations, which restricts its efficacy as a monotherapy[140]. CDK4/6 inhibition by abemaciclib promotes antigen presentation, stimulates IFN-response pathways, and fosters inflammatory remodeling of the tumor microenvironment that supports $CD8^+$ T-cell entry; yet, these benefits can still be offset by PD-L1 upregulation. Checkpoint inhibition removes this barrier, but remains ineffective in immunologically "cold" tumors unless antigen release and innate priming have already taken place[106]. When all three modalities are used together, the antigen release from RT, the inflammatory conditioning by abemaciclib, and the checkpoint release by aPD-L1 synergize to produce supra-additive tumor control. Our results mirror this framework: the RT + aPD-L1 doublet offered no advantage over RT alone, with comparable IFN-γ secretion, $CD4^+$/$CD8^+$ T-cell infiltration, and M1 macrophage accumulation. Similarly, RT plus abemaciclib induced only a small, non-significant increase in IFN-γ and $CD8^+$ T cells, consistent with persistent PD-L1–mediated suppression. The abemaciclib + aPD-L1 combination, lacking RT-driven antigen release, appeared insufficient to prime a strong adaptive response, which likely explains its limited benefit. Only the triplet significantly boosted IFN-γ, enhanced immune infiltration, and produced superior tumor control. An independent report reached a comparable conclusion: adding abemaciclib transformed a

doi:10.6342/NTU202504448

partially effective RT + aPD-L1 regimen into a highly active triplet by intensifying local inflammation and augmenting $CD8^+$ infiltration[141]. Collectively, these observations highlight the non-linear nature of the interaction and emphasize the need to target all three axes of immune evasion concurrently.

Our research uniquely investigates the triple combination of abemaciclib, RT, and anti-PD-L1 antibody, demonstrating significant enhancement of systemic IFN-γ production. This cytokine is a crucial indicator of robust antitumor immunity, mediating effects such as inhibition of MDSCs and polarization of macrophages towards the immunostimulatory M1 phenotype[130]. While previous studies indicated that CDK4/6 inhibitors reduce Treg populations[60], our findings did not show a clear decrease, likely due to RT-induced counteracting effects[142].

Notably, the triple combination significantly elevated the infiltration of CD4+ and CD8+ T cells, alongside an increase in pro-inflammatory macrophages (MCP-1+, CD80+ and iNOS+) and a decrease in immunosuppressive M2 macrophages (CD206+), collectively indicating a profound immunomodulatory shift. Although MCP-1, CD80, and CD206 were employed to distinguish macrophage phenotypes, each has inherent limitations. MCP-1, often linked with M1 polarization, is highly context-dependent and can also contribute to tumor progression by recruiting monocytes that later differentiate into M2-like macrophages[143]. CD80 and CD206 are commonly recognized as M1 and M2 indicators, respectively[144-146], but they capture only a fraction of macrophage

doi:10.6342/NTU202504448

diversity. To address this, we also evaluated iNOS, a functional hallmark of M1 macrophages, and observed that its staining pattern in both 4T1 and EMT6 tumors mirrored the distribution of CD80 and MCP-1, reinforcing evidence of M1-oriented reprogramming under triple therapy with abemaciclib, RT, and aPD-L1[147, 148]. Still, the dichotomous M1/M2 framework is increasingly viewed as overly simplistic, since tumor-associated macrophages frequently exhibit mixed or intermediate states; reliance on single markers risks misinterpretation. Accordingly, current consensus emphasizes multi-marker validation—incorporating additional proteins such as MHC class II and arginase 1 [148, 149]—together with functional assays and transcriptomic or metabolic profiling to more robustly define macrophage reprogramming. Although macrophage phenotypes were characterized using MCP-1, CD80, iNOS and CD206 markers, these markers alone may not comprehensively define macrophage polarization due to their context-dependent expression patterns[143, 144, 146]. Further functional studies and additional phenotypic markers are necessary for complete validation.

In the clinical trial reported by Rugo et al. [121], the combination of abemaciclib with pembrolizumab demonstrated encouraging efficacy but was also associated with substantial grade ≥ 3 adverse events in patients with hormone receptor–positive, HER2-negative metastatic breast cancer. Based on this observation, we deliberately applied sub-IC_{50} doses (100–200 nM) in vitro and the lowest effective murine regimen (50 mg/kg once daily) of abemaciclib[9, 73, 123]. Even at these attenuated levels, abemaciclib enhanced the radiosensitivity of TNBC cells and—when paired with

doi:10.6342/NTU202504448

two 8 Gy fractions of RT plus aPD-L1—improved tumor control without detectable toxicity. Collectively, these findings indicate that future clinical investigations combining CDK4/6 inhibitors with RT and PD-L1 blockade should begin with the minimal feasible abemaciclib exposure and consider upward titration only after confirming safety.

One limitation of this study is that immune activation was assessed solely through serum IFN-γ. We did not measure chemokines in the CXCL9/10/11–CXCR3 pathway, which play a critical role in recruiting $CXCR3^+$ effector T cells and in predicting responses to RT combined with ICIs [150, 151]. Similarly, tumor necrosis factor (TNF)-α influences antigen presentation and T-cell activity but can exert context-dependent, dual effects[152]. Future investigations will therefore incorporate multiplex analyses of CXCL9/10/11, TNF-α, and related mediators to yield a more complete picture of treatment-driven immune modulation.

4.5 SUMMARY

In conclusion, our study provides evidence that combining CDK4/6 inhibition with RT and anti-PD-L1 therapy represents a promising therapeutic approach for treating TNBC. Using immunocompetent murine models (4T1 and EMT6), we demonstrated that this triple therapy effectively suppressed tumor growth and enhanced antitumor immunity. Notably, the treatment significantly elevated systemic IFN-γ levels and increased the infiltration of CD4+ T cells, CD8+ T cells, and pro-inflammatory M1 macrophages within tumors, suggesting a potent reprogramming of

doi:10.6342/NTU202504448

the tumor microenvironment towards an immunostimulatory phenotype (**Figure 4-25**). Further clinical studies are necessary to validate the therapeutic benefits of this combination strategy in patients with advanced or metastatic TNBC.

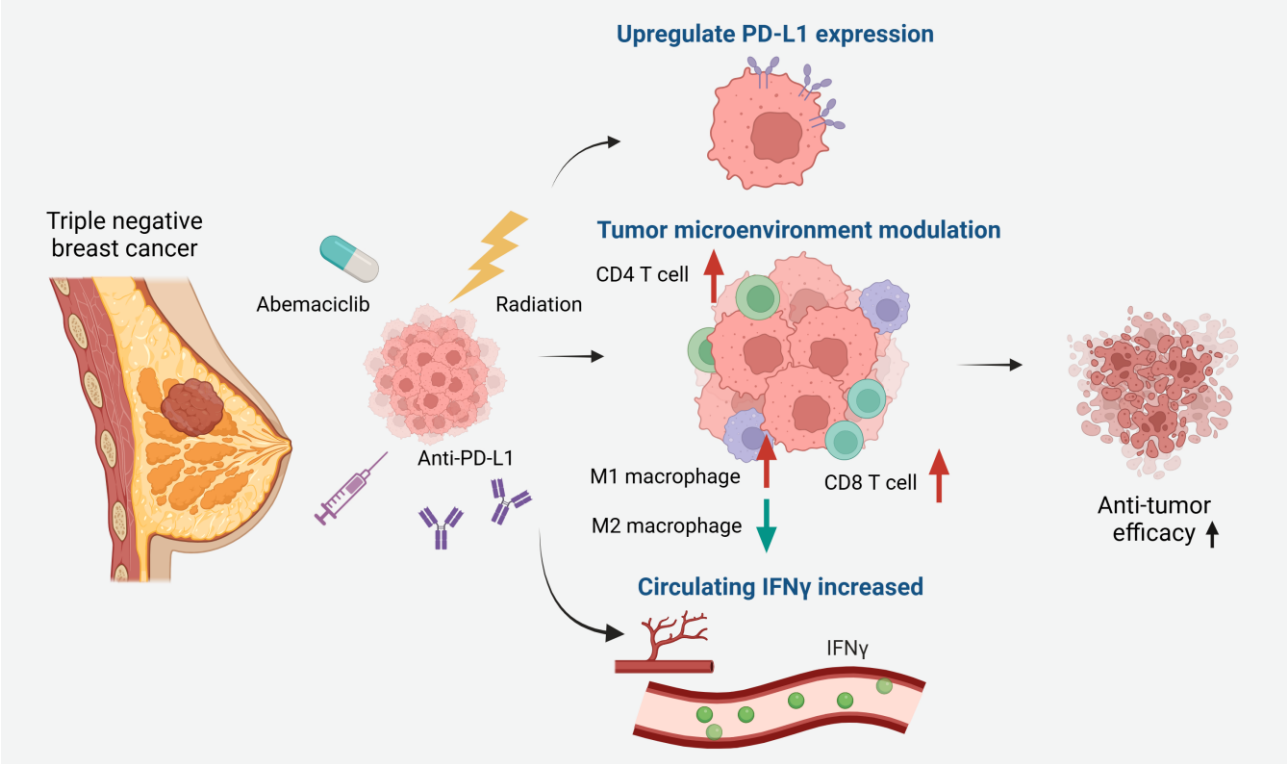

Figure 4-26 Modulation of the tumor microenvironment enhances antitumor efficacy in TNBC through triple combination therapy

doi:10.6342/NTU202504448

CHAPTER 5. CONCLUSION

This thesis aimed to explore and optimize therapeutic strategies for breast cancer treatment by investigating the clinical impact of radiotherapy in early breast cancer and bridging these clinical insights with preclinical evaluations of targeted and immunotherapeutic approaches. We sought to identify effective combinations of radiotherapy with CDK4/6 inhibitors and immunotherapy, thereby connecting clinical practice to innovative therapeutic strategies for improving patient outcomes across different breast cancer subtypes. Our goal was to provide comprehensive insights that could facilitate the development of personalized treatment regimens for patients with varying breast cancer profiles.

In Chapter 2, we analyzed clinical outcomes for patients with early breast cancer receiving modern systemic therapies combined with various radiotherapy approaches. Our findings indicated that SCF-RT alone yielded comparable clinical outcomes to more extensive regional nodal irradiation strategies. Furthermore, additional axillary radiotherapy did not significantly improve outcomes in pathologically N3 patients, suggesting that intensive systemic therapies might be more beneficial than expanding radiotherapy fields in high-risk patients. These clinical insights provided foundational evidence guiding our subsequent preclinical studies, emphasizing the need for more targeted and individualized therapeutic approaches. Our results underscore the importance of balancing

doi:10.6342/NTU202504448

therapeutic efficacy with minimizing unnecessary treatment exposure to enhance patient quality of life.

Chapter 3 focused on the biological mechanisms underlying the radiosensitizing effects of CDK4/6 inhibitors in HR-positive, HER2-negative breast cancer. Our data revealed that CDK4/6 inhibitors significantly enhanced radiosensitivity through suppression of radiation-induced ERK and NF-κB/c-Myc signaling pathways and impaired DNA-DSB repair. These findings highlighted crucial molecular interactions contributing to improved therapeutic efficacy, supporting potential clinical translation to enhance radiotherapy outcomes. This mechanistic understanding provides a strong rationale for integrating CDK4/6 inhibitors into clinical protocols to potentially improve patient responses to radiotherapy.

In Chapter 4, we explored the combined treatment strategy of CDK4/6 inhibitors, radiotherapy, and anti-PD-L1 therapy in immunocompetent TNBC mouse models (4T1 and EMT6). This triple combination demonstrated marked tumor suppression, elevated systemic IFN-γ levels, and increased infiltration of immune effector cells, including CD4+ T cells, CD8+ T cells, and pro-inflammatory M1 macrophages. These changes collectively reprogrammed the tumor microenvironment towards enhanced immunostimulatory activity, showing the potential for combination therapies to improve clinical outcomes in aggressive breast cancer subtypes.

doi:10.6342/NTU202504448

Overall, our study emphasizes the significant clinical and biological benefits of integrating CDK4/6 inhibitor, radiotherapy, and immunotherapy in breast cancer management. The results advocate further clinical investigations of these combination strategies to potentially enhance therapeutic outcomes for patients with advanced breast cancer. The insights gained from our approach provide valuable guidance for future translational and clinical research, potentially leading to more effective and personalized breast cancer treatments. Our work has been published in 3 separate peer-reviewed journals and listed in **Related Publications**.

Building on these findings, future work will pursue a systems-level translational program to define and clinically validate a rational radiotherapy + CDK4/6 inhibitor + immune checkpoint inhibitor paradigm. At the preclinical level, we will comprehensively profile the tumor microenvironment by integrating functional assays of tumor-infiltrating immune cells (e.g., cytokine production and cytotoxicity), assessment of phagocytic activity within myeloid subsets, spatial transcriptomics, and multiplex IHC or immunofluorescence together with immune-related gene-expression panels and macrophage-depletion models, to delineate co-stimulatory pathways and intercellular circuits that govern response. In parallel, we aim to progress from retrospective longitudinal cohorts to prospective clinical trials to evaluate safety and incremental efficacy when escalating from doublet to triplet regimens. To enable precise patient stratification and real-time monitoring, we hope to embed translatable liquid biomarkers—circulating tumor cells (CTCs) and circulating tumor DNA (ctDNA)—for treatment response assessment and minimal residual disease

doi:10.6342/NTU202504448

detection. Collectively, this program is designed to convert mechanistic insight into clinically actionable selection and surveillance frameworks, establishing a clear pathway for the personalized deployment of a radio-immuno-cell-cycle strategy in breast cancer.

The major findings of this dissertation have been published as three peer-reviewed original articles in international journals, including ***Journal of the Formosan Medical Association***[153], ***Translational Oncology***[154], and ***Journal of Cellular Biochemistry***[155]. The list of these publications were presented as in **Publications arising from this dissertation**.

doi:10.6342/NTU202504448

PUBLICATIONS ARISING FROM THIE DISSERTATION

1. Yang WC, Chen YH, Lai SF, Wang CC, Kuo SH, Huang CS. Reassessing regional nodal radiotherapy strategies for breast cancer in the context of modern systemic treatments. J Formos Med Assoc. 2025.
2. Yang WC, Wei MF, Lee YH, Huang CS, Kuo SH. Radiosensitizing effects of CDK4/6 inhibitors in hormone receptor-positive and HER2-negative breast cancer mediated downregulation of DNA repair mechanism and NF-κB-signaling pathway. Transl Oncol. 2024;49:102092.
3. Yang WC, Wei MF, Shen YC, Huang CS, Kuo SH. CDK4/6 inhibitors synergize with radiotherapy to prime the tumor microenvironment and enhance the antitumor effect of anti-PD-L1 immunotherapy in triple-negative breast cancer. J Biomed Sci. 2025;32:79.

doi:10.6342/NTU202504448

REFERENCES

[1] Taiwan Cancer Registry Annual Report. 2018.

[2] Chuang SC, Wu GJ, Lu YS, Lin CH, Hsiung CA. Associations between Medical Conditions and Breast Cancer Risk in Asians: A Nationwide Population-Based Study in Taiwan. PLoS One. 2015;10:e0143410.

[3] Perou CM, Sørlie T, Eisen MB, van de Rijn M, Jeffrey SS, Rees CA, et al. Molecular portraits of human breast tumours. Nature. 2000;406:747–52.

[4] Cheang MC, Chia SK, Voduc D, Gao D, Leung S, Snider J, et al. Ki67 index, HER2 status, and prognosis of patients with luminal B breast cancer. J Natl Cancer Inst. 2009;101:736–50.

[5] Goldhirsch A, Winer EP, Coates AS, Gelber RD, Piccart-Gebhart M, Thürlimann B, et al. Personalizing the treatment of women with early breast cancer: highlights of the St Gallen International Expert Consensus on the Primary Therapy of Early Breast Cancer 2013. Ann Oncol. 2013;24:2206–23.

[6] Voduc KD, Cheang MC, Tyldesley S, Gelmon K, Nielsen TO, Kennecke H. Breast cancer subtypes and the risk of local and regional relapse. J Clin Oncol. 2010;28:1684–91.

[7] American Journal of Cancer Committee on Cancer. AJCC Cancer Staging Manual, 8th edition. Springer. 2017.

[8] Turner NC, Ro J, Andre F, Loi S, Verma S, Iwata H, et al. Palbociclib in Hormone-Receptor-Positive Advanced Breast Cancer. N Engl J Med. 2015;373:209–19.

[9] Adams S, Schmid P, Rugo HS, Winer EP, Loirat D, Awada A, et al. Pembrolizumab monotherapy for previously treated metastatic triple-negative breast cancer: cohort A of the phase II KEYNOTE-086 study. Ann Oncol. 2019;30:397 – 404.

doi:10.6342/NTU202504448

[10] Darby S, McGale P, Correa C, Taylor C, Arriagada R, Clarke M, et al. Effect of radiotherapy after breast-conserving surgery on 10-year recurrence and 15-year breast cancer death: meta-analysis of individual patient data for 10,801 women in 17 randomised trials. Lancet. 2011;378:1707–16.

[11] von Minckwitz G, Untch M, Blohmer JU, Costa SD, Eidtmann H, Fasching PA, et al. Definition and impact of pathologic complete response on prognosis after neoadjuvant chemotherapy in various intrinsic breast cancer subtypes. J Clin Oncol. 2012;30:1796–804.

[12] Ignatiadis M, Sotiriou C. Luminal breast cancer: from biology to treatment. Nat Rev Clin Oncol. 2013;10:494–506.

[13] Cottu P, D'Hondt V, Dureau S, Lerebours F, Desmoulins I, Heudel PE, et al. Letrozole and palbociclib versus chemotherapy as neoadjuvant therapy of high-risk luminal breast cancer. Ann Oncol. 2018;29:2334–40.

[14] Finn RS, Crown JP, Lang I, Boer K, Bondarenko IM, Kulyk SO, et al. The cyclin-dependent kinase 4/6 inhibitor palbociclib in combination with letrozole versus letrozole alone as first-line treatment of oestrogen receptor-positive, HER2-negative, advanced breast cancer (PALOMA-1/TRIO-18): a randomised phase 2 study. The Lancet Oncology. 2015;16:25–35.

[15] Matutino A, Amaro C, Verma S. CDK4/6 inhibitors in breast cancer: beyond hormone receptor-positive HER2-negative disease. Ther Adv Med Oncol. 2018;10:1758835918818346.

[16] Malorni L, Shetty PB, De Angelis C, Hilsenbeck S, Rimawi MF, Elledge R, et al. Clinical and biologic features of triple-negative breast cancers in a large cohort of patients with long-term follow-up. Breast Cancer Res Treat. 2012;136:795–804.

[17] Fallahpour S, Navaneelan T, De P, Borgo A. Breast cancer survival by molecular subtype: a population-based analysis of cancer registry data. CMAJ Open. 2017;5:E734–e9.

[18] Banerji S, Cibulskis K, Rangel-Escareno C, Brown KK, Carter SL, Frederick AM, et al. Sequence analysis of mutations and translocations across breast cancer subtypes. Nature. 2012;486:405–9.

doi:10.6342/NTU202504448

[19] Comprehensive molecular portraits of human breast tumours. Nature. 2012;490:61–70.

[20] Bianchini G, Balko JM, Mayer IA, Sanders ME, Gianni L. Triple-negative breast cancer: challenges and opportunities of a heterogeneous disease. Nat Rev Clin Oncol. 2016;13:674–90.

[21] Lehmann BD, Bauer JA, Chen X, Sanders ME, Chakravarthy AB, Shyr Y, et al. Identification of human triple-negative breast cancer subtypes and preclinical models for selection of targeted therapies. J Clin Invest. 2011;121:2750–67.

[22] Lehmann BD, Jovanović B, Chen X, Estrada MV, Johnson KN, Shyr Y, et al. Refinement of Triple-Negative Breast Cancer Molecular Subtypes: Implications for Neoadjuvant Chemotherapy Selection. PLoS One. 2016;11:e0157368.

[23] Drago JZ, Modi S, Chandarlapaty S. Unlocking the potential of antibody-drug conjugates for cancer therapy. Nat Rev Clin Oncol. 2021;18:327–44.

[24] Bianchini G, De Angelis C, Licata L, Gianni L. Treatment landscape of triple-negative breast cancer - expanded options, evolving needs. Nat Rev Clin Oncol. 2021.

[25] Matsumoto H, Thike AA, Li H, Yeong J, Koo SL, Dent RA, et al. Increased CD4 and CD8-positive T cell infiltrate signifies good prognosis in a subset of triple-negative breast cancer. Breast Cancer Res Treat. 2016;156:237–47.

[26] Emens LA, Cruz C, Eder JP, Braiteh F, Chung C, Tolaney SM, et al. Long-term Clinical Outcomes and Biomarker Analyses of Atezolizumab Therapy for Patients With Metastatic Triple-Negative Breast Cancer: A Phase 1 Study. JAMA Oncol. 2019;5:74–82.

[27] Adams S, Loi S, Toppmeyer D, Cescon DW, De Laurentiis M, Nanda R, et al. Pembrolizumab monotherapy for previously untreated, PD-L1-positive, metastatic triple-negative breast cancer: cohort B of the phase II KEYNOTE-086 study. Ann Oncol. 2019;30:405–11.

[28] Galluzzi L, Humeau J, Buqué A, Zitvogel L, Kroemer G. Immunostimulation with chemotherapy in the era of immune checkpoint inhibitors. Nat Rev Clin Oncol. 2020;17:725–41.

doi:10.6342/NTU202504448

[29] Cortes J, Cescon DW, Rugo HS, Nowecki Z, Im SA, Yusof MM, et al. Pembrolizumab plus chemotherapy versus placebo plus chemotherapy for previously untreated locally recurrent inoperable or metastatic triple-negative breast cancer (KEYNOTE-355): a randomised, placebo-controlled, double-blind, phase 3 clinical trial. Lancet. 2020;396:1817–28.

[30] Delaney G, Jacob S, Featherstone C, Barton M. The role of radiotherapy in cancer treatment: estimating optimal utilization from a review of evidence-based clinical guidelines. Cancer. 2005;104:1129–37.

[31] Strasser-Wozak EM, Hartmann BL, Geley S, Sgonc R, Böck G, Santos AJ, et al. Irradiation induces G2/M cell cycle arrest and apoptosis in p53-deficient lymphoblastic leukemia cells without affecting Bcl-2 and Bax expression. Cell Death Differ. 1998;5:687–93.

[32] Eriksson D, Stigbrand T. Radiation-induced cell death mechanisms. Tumour Biol. 2010;31:363–72.

[33] Tang C, Wang X, Soh H, Seyedin S, Cortez MA, Krishnan S, et al. Combining radiation and immunotherapy: a new systemic therapy for solid tumors? Cancer Immunol Res. 2014;2:831–8.

[34] Seyedin SN, Schoenhals JE, Lee DA, Cortez MA, Wang X, Niknam S, et al. Strategies for combining immunotherapy with radiation for anticancer therapy. Immunotherapy. 2015;7:967–80.

[35] Rodriguez-Ruiz ME, Vitale I, Harrington KJ, Melero I, Galluzzi L. Immunological impact of cell death signaling driven by radiation on the tumor microenvironment. Nat Immunol. 2020;21:120–34.

[36] Sharabi AB, Lim M, DeWeese TL, Drake CG. Radiation and checkpoint blockade immunotherapy: radiosensitisation and potential mechanisms of synergy. Lancet Oncol. 2015;16:e498–509.

[37] Theelen W, Peulen HMU, Lalezari F, van der Noort V, de Vries JF, Aerts J, et al. Effect of Pembrolizumab After Stereotactic Body Radiotherapy vs Pembrolizumab Alone on Tumor Response

doi:10.6342/NTU202504448

in Patients With Advanced Non-Small Cell Lung Cancer: Results of the PEMBRO-RT Phase 2 Randomized Clinical Trial. JAMA Oncol. 2019;5:1276–82.

[38] Ho AY, Barker CA, Arnold BB, Powell SN, Hu ZI, Gucalp A, et al. A phase 2 clinical trial assessing the efficacy and safety of pembrolizumab and radiotherapy in patients with metastatic triple-negative breast cancer. Cancer. 2020;126:850–60.

[39] Bollard J, Miguela V, Ruiz de Galarreta M, Venkatesh A, Bian CB, Roberto MP, et al. Palbociclib (PD-0332991), a selective CDK4/6 inhibitor, restricts tumour growth in preclinical models of hepatocellular carcinoma. Gut. 2017;66:1286–96.

[40] Franco J, Balaji U, Freinkman E, Witkiewicz AK, Knudsen ES. Metabolic Reprogramming of Pancreatic Cancer Mediated by CDK4/6 Inhibition Elicits Unique Vulnerabilities. Cell Rep. 2016;14:979–90.

[41] Logan JE, Mostofizadeh N, Desai AJ, E VONE, Conklin D, Konkankit V, et al. PD-0332991, a potent and selective inhibitor of cyclin-dependent kinase 4/6, demonstrates inhibition of proliferation in renal cell carcinoma at nanomolar concentrations and molecular markers predict for sensitivity. Anticancer Res. 2013;33:2997–3004.

[42] Tripathy D, Bardia A, Sellers WR. Ribociclib (LEE011): Mechanism of Action and Clinical Impact of This Selective Cyclin-Dependent Kinase 4/6 Inhibitor in Various Solid Tumors. Clin Cancer Res. 2017;23:3251–62.

[43] Landis MW, Pawlyk BS, Li T, Sicinski P, Hinds PW. Cyclin D1-dependent kinase activity in murine development and mammary tumorigenesis. Cancer Cell. 2006;9:13–22.

[44] Reddy HK, Mettus RV, Rane SG, Graña X, Litvin J, Reddy EP. Cyclin-dependent kinase 4 expression is essential for neu-induced breast tumorigenesis. Cancer Res. 2005;65:10174–8.

[45] Bartkova J, Lukas J, Müller H, Lützhøft D, Strauss M, Bartek J. Cyclin D1 protein expression and function in human breast cancer. Int J Cancer. 1994;57:353–61.

doi:10.6342/NTU202504448

[46] Umekita Y, Ohi Y, Sagara Y, Yoshida H. Overexpression of cyclinD1 predicts for poor prognosis in estrogen receptor-negative breast cancer patients. Int J Cancer. 2002;98:415–8.

[47] Finn RS, Dering J, Conklin D, Kalous O, Cohen DJ, Desai AJ, et al. PD 0332991, a selective cyclin D kinase 4/6 inhibitor, preferentially inhibits proliferation of luminal estrogen receptor-positive human breast cancer cell lines in vitro. Breast Cancer Res. 2009;11:R77.

[48] Johnston S, Puhalla S, Wheatley D, Ring A, Barry P, Holcombe C, et al. Randomized Phase II Study Evaluating Palbociclib in Addition to Letrozole as Neoadjuvant Therapy in Estrogen Receptor-Positive Early Breast Cancer: PALLET Trial. J Clin Oncol. 2019;37:178–89.

[49] Hortobagyi GN, Lacko A, Sohn J, Cruz F, Ruiz Borrego M, Manikhas A, et al. A phase III trial of adjuvant ribociclib plus endocrine therapy versus endocrine therapy alone in patients with HR-positive/HER2-negative early breast cancer: final invasive disease-free survival results from the NATALEE trial. Ann Oncol. 2025;36:149–57.

[50] Johnston SRD, Harbeck N, Hegg R, Toi M, Martin M, Shao ZM, et al. Abemaciclib Combined With Endocrine Therapy for the Adjuvant Treatment of HR+, HER2-, Node-Positive, High-Risk, Early Breast Cancer (monarchE). J Clin Oncol. 2020;38:3987–98.

[51] Witkiewicz AK, Cox D, Knudsen ES. CDK4/6 inhibition provides a potent adjunct to Her2-targeted therapies in preclinical breast cancer models. Genes Cancer. 2014;5:261–72.

[52] Chen F, Zhang Z, Yu Y, Liu Q, Pu F. HSulf-1 and palbociclib exert synergistic antitumor effects on RB-positive triple-negative breast cancer. Int J Oncol. 2020;57:223–36.

[53] Asghar US, Barr AR, Cutts R, Beaney M, Babina I, Sampath D, et al. Single-Cell Dynamics Determines Response to CDK4/6 Inhibition in Triple-Negative Breast Cancer. Clin Cancer Res. 2017;23:5561–72.

[54] Rao SS, Stoehr J, Dokic D, Wan L, Decker JT, Konopka K, et al. Synergistic effect of eribulin and CDK inhibition for the treatment of triple negative breast cancer. Oncotarget. 2017;8:83925–39.

doi:10.6342/NTU202504448

[55] Ni Y, Schmidt KR, Werner BA, Koenig JK, Guldner IH, Schnepp PM, et al. Death effector domain-containing protein induces vulnerability to cell cycle inhibition in triple-negative breast cancer. Nat Commun. 2019;10:2860.

[56] Tan AR, Wright GS, Thummala AR, Danso MA, Popovic L, Pluard TJ, et al. Trilaciclib plus chemotherapy versus chemotherapy alone in patients with metastatic triple-negative breast cancer: a multicentre, randomised, open-label, phase 2 trial. Lancet Oncol. 2019;20:1587–601.

[57] Malumbres M, Sotillo R, Santamaría D, Galán J, Cerezo A, Ortega S, et al. Mammalian cells cycle without the D-type cyclin-dependent kinases Cdk4 and Cdk6. Cell. 2004;118:493–504.

[58] Hu MG, Deshpande A, Enos M, Mao D, Hinds EA, Hu GF, et al. A requirement for cyclin-dependent kinase 6 in thymocyte development and tumorigenesis. Cancer Res. 2009;69:810–8.

[59] Burton DGA, Stolzing A. Cellular senescence: Immunosurveillance and future immunotherapy. Ageing Res Rev. 2018;43:17–25.

[60] Goel S, DeCristo MJ, Watt AC, BrinJones H, Sceneay J, Li BB, et al. CDK4/6 inhibition triggers anti-tumour immunity. Nature. 2017;548:471–5.

[61] Deng J, Wang ES, Jenkins RW, Li S, Dries R, Yates K, et al. CDK4/6 Inhibition Augments Antitumor Immunity by Enhancing T-cell Activation. Cancer Discov. 2018;8:216–33.

[62] Zhang J, Bu X, Wang H, Zhu Y, Geng Y, Nihira NT, et al. Cyclin D-CDK4 kinase destabilizes PD-L1 via cullin 3-SPOP to control cancer immune surveillance. Nature. 2018;553:91–5.

[63] Schaer DA, Beckmann RP, Dempsey JA, Huber L, Forest A, Amaladas N, et al. The CDK4/6 Inhibitor Abemaciclib Induces a T Cell Inflamed Tumor Microenvironment and Enhances the Efficacy of PD-L1 Checkpoint Blockade. Cell Rep. 2018;22:2978–94.

[64] Ameratunga M, Kipps E, Okines AFC, Lopez JS. To Cycle or Fight-CDK4/6 Inhibitors at the Crossroads of Anticancer Immunity. Clin Cancer Res. 2019;25:21–8.

[65] Teh JLF, Aplin AE. Arrested Developments: CDK4/6 Inhibitor Resistance and Alterations in the Tumor Immune Microenvironment. Clin Cancer Res. 2019;25:921–7.

doi:10.6342/NTU202504448

[66] Hurvitz SA, Martin M, Press MF, Chan D, Fernandez-Abad M, Petru E, et al. Potent Cell-Cycle Inhibition and Upregulation of Immune Response with Abemaciclib and Anastrozole in neoMONARCH, Phase II Neoadjuvant Study in HR(+)/HER2(-) Breast Cancer. Clin Cancer Res. 2020;26:566–80.

[67] O'Brien NA, Tomaso ED, Ayala R, Tong L, Issakhanian S, Linnartz R, et al. Abstract 4756: In vivo efficacy of combined targeting of CDK4/6, ER and PI3K signaling in ER+ breast cancer. Cancer Research. 2014;74:4756–.

[68] Kettner NM, Vijayaraghavan S, Durak MG, Bui T, Kohansal M, Ha MJ, et al. Combined Inhibition of STAT3 and DNA Repair in Palbociclib-Resistant ER-Positive Breast Cancer. Clin Cancer Res. 2019;25:3996–4013.

[69] Teo ZL, Versaci S, Dushyanthen S, Caramia F, Savas P, Mintoff CP, et al. Combined CDK4/6 and PI3Kα Inhibition Is Synergistic and Immunogenic in Triple-Negative Breast Cancer. Cancer Res. 2017;77:6340–52.

[70] Gottgens EL, Bussink J, Leszczynska KB, Peters H, Span PN, Hammond EM. Inhibition of CDK4/CDK6 Enhances Radiosensitivity of HPV Negative Head and Neck Squamous Cell Carcinomas. Int J Radiat Oncol Biol Phys. 2019;105:548–58.

[71] Hashizume R, Zhang A, Mueller S, Prados MD, Lulla RR, Goldman S, et al. Inhibition of DNA damage repair by the CDK4/6 inhibitor palbociclib delays irradiated intracranial atypical teratoid rhabdoid tumor and glioblastoma xenograft regrowth. Neuro Oncol. 2016;18:1519–28.

[72] Huang CY, Hsieh FS, Wang CY, Chen LJ, Chang SS, Tsai MH, et al. Palbociclib enhances radiosensitivity of hepatocellular carcinoma and cholangiocarcinoma via inhibiting ataxia telangiectasia-mutated kinase-mediated DNA damage response. Eur J Cancer. 2018;102:10–22.

[73] Naz S, Sowers A, Choudhuri R, Wissler M, Gamson J, Mathias A, et al. Abemaciclib, a Selective CDK4/6 Inhibitor, Enhances the Radiosensitivity of Non-Small Cell Lung Cancer In Vitro and In Vivo. Clin Cancer Res. 2018;24:3994–4005.

doi:10.6342/NTU202504448

[74] Tao Z, Le Blanc JM, Wang C, Zhan T, Zhuang H, Wang P, et al. Coadministration of Trametinib and Palbociclib Radiosensitizes KRAS-Mutant Non-Small Cell Lung Cancers In Vitro and In Vivo. Clin Cancer Res. 2016;22:122–33.

[75] Hans S, Cottu P, Kirova YM. Preliminary results of the association of Palbociclib and radiotherapy in metastatic breast cancer patients. Radiother Oncol. 2018;126:181.

[76] Meattini I, Desideri I, Scotti V, Simontacchi G, Livi L. Ribociclib plus letrozole and concomitant palliative radiotherapy for metastatic breast cancer. Breast. 2018;42:1–2.

[77] Ragaz J, Jackson SM, Le N, Plenderleith IH, Spinelli JJ, Basco VE, et al. Adjuvant radiotherapy and chemotherapy in node-positive premenopausal women with breast cancer. N Engl J Med. 1997;337:956–62.

[78] Overgaard M, Nielsen HM, Tramm T, Højris I, Grantzau TL, Alsner J, et al. Postmastectomy radiotherapy in high-risk breast cancer patients given adjuvant systemic therapy. A 30-year long-term report from the Danish breast cancer cooperative group DBCG 82bc trial. Radiother Oncol. 2022;170:4–13.

[79] McGale P, Taylor C, Correa C, Cutter D, Duane F, Ewertz M, et al. Effect of radiotherapy after mastectomy and axillary surgery on 10-year recurrence and 20-year breast cancer mortality: meta-analysis of individual patient data for 8135 women in 22 randomised trials. Lancet. 2014;383:2127–35.

[80] Whelan TJ, Olivotto IA, Parulekar WR, Ackerman I, Chua BH, Nabid A, et al. Regional Nodal Irradiation in Early-Stage Breast Cancer. N Engl J Med. 2015;373:307–16.

[81] Poortmans PM, Weltens C, Fortpied C, Kirkove C, Peignaux-Casasnovas K, Budach V, et al. Internal mammary and medial supraclavicular lymph node chain irradiation in stage I-III breast cancer (EORTC 22922/10925): 15-year results of a randomised, phase 3 trial. Lancet Oncol. 2020;21:1602–10.

doi:10.6342/NTU202504448

[82] Jagsi R, Pierce L. Radiation therapy to the internal mammary nodal region in breast cancer: the debate continues. Int J Radiat Oncol Biol Phys. 2013;86:813–5.

[83] Bazan JG, White JR. Internal Mammary Nodal Irradiation Debate for Node-Positive Breast Cancer-Has the Needle Moved? JAMA Oncol. 2022;8:780.

[84] Thorsen LB, Offersen BV, Danø H, Berg M, Jensen I, Pedersen AN, et al. DBCG-IMN: A Population-Based Cohort Study on the Effect of Internal Mammary Node Irradiation in Early Node-Positive Breast Cancer. J Clin Oncol. 2016;34:314–20.

[85] Hennequin C, Bossard N, Servagi-Vernat S, Maingon P, Dubois JB, Datchary J, et al. Ten-year survival results of a randomized trial of irradiation of internal mammary nodes after mastectomy. Int J Radiat Oncol Biol Phys. 2013;86:860–6.

[86] Kim YB, Byun HK, Kim DY, Ahn SJ, Lee HS, Park W, et al. Effect of Elective Internal Mammary Node Irradiation on Disease-Free Survival in Women With Node-Positive Breast Cancer: A Randomized Phase 3 Clinical Trial. JAMA Oncol. 2022;8:96–105.

[87] Donker M, van Tienhoven G, Straver ME, Meijnen P, van de Velde CJ, Mansel RE, et al. Radiotherapy or surgery of the axilla after a positive sentinel node in breast cancer (EORTC 10981-22023 AMAROS): a randomised, multicentre, open-label, phase 3 non-inferiority trial. Lancet Oncol. 2014;15:1303–10.

[88] Choi J, Kim YB, Shin KH, Ahn SJ, Lee HS, Park W, et al. Radiation Pneumonitis in Association with Internal Mammary Node Irradiation in Breast Cancer Patients: An Ancillary Result from the KROG 08-06 Study. J Breast Cancer. 2016;19:275–82.

[89] Overgaard M, Hansen PS, Overgaard J, Rose C, Andersson M, Bach F, et al. Postoperative radiotherapy in high-risk premenopausal women with breast cancer who receive adjuvant chemotherapy. Danish Breast Cancer Cooperative Group 82b Trial. N Engl J Med. 1997;337:949–55.

doi:10.6342/NTU202504448

[90] Overgaard M, Jensen MB, Overgaard J, Hansen PS, Rose C, Andersson M, et al. Postoperative radiotherapy in high-risk postmenopausal breast-cancer patients given adjuvant tamoxifen: Danish Breast Cancer Cooperative Group DBCG 82c randomised trial. Lancet. 1999;353:1641–8.

[91] Tseng YD, Uno H, Hughes ME, Niland JC, Wong YN, Theriault R, et al. Biological Subtype Predicts Risk of Locoregional Recurrence After Mastectomy and Impact of Postmastectomy Radiation in a Large National Database. Int J Radiat Oncol Biol Phys. 2015;93:622–30.

[92] Slamon D, Eiermann W, Robert N, Pienkowski T, Martin M, Press M, et al. Adjuvant trastuzumab in HER2-positive breast cancer. N Engl J Med. 2011;365:1273–83.

[93] Bartels SAL, Donker M, Poncet C, Sauvé N, Straver ME, van de Velde CJH, et al. Radiotherapy or Surgery of the Axilla After a Positive Sentinel Node in Breast Cancer: 10-Year Results of the Randomized Controlled EORTC 10981-22023 AMAROS Trial. J Clin Oncol. 2023;41:2159–65.

[94] Lin PH, Kuo WH, Huang AC, Lu YS, Lin CH, Kuo SH, et al. Multiple gene sequencing for risk assessment in patients with early-onset or familial breast cancer. Oncotarget. 2016;7:8310–20.

[95] Hortobagyi GN, Stemmer SM, Burris HA, Yap YS, Sonke GS, Hart L, et al. Overall Survival with Ribociclib plus Letrozole in Advanced Breast Cancer. N Engl J Med. 2022;386:942–50.

[96] Chou TC. Drug combination studies and their synergy quantification using the Chou-Talalay method. Cancer Res. 2010;70:440–6.

[97] Collins A, Yuan L, Kiefer TL, Cheng Q, Lai L, Hill SM. Overexpression of the MT1 melatonin receptor in MCF-7 human breast cancer cells inhibits mammary tumor formation in nude mice. Cancer Lett. 2003;189:49–57.

[98] Zhang M, Zhang L, Hei R, Li X, Cai H, Wu X, et al. CDK inhibitors in cancer therapy, an overview of recent development. Am J Cancer Res. 2021;11:1913–35.

[99] Ahmed KM, Li JJ. NF-kappa B-mediated adaptive resistance to ionizing radiation. Free Radic Biol Med. 2008;44:1–13.

doi:10.6342/NTU202504448

[100] Gabay M, Li Y, Felsher DW. MYC activation is a hallmark of cancer initiation and maintenance. Cold Spring Harb Perspect Med. 2014;4.

[101] Kuo SH WM, lee YS, Tzeng YS, Cheng AL, Huang CS. Overexpression of MAP3K1 is closely associated with the prognosis of patients with hormone receptor-positive early breast cancer. Abstract 502. EACR-AACR-SIC: Special Conference2017.

[102] Ouellette MM, Zhou S, Yan Y. Cell Signaling Pathways That Promote Radioresistance of Cancer Cells. Diagnostics (Basel). 2022;12.

[103] Paramanantham A, Jung EJ, Go SI, Jeong BK, Jung JM, Hong SC, et al. Activated ERK Signaling Is One of the Major Hub Signals Related to the Acquisition of Radiotherapy-Resistant MDA-MB-231 Breast Cancer Cells. Int J Mol Sci. 2021;22.

[104] Petroni G, Buqué A, Yamazaki T, Bloy N, Liberto MD, Chen-Kiang S, et al. Radiotherapy Delivered before CDK4/6 Inhibitors Mediates Superior Therapeutic Effects in ER(+) Breast Cancer. Clin Cancer Res. 2021;27:1855–63.

[105] Pesch AM, Hirsh NH, Chandler BC, Michmerhuizen AR, Ritter CL, Androsiglio MP, et al. Short-term CDK4/6 Inhibition Radiosensitizes Estrogen Receptor-Positive Breast Cancers. Clin Cancer Res. 2020;26:6568–80.

[106] Yang Y, Luo J, Chen X, Yang Z, Mei X, Ma J, et al. CDK4/6 inhibitors: a novel strategy for tumor radiosensitization. J Exp Clin Cancer Res. 2020;39:188.

[107] Jin MH, Oh DY. ATM in DNA repair in cancer. Pharmacol Ther. 2019;203:107391.

[108] Dean JL, McClendon AK, Knudsen ES. Modification of the DNA damage response by therapeutic CDK4/6 inhibition. J Biol Chem. 2012;287:29075–87.

[109] Hagen KR, Zeng X, Lee MY, Tucker Kahn S, Harrison Pitner MK, Zaky SS, et al. Silencing CDK4 radiosensitizes breast cancer cells by promoting apoptosis. Cell Div. 2013;8:10.

[110] Chen P, Lee NV, Hu W, Xu M, Ferre RA, Lam H, et al. Spectrum and Degree of CDK Drug Interactions Predicts Clinical Performance. Mol Cancer Ther. 2016;15:2273–81.

doi:10.6342/NTU202504448

[111] Lawrence T. The nuclear factor NF-kappaB pathway in inflammation. Cold Spring Harb Perspect Biol. 2009;1:a001651.

[112] Sethi G, Ahn KS, Aggarwal BB. Targeting nuclear factor-kappa B activation pathway by thymoquinone: role in suppression of antiapoptotic gene products and enhancement of apoptosis. Mol Cancer Res. 2008;6:1059–70.

[113] Brach MA, Hass R, Sherman ML, Gunji H, Weichselbaum R, Kufe D. Ionizing radiation induces expression and binding activity of the nuclear factor kappa B. J Clin Invest. 1991;88:691–5.

[114] Paul A, Edwards J, Pepper C, Mackay S. Inhibitory-κB Kinase (IKK) α and Nuclear Factor-κB (NFκB)-Inducing Kinase (NIK) as Anti-Cancer Drug Targets. Cells. 2018;7.

[115] Prescott JA, Cook SJ. Targeting IKKβ in Cancer: Challenges and Opportunities for the Therapeutic Utilisation of IKKβ Inhibitors. Cells. 2018;7.

[116] Figura NB, Potluri TK, Mohammadi H, Oliver DE, Arrington JA, Robinson TJ, et al. CDK 4/6 inhibitors and stereotactic radiation in the management of hormone receptor positive breast cancer brain metastases. J Neurooncol. 2019;144:583–9.

[117] Beddok A, Xu HP, Henry AA, Porte B, Fourquet A, Cottu P, et al. Concurrent use of palbociclib and radiation therapy: single-centre experience and review of the literature. Br J Cancer. 2020;123:905–8.

[118] Wei L, Leibowitz BJ, Wang X, Epperly M, Greenberger J, Zhang L, et al. Inhibition of CDK4/6 protects against radiation-induced intestinal injury in mice. J Clin Invest. 2016;126:4076–87.

[119] Franco R, Cao JQ, Yassa M, Hijal T. Safety of CDK4/6 Inhibitors Combined with Radiotherapy in Patients with Metastatic Breast Cancer: A Review of the Literature. Curr Oncol. 2023;30:5485–96.

[120] Kubeczko M, Jarząb M, Gabryś D, Krzywon A, Cortez AJ, Xu AJ. Safety and feasibility of CDK4/6 inhibitors treatment combined with radiotherapy in patients with HR-positive/HER2-negative breast cancer. A systematic review and meta-analysis. Radiother Oncol. 2023;187:109839.

doi:10.6342/NTU202504448

[121] Rugo HS, Kabos P, Beck JT, Jerusalem G, Wildiers H, Sevillano E, et al. Abemaciclib in combination with pembrolizumab for HR+, HER2- metastatic breast cancer: Phase 1b study. NPJ Breast Cancer. 2022;8:118.

[122] Schmid P, Cortes J, Pusztai L, McArthur H, Kümmel S, Bergh J, et al. Pembrolizumab for Early Triple-Negative Breast Cancer. N Engl J Med. 2020;382:810–21.

[123] Pulaski BA, Ostrand-Rosenberg S. Reduction of established spontaneous mammary carcinoma metastases following immunotherapy with major histocompatibility complex class II and B7.1 cell-based tumor vaccines. Cancer Res. 1998;58:1486–93.

[124] Kim K, Skora AD, Li Z, Liu Q, Tam AJ, Blosser RL, et al. Eradication of metastatic mouse cancers resistant to immune checkpoint blockade by suppression of myeloid-derived cells. Proc Natl Acad Sci U S A. 2014;111:11774–9.

[125] Taylor BC, Sun X, Gonzalez-Ericsson PI, Sanchez V, Sanders ME, Wescott EC, et al. NKG2A Is a Therapeutic Vulnerability in Immunotherapy Resistant MHC-I Heterogeneous Triple-Negative Breast Cancer. Cancer Discov. 2024;14:290–307.

[126] Akbay EA, Koyama S, Carretero J, Altabef A, Tchaicha JH, Christensen CL, et al. Activation of the PD-1 pathway contributes to immune escape in EGFR-driven lung tumors. Cancer Discov. 2013;3:1355–63.

[127] Wen-Chi Yang M-FW, Yi-Hsuan Lee, Chiun-Sheng Huang, Sung-Hsin Kuo. Radiosensitizing effects of CDK4/6 inhibitors in hormone receptor-positive and HER2-negative breast cancer mediated downregulation of DNA repair mechanism and NF-κB-signaling pathway. Tanslatinoal Oncology. 2024;in revision.

[128] Gao X, Leone GW, Wang H. Cyclin D-CDK4/6 functions in cancer. Adv Cancer Res. 2020;148:147–69.

doi:10.6342/NTU202504448

[129] Bernhardt T, Kriesen S, Manda K, Schlie C, Panzer R, Hildebrandt G, et al. Induction of Radiodermatitis in Nude Mouse Model Using Gamma Irradiator IBL 637. Skin Pharmacol Physiol. 2022;35:224–34.

[130] Ni L, Lu J. Interferon gamma in cancer immunotherapy. Cancer Med. 2018;7:4509–16.

[131] Guarducci C, Bonechi M, Boccalini G, Benelli M, Risi E, Di Leo A, et al. Mechanisms of Resistance to CDK4/6 Inhibitors in Breast Cancer and Potential Biomarkers of Response. Breast Care (Basel). 2017;12:304–8.

[132] Robinson TJ, Liu JC, Vizeacoumar F, Sun T, Maclean N, Egan SE, et al. RB1 status in triple negative breast cancer cells dictates response to radiation treatment and selective therapeutic drugs. PLoS One. 2013;8:e78641.

[133] George MA, Qureshi S, Omene C, Toppmeyer DL, Ganesan S. Clinical and Pharmacologic Differences of CDK4/6 Inhibitors in Breast Cancer. Front Oncol. 2021;11:693104.

[134] Pesch AM, Hirsh NH, Michmerhuizen AR, Jungles KM, Wilder-Romans K, Chandler BC, et al. RB expression confers sensitivity to CDK4/6 inhibitor-mediated radiosensitization across breast cancer subtypes. JCI Insight. 2022;7.

[135] Shrestha M, Wang DY, Ben-David Y, Zacksenhaus E. CDK4/6 inhibitors and the pRB-E2F1 axis suppress PVR and PD-L1 expression in triple-negative breast cancer. Oncogenesis. 2023;12:29.

[136] Wu CT, Chen WC, Chang YH, Lin WY, Chen MF. The role of PD-L1 in the radiation response and clinical outcome for bladder cancer. Sci Rep. 2016;6:19740.

[137] Hampe L, Küffer S, Niemeier T, Scheele NC, Hampe LZ, Riedl AL, et al. Effects of chemoradiotherapy on surface PD-L1 expression in esophageal cancer and its implications for immunotherapy. Front Immunol. 2024;15:1509051.

[138] Shen N, Yang C, Zhang X, Tang Z, Chen X. Cisplatin nanoparticles possess stronger anti-tumor synergy with PD1/PD-L1 inhibitors than the parental drug. Acta Biomater. 2021;135:543–55.

doi:10.6342/NTU202504448

[139] Zhu S, Zhang T, Zheng L, Liu H, Song W, Liu D, et al. Combination strategies to maximize the benefits of cancer immunotherapy. J Hematol Oncol. 2021;14:156.

[140] Wang NH, Lei Z, Yang HN, Tang Z, Yang MQ, Wang Y, et al. Radiation-induced PD-L1 expression in tumor and its microenvironment facilitates cancer-immune escape: a narrative review. Ann Transl Med. 2022;10:1406.

[141] Wang L, Wu Y, Kang K, Zhang X, Luo R, Tu Z, et al. CDK4/6 inhibitor abemaciclib combined with low-dose radiotherapy enhances the anti-tumor immune response to PD-1 blockade by inflaming the tumor microenvironment in Rb-deficient small cell lung cancer. Transl Lung Cancer Res. 2024;13:1032–46.

[142] Muroyama Y, Nirschl TR, Kochel CM, Lopez-Bujanda Z, Theodros D, Mao W, et al. Stereotactic Radiotherapy Increases Functionally Suppressive Regulatory T Cells in the Tumor Microenvironment. Cancer Immunol Res. 2017;5:992–1004.

[143] Yoshimura T. The chemokine MCP-1 (CCL2) in the host interaction with cancer: a foe or ally? Cell Mol Immunol. 2018;15:335–45.

[144] Takada Y, Hisamatsu T, Kamada N, Kitazume MT, Honda H, Oshima Y, et al. Monocyte chemoattractant protein-1 contributes to gut homeostasis and intestinal inflammation by composition of IL-10-producing regulatory macrophage subset. J Immunol. 2010;184:2671–6.

[145] Li W, Katz BP, Spinola SM. Haemophilus ducreyi-induced interleukin-10 promotes a mixed M1 and M2 activation program in human macrophages. Infect Immun. 2012;80:4426–34.

[146] Xu ZJ, Gu Y, Wang CZ, Jin Y, Wen XM, Ma JC, et al. The M2 macrophage marker CD206: a novel prognostic indicator for acute myeloid leukemia. Oncoimmunology. 2020;9:1683347.

[147] Lu G, Zhang R, Geng S, Peng L, Jayaraman P, Chen C, et al. Myeloid cell-derived inducible nitric oxide synthase suppresses M1 macrophage polarization. Nat Commun. 2015;6:6676.

doi:10.6342/NTU202504448

[148] Mei M, Tang L, Zhou H, Xue N, Li M. Honokiol prevents lung metastasis of triple-negative breast cancer by regulating polarization and recruitment of macrophages. Eur J Pharmacol. 2023;959:176076.

[149] Liu L, Stokes JV, Tan W, Pruett SB. An optimized flow cytometry panel for classifying macrophage polarization. J Immunol Methods. 2022;511:113378.

[150] House IG, Savas P, Lai J, Chen AXY, Oliver AJ, Teo ZL, et al. Macrophage-Derived CXCL9 and CXCL10 Are Required for Antitumor Immune Responses Following Immune Checkpoint Blockade. Clin Cancer Res. 2020;26:487–504.

[151] Tokunaga R, Zhang W, Naseem M, Puccini A, Berger MD, Soni S, et al. CXCL9, CXCL10, CXCL11/CXCR3 axis for immune activation - A target for novel cancer therapy. Cancer Treat Rev. 2018;63:40–7.

[152] Mercogliano MF, Bruni S, Elizalde PV, Schillaci R. Tumor Necrosis Factor α Blockade: An Opportunity to Tackle Breast Cancer. Front Oncol. 2020;10:584.

[153] Yang WC, Chen YH, Lai SF, Wang CC, Kuo SH, Huang CS. Reassessing regional nodal radiotherapy strategies for breast cancer in the context of modern systemic treatments. J Formos Med Assoc. 2025.

[154] Yang WC, Wei MF, Lee YH, Huang CS, Kuo SH. Radiosensitizing effects of CDK4/6 inhibitors in hormone receptor-positive and HER2-negative breast cancer mediated downregulation of DNA repair mechanism and NF-κB-signaling pathway. Transl Oncol. 2024;49:102092.

[155] Yang WC, Wei MF, Shen YC, Huang CS, Kuo SH. CDK4/6 inhibitors synergize with radiotherapy to prime the tumor microenvironment and enhance the antitumor effect of anti-PD-L1 immunotherapy in triple-negative breast cancer. J Biomed Sci. 2025;32:79.

doi:10.6342/NTU202504448